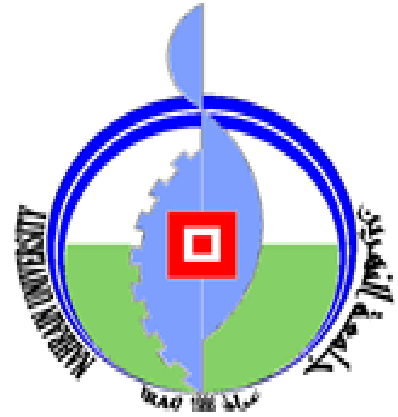


Republic of Iraq
Ministry of Higher Education and Scientific Research
Al-Nahrain University/ College of Science
Department of Physics



Structure Evolution in the even-even Ba nuclei with IBM

A Thesis

Submitted to College of Science / Al-Nahrain University as a partial
Fulfillment of the Requirements for the Degree of Master of science in
Physics .

By

Ghofran A. Hrata

B.Sc. Physics/College of Science/Al-Nahrain University (2014)

Supervised by

Prof. Dr. SAAD N. ABOOD

2016 A.D

1437 H.D

Supervisor Certification

We certify that this thesis entitled "**Structure Evolution in the even-even Ba nuclei with IBM**" was prepared under our supervision at the University of Al-Nahrain Collage of Science Department of Physics, in partial fulfillment of the requirements for the degree of Master of science in physics.

Signature: *Saad N. Abood*

Name: Saad N. Abood

Scientific Degree: Professor

Date: 6 / 9 / 2016

In view of available recommendation, I forward this thesis for debate by the examining committee.

Signature: *Saad N. Abood*


Name: Saad Naji Abood


Scientific Degree: Professor


Date: 6 / 9 / 2016

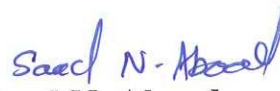
Committee Certification

We, the examining committee certify that we have read this thesis entitled " **Structure Evolution in the even-even Ba Nuclei with IBM** " and examined the student " Ghofran A. Ali " in its contents and that in our opinion, it is accepted for the Degree of Master of Science in Physics.

Signature: 
Name: **Dr. Nada Fadhil Tawfiq**
Scientific Degree: Professor
Date: 15 / 3 / 2017
(Chairman)

Signature: 
Name: **Dr. Mahdi Hadi Jasim**
Scientific Degree: Assis. Prof.
Date: 19 / 3 / 2017
(Member)

Signature: 
Name: **Dr. Mudar Ahmed Abdulsattar**
Scientific Degree: Chief Researchers
Date: 19 / 3 / 2017
(Member)

Signature: 
Name: **Dr. Saad N. Abood**
Scientific Degree: Professor
Date: 15 / 3 / 2017
(Member/ Supervisor)

I, hereby certify upon the decision of the examining committee.


Signature: 
Name: **Dr. Hadi M. A. Abood**
Scientific Degree: Professor
Title: Dean of College of Science
Date: 23 / 3 / 2017

Table of Contents

	Page
List of Figures	i
List of Tables	ii
Abstract	iii
Chapter One - Introduction	1
1.1 The Aims of Presented Research Work	5
1.2 Talk Layout	6
Chapter Two - Theoretical Considerations	7
2.1 Macroscopic Models	7
2.1.1 Spherical Shapes	7
2.1.2 Non-Spherical Shapes	9
2.2 Microscopic Models	12
2.2.1 Pairing-Coupling Scheme	12
2.2.2 Paring-Plus-Quadrupole Model	14
2.2.3 Dynamic Deformation Model (DDM)	15
2.2.4 Other Microscopic Models	17
2.3 Phenomenological Models	17
2.3.1 Group Theoretical Model- The Interacting Boson Model (IBM)	17
2.3.1.1 The Vibrational SU(5) Symmetry	22
2.3.1.2 The Rotational SU(3) Symmetry	25
2.3.1.3 The Gamma Unstable O(6) Symmetry	27
2.3.1.4 The Potential Energy Surface	31
2.3.2. Interacting Boson Model-2 (IBM-2)	32
2.3.2.1 Mixed-Symmetry States	36
Chapter Three - Results and Discussion	39
3.1 IBM-1 Results	39
3.1.1 Energy Spectra	39
3.1.2 Potential Energy Surface	60
3.1.3 Electric Transition Probability B(E2)	60
3.1.4 Magnetic Transition Probability B(M1) and Mixing Ratio $\delta(E2/M1)$	69
3.2 IBM-2 Results	73
3.2.1 Energy Spectra	73
3.2.2 Electric Transition Probability B(E2)	76
3.2.3 Magnetic Transition Probability B(M1) and Mixing Ratio (E2/M1)	78
3.2.4 Electric Monopole Matrix Element $\rho(E0)$	81
3.2.5 Mixed Symmetry States in ¹²⁰⁻¹⁴⁸ Ba Isotopes	82
3.3 Dynamic Deformation Model (DDM) Results	88
3.3.1 Energy Spectra	88
3.3.2 Potential Energy Surface	89
3.3.3 Electric Transition Probability B(E2)	91
3.3.4 Magnetic Transition Probability B(M1) and Mixing Ratio $\delta(E2/M1)$	93
3.3.4 Electric Monopole Transition Matrix element $\rho(E0)$	94
Chapter Four	96
4.1 Concluding Remarks	96
4-2 Suggestions for Future Work	98
References	100

List of Figures

Figures	Page
2.1 Typical spectrum of a nucleus exhibiting the SU(5) symmetry. The states are labeled by the quantum numbers $J^\pi(n_d, \nu, n_\Delta)$. The spectrum is broken up into a number of bands.	22
3.1 Comparison between experimental data, IBM-1, IBM-2 and DM calculated energy levels for ^{120}Ba .	46
3.2 Comparison between experimental data, IBM-1, IBM-2 and DM calculated energy levels for ^{122}Ba .	47
3.3 Comparison between experimental data, IBM-1, IBM-2 and DM calculated energy levels for ^{124}Ba .	48
3.4 Comparison between experimental data, IBM-1, IBM-2 and DM calculated energy levels for ^{126}Ba .	49
3.5 Comparison between experimental data, IBM-1, IBM-2 and DM calculated energy levels for ^{128}Ba .	50
3.6 Comparison between experimental data, IBM-1, IBM-2 and DM calculated energy levels for ^{130}Ba .	51
3.7 Comparison between experimental data, IBM-1, IBM-2 and DM calculated energy levels for ^{132}Ba .	52
3.8 Comparison between experimental data, IBM-1, IBM-2 and DM calculated energy levels for ^{134}Ba .	53
3.9 Comparison between experimental data, IBM-1, IBM-2 and DM calculated energy levels for ^{136}Ba .	54
3.10 Comparison between experimental data, IBM-1, IBM-2 and DM calculated energy levels for ^{140}Ba .	55
3.11 Comparison between experimental data, IBM-1 and IBM-2 calculated energy levels for ^{142}Ba .	56
3.12 Comparison between experimental data, IBM-1 and IBM-2 calculated energy levels for ^{144}Ba .	57
3.13 Comparison between experimental data, IBM-1 and IBM-2 calculated energy levels for ^{146}Ba .	58
3.14 Comparison between experimental data, IBM-1 and IBM-2 calculated energy levels for ^{148}Ba .	59

List of Tables

Tables	Page
3-1 IBM-1 Hamiltonian parameters for $^{120-148}\text{Ba}$ isotopes.	39
3-2 Experimental and theoretical values of energy ratios in Ba isotopes.	41
3-3 Experimental and theoretical values of β_{\min} , E_d , V_{PO} energy difference $E(2_2^+) - E(4_1^+)$ and $Q(2_1^+)$ in Ba isotopes.	44
3-4 The root mean square deviations (RMSD) between experimental and calculated energy levels for $^{120-148}\text{Ba}$ isotopes.	45
3-5 The effective boson charges used in IBM-1 for the calculation of $B(E2)$ transition probabilities for $^{120-148}\text{Ba}$ isotopes.	61
3-6 Experimental and theoretical values of Electric Transition Probabilities $B(E2; J_i^+ \rightarrow J_f^+)$ in e^2b^2 Units for Ba isotopes.	62
3-7 Branching Ratios of $^{120-148}\text{Ba}$ isotopes.	66
3-8 Magnetic Transition Probability $B(M1; J_f^+ \rightarrow J_i^+)$ for $^{120-148}\text{Ba}$ isotopes in μ_N^2 .	70
3-9 Mixing Ratio $\delta(E2/M1)$ for $^{120-148}\text{Ba}$ in eb/μ_N units.	71
3-10 Parameters used in IBM-2 Hamiltonian for $^{120-148}\text{Ba}$ nuclei (all in MeV except χ_ν and χ_π are dimensionless).	74
3-11 Variation of the 2_2^+ , 3_1^+ , 2_3^+ , 4_2^+ and 4_3^+ energies as a function of Majorana parameters ξ_2 .	76
3-12 Effective charge used in E2 transition calculations ($e_\pi = 0.2032 e.b$).	77
3-13 Experimental and IBM-2 calculations for g-factors for $^{120-148}\text{Ba}$ μ_N units.	80
3-14: Monopole Matrix Element $\rho(E0)$ in $e.b$ for $^{120-148}\text{Ba}$ isotopes in IBM-2.	81
3-15 $X(E0/E2)$ $^{120-148}\text{Ba}$ isotopes in IBM-2.	82
3-16 B(M1) calculated to first excited states in μ_N^2 units for $^{120-148}\text{Ba}$ isotopes.	84
3-17 Experimental and calculated for 1^+ level for $^{126-142}\text{Ba}$ isotopes in MeV units.	87
3-18 The root-mean-square (rms) values of β and γ deformation parameters of ground state and excited states in $^{120-140}\text{Ba}$ isotopes.	89
3-19 Quadrupole moment for ground band, beta and gamma bands for $^{120-140}\text{Ba}$ isotopes in $e.b$ units.	92
3-20 Magnetic dipole moment in μ_N units and g-factors for $^{120-146}\text{Ba}$ μ_N units in DDM.	93
3-21 Monopole Matrix Element $\rho(E0)$ in $e.b$ for $^{120-140}\text{Ba}$ isotopes in DDM.	94
3-22 $X(E0/E2)$ $^{120-148}\text{Ba}$ isotopes in DDM.	95

ABSTRACT

The nuclear structure and electromagnetic transitions of even–even neutron-rich $^{120-148}\text{Ba}$ isotopes was studied in the framework of the collective models Interacting Boson Model (IBM-1 and IBM-2) and Dynamic Deformation Model (DDM). The reduced transition probabilities $B(E2)$, $B(M1)$, monopole matrix element $\rho(E0)$, mixing ratio $\delta(E2/M1)$ and $X(E0/E2)$ of these isotopes was calculated. A set of parameters was used in the calculation to approach the values with the measured data. It was pointed out that Interacting Boson Model (IBM-1 and IBM-2) are equitably reliable for the description of spectra and other nuclear properties. It was found that there is a rapid transition between spherical and rotational shapes.

In this work, we depend on new methods to evaluate the effective charges for proton and neutron boson (e_π) and (e_ν), and new method to calculate the gyromagnetic ratio for proton boson (g_π) and (g_ν).

Mixed symmetry states are also studied. It is found that some of the mixed symmetry states with moderate high spins change very fast with respect to the Majorana interaction. Under certain conditions, they become the yrast state or yrare state. These states are difficult to decay and become very stable. This study suggests that a possible new mode of isomers may exist due to the special nature in their proton and neutron degrees of freedom for these isotopes.

The mixed-symmetry 2_3^+ , 2_4^+ , 3_1^+ and 1^+ states or at least a fragment of it have been identified in Ba isotopes. This enables us to trace the evolution of the one-phonon and two-phonon states in the even-even barium isotopic chain from the γ -soft nuclei near $N = 82$ to the deformed nuclei towards mid-shell.

The Dynamic Deformation Model (**DDM**) of Kumar and Baranger is employed for studying variations of the nuclear structure of light $^{120-140}\text{Ba}$ isotopes. The potential energy surface parameters have been calculated and the low-lying levels spectrum is predicted along with the static and transition E2 moments. Comparison with experiment data and with other theories supports the validity of our treatment.

The recent developments of the dynamic deformation model (**DDM**) make it readily applicable to a wide range of nuclei in periodic table. We study of the even-mass barium isotopes from $N= 64$ to the closed neutron shell at $N= 84$. Within this region there is experimental evidence for nuclei with the characteristics of vibrational, rotational or γ -soft level sequences. We show that the **DDM** model is well able to account for these features as typified by energy levels, electric quadrupole moments and gamma transition probabilities across this region when the only parameter which changes is the neutron number. For comparison the experimental data were also fitted to IBM-2 and the results from these fits are in general in good agreement with those from the DDM.

Supervisor Certification

We certify that this thesis entitled "**Structure Evolution in the even-even Ba nuclei with IBM**" was prepared under our supervision at the University of Al-Nahrain Collage of Science Department of Physics, in partial fulfillment of the requirements for the degree of Master of science in physics.

Signature:

Name: Saad N. Abood

Scientific Degree: Professor

Date: / / 2016

In view of available recommendation, I forward this thesis for debate by the examining committee.

Signature:

Name: Saad Naji Abood

Scientific Degree: Professor

Date: / / 2016

CHAPTER ONE

INTRODUCTION

The atomic nucleus is a fascinating physical object. With a size measured in units of 10^{-15} m its dimensions are far beyond the abilities of human imagination. It is remarkable that an atomic nucleus only makes up about 0.001% of the volume of its atom leaving the rest empty. Yet, atomic nuclei comprise more than 99.9% of the mass of all visible matter. Our contemporary idea of the properties of the atomic nucleus can be traced back to its groundbreaking discovery together with the development of the model of the atom by Rutherford in 1911 [1]. Since then, nuclear scientists have made tremendous progress in the description of the atomic nucleus. But even today not all properties of the atomic nucleus have been fully understood.

The atomic nucleus is a mesoscopic quantum system consisting of 1~300 interacting nucleons of two different species, namely protons and neutrons. However, their interaction is still subject to ongoing investigations. Recent attempts to model realistic interactions try to deduce the interactions between the nucleons from the fundamentals of *QCD*, e.g. [2], and involve different degrees of many body terms. Given these considerations one would expect the structure of the nucleus to be chaotic and complicated. However, empirical data on level schemes, in particular of even-even nuclei all across the nuclear chart reveal a different observation. In fact, almost all even-even nuclei exhibit some surprisingly simple parts of their level schemes whose patterns are repeating in different regions of the nuclear chart. One well-known example are the first two excited states of even-even nuclei that in most cases are of angular momentum $J^+ = 2^+$ and $J^+ = 4^+$. The ratio of their excitation energies, $R_{4/2} = E(4_1^+ / 2_1^+)$, exhibits a very uniform behavior as a function of the distance from the nuclear magic numbers.

While a unified description of nuclear structure is still not available, different approaches have been established to describe certain features of the nuclei. For nuclei near closed shells the nuclear shell model [3] is capable of a good description, provided that the underlying single-particle energies and interactions are known. Nuclei further away of closed shells exhibit characteristic features that can be described by the phenomenon of quadrupole collectivity, which arises from a coherent motion of the nucleons, a phenomenon that can be observed in numerous even-even nuclei across the nuclear chart. A very successful theoretical framework for the description of collectivity has been found in the geometrical model introduced by Bohr and Mottelson [Boh98], treating the nucleus as a shaped object which can be subject to excitations of vibrational and rotational character. A different ansatz was developed in terms of algebraic models, among which the **Interacting Boson Model (IBM)** [4] is the most widely known. Short introductory chapters on all of the above-mentioned theoretical models will be given in the subsequent chapters.

The models which describe the different phenomena of quadrupole collectivity allow for the deduction of simple rules for experimental signatures—experimentally

accessible quantities that are characteristic of the respective theoretical models and can, thus, help in guiding experimentalists to design and perform dedicated experiments. Experimental results on the quantities serving as signatures of given theoretical models are the most crucial testing ground for the applicability of a model. Such observables can be relative quantities like decay branching ratios or γ -ray multipole mixing ratios. However, absolute quantities, for example in the form of selection rules for electromagnetic transitions, allow for more substantial interpretations of experimental data.

Interest in the $A = 130$ region of light Ba isotopes ($N < 82$) was renewed in 1985 on the recognition that some of these nuclei are good examples of the $O(6)$ dynamic symmetry of the Interacting Boson Model (IBM) [4]. Later, in 2000, with the identification of ^{134}Ba as a good example of the newly proposed analytically solvable $E(5)$ critical point symmetry on the $U(5)$ - $O(6)$ path by Iachello [5], and by Casten and Zamfir [6], interest in the Ba isotopes ($N < 82$) was renewed. Kumar and Gupta [7] extended the highly successful microscopic theory in the dynamic pairing plus quadrupole (DPPQ) model of Kumar-Baranger [8] to the $A = 130$ region, by using the appropriate Nilsson spherical single-particle energies, and applied it to the study of the neutron-deficient Ba isotopes.

Puddu *et al.*, [9] used the Interacting Boson Model (IBM-2) to predict the general trend of variation with N of the level structures and E2 moments in Xe, Ba and Ce ($N < 82$). Castanos *et al.*, [10] derived the effective Hamiltonian in IBM-1 in terms of Casimir operators with seven adjustable coefficients to study the groups of nuclei including light Ba isotopes. In Ba they obtained 2_γ below 4_g for all N , contrary to experiment. Hamilton *et al.*, [11] studied the γ decay from the 2_3^+ state at about 2-MeV excitation in the nuclei ^{140}Ba , ^{142}Ce , and ^{144}Nd , with 84 neutrons and is shown to be consistent with its identification as the lowest state of mixed symmetry in the $U(5)$ limit of the neutron-proton version of the interacting-boson model.

Novoselsky and Talmi [12] used a larger boson energy ε on shell model considerations in IBM-2 application. They kept χ the coefficient of $[dd^+]$ term constant and varied coefficients of other terms in the IBM Hamiltonian to better reproduce the odd-even spin staggering. Sevrin *et al.*, [13] added the $SU(3)$ term to $O(6)$ to generate some rigid triaxiality in IBM-2 to better reproduce the odd-even spin staggering in the $K = 2^+\gamma$ -band.

The energy level spectrum and the interband $B(E2)$ ratios were calculated for $^{130-134}\text{Ba}$ [14]. The problem of computation of the resulting large matrix size restricted the analysis to a maximum of four neutron pairs (and four proton pairs).

Yu-Xin LIU *et al.*, in 1994 [15] studied the an IBM-2 description of the staggering phenomenon in $^{128-140}\text{Ba}$ isotopes. By introducing the quadrupole interactions among like bosons into the Hamiltonian, the staggering phenomenon in the quasi-gamma band is reproduced pretty well. The physical mechanism behind the improvement is discussed.

Kumar and Gupta (2001) [16] employed the dynamic pairing plus quadrupole model of Kumar and Baranger for studying variations of the nuclear structure of light Ba isotopes with $A = 122-134$. The potential energy surface parameters have been calculated and the low-spin level spectrum is predicted along with the static and transition $E2$ moments. Comparison with experiment and with other theories supports the validity of our treatment.

Mittal and Vidya Devi [17] in 2010 studied $^{126-136}\text{Ba}$ isotopes within IBM-1. IBM-1 is used to describe the nuclear structure of these isotopes. The structure of such isotopes was undertaken to provide more detail on the neutron rich isotope. boson model is used to calculate the ground, beta and gamma band energy spectra and the $B(E2)$ transition probabilities of $^{126-136}\text{Ba}$ nuclei.

P. G. Bizzeti *et al.*, in 2010 [18] investigate the possible X(5) character of ^{122}Ba , suggested by the ground-state band energy pattern, the lifetimes of the lowest yrast states of ^{122}Ba have been measured, via the recoil distance Doppler-shift method. The relevant levels have been populated by using the $^{108}\text{Cd}(^{16}\text{O}, 2n)^{122}\text{Ba}$ and the $^{112}\text{Sn}(^{13}\text{C}, 3n)^{122}\text{Ba}$ reactions. The $B(E2)$ values deduced in the present work are compared to the predictions of the X(5) model and to calculations performed in the framework of the IBM-1 and IBM-2 models.

Turkan [19] in 2010 studied the electromagnetic characteristics of $^{124-136}\text{Ba}$ isotopes Performed in the Framework of IBM-1 and IBM-2. In this study It was pointed out that the level scheme of the transitional nuclei $^{124-136}\text{Ba}$ also can be studied by both characteristics (IBM-1 and IBM-2) of the interacting boson model and an adequate point of the model leading to $E2$ transitions is therefore confirmed. Most of the $\delta(E2/M1)$ mixing ratios that are still not known so far are stated and the set of parameters used in these calculations is the best approximation that has been carried out so far. It has turned out that the interacting boson approximation is fairly reliable for the calculation of spectra in the entire set of $^{124-136}\text{Ba}$ isotopes.

Kumar *et al.*, in [2010] [20] study the nuclear structure of $^{122-134}\text{Ba}$ isotopes using IBM-1. In this work calculated the level spectra of $^{122-134}\text{Ba}$ using the phenomenological IBM-1 model.

Subber and AL-Khudair in 2011 [21] studied the Nuclear structure of the neutron-rich $^{140-148}\text{Ba}$ isotopes. The level structure of even-even neutron-rich $^{140-148}\text{Ba}$ isotopes was studied in the framework of the interacting boson model. The reduced transition probabilities $B(E2)$ of these nuclei was calculated. A set of parameters was used in the calculation to approach the values with the measured data. It was pointed out that interacting boson approximations are equitably reliable for the description of spectra and other properties. It was found that there is a rapid transition between spherical and rotational shapes.

Mittal and Vidya Devi in 2011 [22] studied $^{122-132}\text{Xe}$ and $^{122-136}\text{Ba}$ nuclei using IBM-1. In this study presented the calculation of energy levels and $B(E2)$ values of these

nuclei. Using the best fitted values of the parameters in the Hamiltonian of IBM-1 model and has been calculated the energy levels and $B(E2)$ values for number of some transitions in $^{122-132}\text{Xe}$ and $^{122-136}\text{Ba}$ nuclei. Results are compared with experimental data and other theoretical models. It has turned out that IBM-1 fairly reliable for the calculation of spectra to the entire set of $^{122-132}\text{Xe}$ and $^{122-136}\text{Ba}$ nuclei.

Subber and AL-Khudair in 2012 [23] studied the $\delta(E2/M1)$ and $X(E0/E2)$ mixing ratios in ^{134}Ba by means of IBM-2. In this study showed that the ^{134}Ba isotope ($Z = 56$) lies in the transitional region closer to the vibrational range of nuclei. Energy levels $B(E2)$, $B(M1)$ and the mixing ratios $\delta(E2/M1)$ and $X(E0/E2)$ for selected transitions were calculated in the framework of the proton-neutron interacting boson model (IBM-2). All results were compared with experimental data. Some experimental $X(E0/E2)$ ratios were calculated from available experimental data. Majorana parameters were found to have a great effect on the calculated energy levels of the 2_3^+ and 2_4^+ , which indicate that both of them have mixed symmetry properties.

Gupta in 2013 [24], the shape-phase transition at $N = 88-90$, and the role of $Z = 64$ subshell effect therein has been a subject of study on empirical basis and in the context of the $N_p N_n$ scheme, but a microscopic view of the same has been lacking. The dynamic pairing plus quadrupole model (DPPQ) is employed to predict the occupation probabilities of the neutron and proton deformed, single-particle orbitals. The nuclear structure of Ba–Dy ($N > 82$) nuclei is studied and the shape equilibrium parameters derived.

Thomas Möller in 2014 [25] The results on $B(M1; 2_{1,i}^+ \rightarrow 2_1^+)$ values of the nuclei $^{130,132}\text{Ba}$ complete the experimental data on the evolution of the one quadrupole-phonon state of mixed proton-neutron symmetry ($2_{1,Ms}^+$) in the $A= 130$ mass region. The results support the previous observation of increased fragmentation of the $2_{1,Ms}^+$ state for mid-shell nuclei, although one candidate of a $2_{1,Ms}^+$ state of ^{130}Ba , if confirmed, would alter this interpretation.

Gupta in 2015 [26], nuclear level structures of $^{122-134}\text{Ba}$ isotopes have been studied empirically in relation to the analytic symmetries of the interacting boson model IBM-1 and in the calculation of the IBM-1 Hamiltonian. Comparison is made with experiment and with the microscopic dynamic pairing plus quadrupole model predictions available from our previous studies. The variation of the structure of states in the 2_2^+ bands and of the $0_{2,3}^+$ bands, with neutron number N , have been studied. Relation of odd-even spin staggering in the 2_2^+ bands with the β -softness is illustrated. A comparison is made with predictions of the various analytical symmetries.

Gupta in 2015 [27], Rich experimental data is available for light Ba isotopes $N < 82$ have been studied. An attempt has been made in a dynamic deformation model using pairing plus quadrupole interactions and two full major shell configuration space

1.1 The Aims of Presented Research Work

In the context of the main aim of the present study, namely to investigate the following nuclear properties:

1- The objective of the present study is to test the capabilities of **IBM-1**, **IBM-2** models and to give an insight on the variation of the nuclear structure and electromagnetic transitions of $^{120-148}\text{Ba}$ isotopes with neutron number N . We have done a detailed study of the energy systematics of $^{120-148}\text{Ba}$ isotopes and the $E2$, $M1$ transition rates in their decay, mixing ratios $\delta(E2/M1)$ and monopole transition probability $B(E0)$ and $X(E0/E2)$. In the this work, we study the shape transition of light Ba isotopes in comparison with the predictions of the various analytical symmetries for this region.

2- Our work represents an attempt in the dynamic deformation model (**DDM**) for analyzing the nuclear structure of Ba isotopes varying with neutron number N . We give a brief account of our method and we present the results and compare a large amount of data with experiment and the results of other IBM-1 and IBM-2 calculations in all of the above three methods. We discuss the successes and the limitations of our method and give our conclusions.

3- The main purpose of this work is to test the possible X(5) character of the Ba nucleus by energy level in the ground state (g.s.) band to deduce the $E2$ strengths of the transitions de-exciting its levels and, possibly, to identify the excited β band [the $s = 2$ band according to X(5) terminology].

4- To study the mixed-symmetry states characteristics of the eigenstates through the study of various quantities for instance, correlation in the electromagnetic transition probabilities.

5- In the present study we focus our attention on Ba isotopes that are usually interpreted as soft in γ [or close to the SO(6) limit of the IBM] and we investigate to what extent the observed signature splitting in the γ -band signals the occurrence of more rigid triaxiality.

6- Investigate the balance and the interplay between the nuclear collectivity, the shell structures, and the isospin degree of freedom, we will try to clarify this relation. In this respect, there are three physics questions that need to be addressed:

* What is the impact of the underling microscopic structure on the properties of mixed symmetry states in low-collective vibrational nuclei from the Ba nucleus?

* How do mixed symmetry states evolve with increasing nuclear deformation?

* How does the balance between the number of valence protons and neutrons influence the properties of the mixed symmetry states ?

7- Study the potential energy surface within IBM-1 and DDM .

1.2 Talk Layout

This thesis is organized as follows. The next Chapter gives a details summary of the nuclear structure models used in this work: the IBM and the DDM. The discussion of the results are described in Chapter 3. The results of this thesis are summarized in Chapter four and an outlook for future applications is given.

Chapter Two

THEORETICAL CONSIDERATIONS

During the past thirty years, a large number of nuclear models and methods have been developed. The spherical shell model has been extended so that it can be employed for quite heavy nuclei [28,29]. However, there are serious problems connected with configuration space truncation and there are indications, especially from nuclear reaction studies, that the "extra" configurations cannot be left out of a satisfactory theory of atomic nuclei. Furthermore, such spherical models cannot describe nuclear fission. This is not a matter of concern only for people interested in transuranic nuclei! Any nucleus can fission if it is given enough energy and angular momentum. The limiting angular momentum reaches a peak value [30] of ~ 95 at $A \sim 130$ but drops off to zero on *both* sides of this mass number.

The first two sections of this chapter will present a brief summary of some of the macroscopic and microscopic nuclear models of collective excitations. Section 3 will present a detailed discussion of the recently proposed phenomenological model (Interacting Boson Model (IBM)).

2.1. MACROSCOPIC MODELS

The understanding of nuclear excitations in terms of the specific interactions of the single nucleons comprising a nucleus is the fundamental problem of nuclear physics. The shell model has been shown to provide this level of understanding in many nuclear systems. However, this success has been limited in even-even nuclei to systems with relatively few particles outside of closed shells or the region $A \leq 50$. To date, no complete shell model description of a heavy even-even nucleus far from a closed shell exists.

The nuclear systems composed of many particles, however, exhibit structures that can be easily understood when the gross properties of these nuclei are taken into account. For example, there is considerable evidence that the low-lying excitations of even-even nuclei with $A \geq 100$ are predominantly of a collective nature, that is, the correlated oscillations of many particles with respect to a core of spectator nucleons. In addition, the onset of structures that can be attributed to the excitation of only a few (2 to 4) particles occurs at a much higher energy.

The understanding of the collective excitations of nuclei has long been viewed in terms of the macroscopic properties of the nucleus. One of the earliest attempts at this type of description was the classical Liquid Drop Model (LDM) [31] which tried to describe such bulk properties of nuclei as binding energies and the onset of fission.

The most successful of the macroscopic descriptions of nuclear excitations is that of A. Bohr and B. Mottelson (BM) [32,33].

An excellent detailed description of the collective properties of nuclei is presented in their text (Ref. 33). In addition, numerous excellent review articles [34,35] have appeared, which present the BM model in great detail; therefore, the discussion here will be restricted to a general presentation of the model and the characteristic features of the different excitations expected from a phenomenological approach.

2. 1. 1. Spherical Shapes

In the BM description, the competition between short-range and long-range interactions between nucleons gives rise to surface vibrations about an equilibrium shape

that can be spherical or deformed, whether or not axially symmetric.

The surface of a nucleus can be expressed in terms of [36]:

$$R = R_o \left[1 + \sum_{\lambda, \mu} \alpha_{\lambda\mu} Y_{\lambda}^{\mu}(\theta, \phi) \right] \dots\dots\dots(2-1)$$

where R_o is a constant and Y_{λ}^{μ} are the usual spherical harmonics (Legendre polynomials). The collective motions are then obtained by the time variation of the α_{λ}^{μ} 's. In the usual quadratic approximation, the kinetic energy can be written as [36]:

$$T = \frac{1}{2} \sum_{\lambda\mu} B_{\lambda} \left| \dot{\alpha}_{\lambda\mu} \right|^2 \dots\dots\dots(2-2)$$

Similarly, the expression for the potential energy becomes [36]

$$V = \frac{1}{2} \sum_{\lambda\mu} C_{\lambda} \left| \alpha_{\lambda\mu} \right|^2 \dots\dots\dots(2-3)$$

Equations (2-2) and (2-3) correspond to the familiar simple harmonic oscillator for each variable $\alpha_{\lambda\mu}$, where the associated frequency for each $\alpha_{\lambda\mu}$ is given by [36]:

$$\omega_{\lambda} = \left(\frac{C_{\lambda}}{B_{\lambda}} \right) \dots\dots\dots(2-4)$$

The oscillations associated with $\lambda = 0$ and $\lambda = 1$ are not of concern here, since they correspond to density oscillations (which will occur at high excitation energies) and vibrations of the center of mass, respectively. The frequency, ω_{λ} , rapidly increases [37] as a function of λ .

Therefore, the lowest order vibrations will be of order $\lambda = 2$, or quadrupole oscillations. Since we are only interested in low-lying excitations, the only other order which will be discussed is $\lambda = 3$.

Consider first the situation for $\lambda = 2$. A phonon, a quantum of vibration, of type A carries angular momentum equal to λ and parity $(-)^{\lambda}$. Therefore, for a nucleus which can oscillate about a spherical shape, the first excited state will have spin-parity of 2^{+} . The next quadrupole excitation will correspond to the coupling of two $\lambda = 2$ phonons, i.e., $n_{\lambda=2} = 2$, and will be a degenerate triplet of states with J^{π} values of $0^{+}, 2^{+}, 4^{+}$ at twice the excitation energy of the first 2^{+} state. (Recall the energy for a simple harmonic vibrator is of the form $E_n = \hbar\omega (n + 3/2)$). In actual situations, one expects that the degeneracies will be broken, but the predicted occurrence of levels at approximately the appropriate energies should correspond to what is actually observed.

An energy spectrum is not sufficient to identify the structure of a nucleus; knowledge of the wave functions of the states is crucial. The most frequent means of probing the wave functions is by investigating the reduced transition probability, $B(E\lambda)$, for the γ -ray decay of one level to another, since this involves the overlap of two wave functions connected by the transition operator, which is a familiar multipole operator $M(E\lambda)$. The $B(E\lambda)$ values are simply related to the multipole operator, $M(E\lambda)$, via [36]:

$$B(E\lambda : J_i \rightarrow J_f) = \frac{1}{2J_i + 1} \left| \langle J_f || M(E\lambda) || J_i \rangle \right|^2 \dots\dots\dots(2-5)$$

One can label the collective excitations by the number of phonons, n_{λ} , and the angular momentum J . Transitions will only occur between states connected by $\Delta n_{\lambda} = \pm 1$. The $B(E\lambda)$ values for allowed transitions between two levels are given by [34]:

$$\sum B(E\lambda : n_\lambda J_i \rightarrow n_\lambda - 1 J_f) = n_\lambda B(E\lambda : n_\lambda = 1 \rightarrow n_\lambda = 0) \dots \dots \dots (2-6)$$

The summation on the left-hand-side of the equation is over all states to which the initial state can decay, given the selection rules of the $B(E\lambda)$ operator. For example, consider the 4_1^+ level (the subscript refers to the first occurrence of a 4^+ state) of the two $\lambda = 2$ phonon triplet. Here $n_2 = 2$, and the only state to which the 4_1^+ state can decay is the $n_2 = 1$ 2_1^+ state. Therefore, Eq. (2-6) reduces to :

$$\begin{aligned} B(E2 : n_2 = 2 4_1^+ \rightarrow n_2 = 1 2_1^+) \\ = 2B(E2 : 2_1^+ = 1 \rightarrow 0_1^+) \dots \dots \dots (2-7) \end{aligned}$$

In addition, Eq. (2-6) implies that for any higher-lying state, for example, the 2^+ of the three-phonon quintuplet, the sum of all transition probabilities will be equal to the phonon number of the initial level times $B(E2 : 2_1^+ \rightarrow 0_1^+)$, although the individual transitions to the lower $n_2 = 2$ states will not be necessarily of equal strength. The actual branching ratios are determined by the respective coefficients of fractional parentage (*cfp*) for the coupling of particles with angular momentum λ . In particular, for $\lambda = 2, 3, 4$ these have been tabulated by Bayman and Lande [38].

In addition to quadrupole oscillations, oscillations corresponding to $\lambda = 3$, known as octupole vibrations, may occur at approximately the energy of the $\lambda = 2$ two-phonon triplet [36].

Again, an energy spectrum given by $E \propto \hbar\omega_3$ occur, with the lowest state being a 3^- level. In addition to the multiple octupole excitations, negative-parity states characterized by a mixture of quadrupole and octupole vibrations may occur. The lowest excitations of this type, namely with $n_2 = 1$ and $n_3 = 1$, will consist of five degenerate states with spin-parity $1^-, 2^-, 3^-, 4^-, 5^-$. However, because both the octupole vibration and any higher order coupling of vibrations occur relatively high in excitation energy, there is a greater probability that these states will mix with non-collective excitations, so that their simple structure may be obscured.

2.1.2 Non-Spherical Shapes

As mentioned earlier, a particular nuclear shape emerges as a result of the competition between long-range and short-range interactions. The particular effective interactions that are important to the BM description are the short-range monopole pairing interaction and the long-range quadrupole-quadrupole interaction between nucleons. A more detailed discussion of these interactions is presented in numerous review articles, in particular, Ref. [34] and in the next section. The pairing interaction tends to make the nucleus spherical; also, the strength of this interaction is proportional to the number of particles, N , outside of the closed shell. The quadrupole-quadrupole interaction favors a non-spherical shape because of the characteristic range [34]; here the strength of the interaction is proportional to N^2 . Near closed shells, the pairing interaction will dominate, but toward the middle of the shell, where $N^2 \gg N$, the quadrupole interaction will dominate the pairing force and, hence, the nucleus will assume a permanent deformation.

To describe the surface of a non-spherical nucleus, it is convenient to transform Eq. (2-1) into the coordinate system fixed with respect to the nucleus. Therefore, for a quadrupole shape, Eq. (2-1) becomes [36]:

$$R = R_o \left[1 + \sum_{\mu} \alpha_{2\mu} Y_2^{\mu}(\theta', \phi') \right] \dots\dots\dots(2-8)$$

where the $\alpha_{2\mu}$ are related to the earlier $a_{2\mu}$ via [36]:

$$a_{2\nu} = \sum_{\mu} \alpha_{2\mu} D_{\mu\nu}^2(\Theta, \Phi, \Psi) \quad (2-9)$$

where the $D_{\mu\nu}^2$ are the usual rotation matrices and θ, Φ, Ψ are the Euler angles, which relate the body-fixed and space-fixed axes. Since [36] $\alpha_{12} = \alpha_{2-1} = 0$ and $\alpha_{22} = \alpha_{2-2}$, there are only five parameters needed to describe the system, namely the Euler angles θ, Φ, Ψ , and α_{20} and α_{22} . For convenience, the parameters a_{20} and a_{22} are replaced by β and γ via the following relations [36]:

$$\begin{aligned} \alpha_{20} &= \beta \cos \gamma \\ \alpha_{22} &= \frac{1}{\sqrt{2}} \beta \sin \gamma \dots\dots\dots(2-10) \end{aligned}$$

The parameter β is a measure of the degree of quadrupole deformation, while γ is a measure of the departure from axial symmetry. The expression for the kinetic energy is given by [36]:

$$T = -\frac{\hbar^2}{2B} \left[\frac{1}{\beta^4} \frac{\partial}{\partial \beta} \beta^4 \frac{\partial}{\partial \beta} + \frac{1}{\beta^2} \frac{1}{\sin 3\gamma} \frac{\partial}{\partial \gamma} \sin 3\gamma \frac{\partial}{\partial \gamma} - \frac{1}{4} \sum_k \frac{J_k^2}{\sin^2(\gamma - \frac{2}{3}\pi k)} \right] \dots\dots\dots(2-11)$$

where the J_k are the angular momentum operators associated with the Euler angles. This kinetic energy, together with the appropriate potential energy, will be referred to as the Bohr Hamiltonian.

Three types of potentials will be discussed. The most familiar, which corresponds to the symmetric rotor, occurs for $\beta \neq 0, \gamma = 0$. The other two correspond to asymmetric rotors: the triaxial rotor, where $V = V(\beta, \gamma_o)$ for a specific $\gamma_o \neq 0$, and the γ -unstable rotor, where $V = V(\beta)$ (i.e., independent of γ).

The symmetric rotor is characterized by a quadrupole deformation β which may be positive or negative, referring to prolate or oblate shapes, respectively. Empirically, most deformed nuclei are prolate. Two types of collective excitations may occur: the nucleus may rotate about an axis perpendicular to the axis of symmetry or the nucleus may oscillate about its equilibrium shape. These oscillations may be along the symmetry axis, β vibrations, or such as to introduce asymmetries, γ vibrations. In either case, rotations will again be built upon the intrinsic structure at excitation energy, E_{vib} . In all of these cases, the energy spectrum can be simply expressed as [39]:

$$E = \frac{\hbar^2}{2I} [J(J+1) - K^2] + E_{vib} \dots\dots\dots(2-12)$$

where I is the moment of inertia and K is the projection of angular momentum onto the symmetry axis. For the rotations built upon the ground state and β vibrations, $K = 0$ and the

spin sequence will be $0^+, 2^+, 4^+ \dots$. For the γ vibrations $K = 2$ and the sequence of levels will be $2^+, 3^+, 4^+ \dots$ (The derivation of these spin sequences may be found in numerous references such as Refs. [33,36]).

The transition probabilities again provide a convenient probe of the wave functions. For transitions between states belonging to the same rotational band labelled by K one obtains [37]

$$B(E2: J_i K \rightarrow J_f K) = e^2 Q_o^2 \left| \langle J_i 2K0 | J_f K \rangle \right|^2 \quad (2-13)$$

where Q_o is the intrinsic quadrupole moment (see Chap. 4 of Ref. 36) and the right-hand-side contains the usual *Clebsch-Gordon coefficient*. For deformed nuclei Q_o is large ; thus, enhanced transitions occur within a band. In general, for transitions between bands K_i and K_f , the branching ratios are given by [40]:

$$\frac{B(E2: J_i K_i \rightarrow J_f K_f)}{B(E2: J_i K_i \rightarrow J'_f K_f)} = \frac{\langle J_i K 2K_i - K_f | J_f K_f \rangle^2 M(K_i, K_f)}{\langle J_i K 2K_i - K_f | J'_f K_f \rangle^2 M(K_i, K_f)} \quad (2-14)$$

where the matrix element $M(K_i, K_f)$ only depends on the intrinsic structure of the bands and not on the particular states in question. This means that the branching ratio, commonly referred to as the *Alaga ratio*, from an initial state to two levels of the same rotational band only depends on the J and K of the various states and not on the intrinsic structure, since the same matrix element M appears in both numerator and denominator of Eq. (2-14).

(Note: this description only holds for $2 \leq K_i + K_f$. The cases when $K_i + K_f \leq 2$, or where multipolarities other than electric quadrupole are involved, are discussed in Ref. 40).

Davydov and coworkers [41, 42] have performed extensive investigations of the properties of nuclei with rigid asymmetric deformations. In their model, which consists of the Bohr Hamiltonian with a γ -dependent potential, the nucleus is described by γ and β , where γ may be determined by the energy of the 2_2^+ state. Unlike the case for a symmetric rotor, the 2_2^+ level and associated states are rotational excitations rather than members of a γ -vibration.

Vibrations can be added to this triaxial structure by introducing μ , the "non-adiabaticity" parameter [43]. The parameter μ is a measure of the importance of the rotation-vibration interaction. For $\mu < 1/3$ the distinction between rotations and vibrations is clear, while for $\mu > 1/3$, the nucleus is considered "soft" and the distinction is not as obvious. The definition of μ and the values for many nuclei are presented in Ref. [43]. It should be noted that only by introducing the non-adiabaticity parameter can excited 0^+ states be incorporated into the triaxial description.

A discussion of the Bohr Hamiltonian with a potential that is defined to be independent of γ was presented by Wilets and Jean [44]. A particular example of a γ -unstable potential is the displaced harmonic oscillator where [44]:

$$V(\beta) = \frac{1}{2}(\beta - \beta_o)^2 \dots \dots \dots (2-15)$$

One result of a γ -independent potential is that the Bohr Hamiltonian can be expressed by two equations, one that depends only on β and one that depends only on γ , with the separation parameter Λ given by [44]:

$$\Lambda = \tau(\tau + 3) \dots \dots \dots (2-16)$$

In conclusion, the model of Bohr and Mottelson can be used to describe a variety of nuclear shapes: spherical, non-spherical, symmetric and asymmetric. To these shapes odd nucleons may be coupled, as described in Ref. [45,46]. However, as presented here, the Bohr and Mottelson prescription is strictly phenomenological. The next section will present several attempts at a microscopic description of some of the ideas presented here.

2.2. MICROSCOPIC MODELS

As mentioned in the previous section, the actual shape of a nucleus in the macroscopic description arises from the competition between the effective short-range pairing interaction and long-range quadrupole interaction between nucleons. After a presentation of the formalism necessary in order to understand the pairing interaction which occurs in many models, several different attempts at generating the phenomenological properties of nuclei from a more fundamental basis will be discussed.

2.2.1. Pair-Coupling Scheme

The pairing interaction is strongest for a state in which the particles occupy the orbitals in pairs coupled to angular momentum zero, so that the entire state has angular momentum zero. All states for which a pair of particles are not coupled to angular momentum zero will occur much higher in energy. A convenient quantum number is the seniority, ν , which counts the number of particles not pair-wise coupled to spin zero. The pairing interaction, therefore, produces a large energy gap between the $\nu = 0$ 0^+ state and all states with $\nu \neq 0$. To simplify the discussion of the pairing force, the language of second quantization will be used, in which a shell model state will be written as $a_\nu^+ |0\rangle$, where a_ν^+ defines a creation operator operating on the vacuum $|0\rangle$. The single particle annihilation operator a_ν has the property $a_\nu^+ |0\rangle = 0$. This formalism is very common and the properties, such as commutation rules for the operators, will not be discussed here, but may be found in numerous references, such as Refs. [34, 47], and [48].

In this formalism, the pairing interaction in a single j shell with strength G is written as [34]:

$$V_{pair} = -G \sum_{\nu\omega} a_\nu^+ a_{-\nu}^+ a_{-\omega} a_\omega \dots \dots \dots (2-17)$$

which destroys a pair of particles in the ω orbit and creates a pair in the ν orbit, with the sum being performed over all ν and ω orbitals. However, in most nuclear systems, the single j shell approximation is not valid. With the method of *Bardeen, Cooper, and Schrieffer (BCS)* [49], the ground state wave function for a nucleus in the case of non-degenerate orbitals can be written in the form [34, 50]:

$$\Phi_0^{BCS} = \prod_{\nu} (U_\nu + V_\nu a_\nu^+ a_{-\nu}^+) |0\rangle \dots \dots \dots (2-18)$$

where the U_ν and V_ν are subject to [34]:

$$U_\nu^2 + V_\nu^2 = 1 \dots \dots \dots (2-19)$$

$$2 \sum_{\nu} V_\nu^2 = N \dots \dots \dots (2-20)$$

and N is the total number of particles.

To discuss the properties of excited states, it is simplest to transform from the single-particle to quasi-particle description of the individual nucleons, as first performed by Bogoliubov and Valatin [51, 52]. Here the correlated ground state of Eq. (2-18) is defined as the quasi-particle vacuum $|0^{\sim}\rangle$ and the quasi-particle operators α_v^+ and β_v^+ are related to the earlier single-particle operators a_v^+ , α_v via [34]:

$$\begin{aligned} \alpha_v^+ &= U_v a_v^+ - V_v a_{-v} \\ \beta_v^+ &= U_v a_{-v}^+ - V_v a_v \dots\dots\dots(2-21) \end{aligned}$$

with similar relations for the destruction operators. The quasi-particle vacuum is defined such that $a_v^+ |0^{\sim}\rangle = 0$.

The quasi-particle formalism does not guarantee the conservation of particles at all times. The probability, V_v^2 , that a state v will be occupied by a pair of quasi-particles is given by [34]:

$$V_v^2 = \frac{1}{2} [1 - (\varepsilon_v - \lambda) / E_v] \dots\dots\dots(2-22)$$

where

$$E_v = \sqrt{(\varepsilon_v - \lambda)^2 + \Delta^2} \dots\dots\dots(2-23)$$

$$\Delta = G \sum_v U_v V_v \dots\dots\dots(2-24)$$

Several quantities appear in these expressions: ε_v is the single-particle energy, which is related to the quasi-particle energy E_v via Eq. (2-23); λ is the energy of the Fermi surface; Δ , the gap parameter, determines the diffuseness of the Fermi surface.

Several consequences of Eq. (2-22) should be noted. The Fermi surface is no longer sharp, but states above the level determined by λ have a finite probability of being full and levels below λ have a finite probability of being empty. Therefore, the total number of particles in the ground state wave function given by Eq. (2-18) will only on the average correspond to a certain number of particles N .

Typically, the root-mean-square fluctuation in particle number is two or three [34]. Also, in even-even nuclei, where the simplest intrinsic excitation corresponds to the breaking of a pair, or the creation of two quasi-particles, the minimum energy, 2Δ , for such an excitation will occur when $\varepsilon = \lambda$. Therefore, the energy spectra of even-even nuclei will have a characteristic gap, the pairing gap, between the ground state and the first intrinsic excitation.

The gap parameter Δ can be determined in a number of ways. Since the ground state of an odd nucleus consists of one quasi-particle, while, obviously, the even-even ground state has none, the odd-even mass difference is one measure of Δ . One reasonable empirical definition of the odd-even mass difference for neutrons, $P_n(Z,N)$, is given by [48]:

$$P_n(Z, N) = \frac{1}{4} [-S_n(Z, N+1) + 2S_n - S_n(Z, N-1)] \dots\dots\dots(2-25)$$

where Z and N here are the proton and neutron numbers, respectively, and $S_n(Z,N)$ is the neutron separation energy, which is related to the total binding, $E(Z,N)$, by the formula

$$S_n(Z, N) = E(Z, N) - E(Z, N-1) \dots\dots\dots(2-26)$$

Analogous relations can be obtained for P_p , the proton odd-even mass difference.

Two quasi-particle excitations frequently occur at energies less than the value of 2Δ , as determined from odd-even mass differences. (The systematics of two quasi-particle excitations in the region $A = 150-190$ is shown in Figure 35 of Ref. [34]; frequently the lowest states occur at energies 10-15 percent below the energy predicted by $2P_n$ or $2P_p$). This effect is known as "blocking", because the quasi-particle excitation prevents the states involved in the excitation from participating in the correlated state. Several attempts at generating the empirical values of Δ have been made. The simplest understanding of how blocking effects contribute comes from examining the relevant form of Eq. (2-18) for a two quasi-particle excitation [48]:

$$\Phi_{\nu\omega} = a_{\nu}^{+} a_{-\omega}^{+} \prod_{\mu \neq \nu\omega} (U_{\mu} + V_{\mu} a_{\mu}^{+} a_{-\mu}^{+}) |0\rangle \dots\dots\dots(2-27)$$

Although the product in Eq. (2-27) does not include the ν and ω orbitals involved in the new state, the U and V are still the values obtained when no state is blocked. If one defines an effective number, Γ , of single particle orbits that contribute to the pairing energy as [34]:

$$\Gamma = \frac{2\Delta}{G} = 2 \sum_{\mu} U_{\mu} + V_{\mu} \dots\dots\dots(2-28)$$

one finds that a reduction of T due to a two quasi-particle excitation is equivalent to a reduced value of Δ , or alternate values of U and V . The calculations of Refs. [48] and [53] are able to reproduce the empirical reduction of the pairing gap, as observed for the lowest two quasi-particle states.

2.2.2. Pairing-Plus-Quadrupole Model (PPQ)

About 46 years ago Kumar and Baranger (**KB**) developed a Pairing-Plus-Quadrupole Model (**PPQ**) [54-57] in which they calculated the low-lying collective excitations in transitional nuclei. Until recently this model had been found very successful in reproducing many empirical quantities such as energy levels, $B(E2)$ values and quadrupole moments in the *W-Os-Pt* nuclei

The uniqueness of the Kumar and Baranger description is the coupling of microscopic techniques to a macroscopic problem. Kumar and Baranger begin with a generalized Bohr Hamiltonian [58]:

$$H = V(\beta, \gamma) T_{rot} + T_{vib} \dots\dots\dots(2-29)$$

where $V(\beta, \gamma)$ is the potential energy of deformation; T_{rot} the rotational kinetic energy is,

$$T_{rot} = \frac{1}{2} [I_1(\beta, \gamma) \omega_1^2 + I_2(\beta, \gamma) \omega_2^2 + I_3(\beta, \gamma) \omega_3^2] \dots\dots\dots(2-30)$$

and the vibrational kinetic energy, T_{vib} is written

$$T_{vib} = \frac{1}{2} B_{\beta\beta}(\beta, \gamma) \dot{\beta}^2 + B_{\beta\gamma}(\beta, \gamma) \dot{\beta} \dot{\gamma} + \frac{1}{2} B_{\gamma\gamma}(\beta, \gamma) \dot{\gamma}^2 \dots\dots\dots(2-31)$$

The three principal moments of inertia I_1, I_2, I_3 and the vibrational inertia parameters $B_{\beta\beta}, B_{\beta\gamma}, B_{\gamma\gamma}$ and B are chosen to be arbitrary functions of β and γ ; $\omega_1, \omega_2, \omega_3$ are the components of the angular velocity on the intrinsic axes. This form of the Hamiltonian is the most general that can be obtained, given the condition that the velocities can only occur to no higher order than quadratic [58].

Seven functions of β and γ appear in the Hamiltonian; $V(\beta, \gamma)$, the three moments of inertia I , and the three parameters B . Kumar and Baranger calculate the inertia parameters from a microscopic pairing-plus-quadrupole model based on the fully self-consistent time-dependent Hartree-Fock picture. The potential energy $V(\beta, \gamma)$ is

calculated using the Nilsson Model [45] single-particle energies and wave functions and a pairing force, incorporating the *BCS* techniques. The seven functions of the *KB* Hamiltonian are calculated numerically at every point in a large $\beta - \gamma$ mesh.

2.2.3. Dynamic Deformation Model (DDM)

The dynamic deformation model has been developed over many years starting from the Paring Plus Quadrupole model (*PPQ*) of Kumar and Baranger [57]. The *DDM* is an ambitious attempt to the collective spherical-transitional-deformed transitions and to span from the s-d shell to heavy nuclei using a microscopic theory of collective motion. No fitting parameters are required to obtain the data for a particular nucleus.

A full description of the *DDM* is given in reference [59] and references therein. Here we present only the results of our application of the new version [60] of the *DDM* to the tellurium isotopes.

The detailed formalism and early results may be found in Kumar *et al.*, [59] and Kumar [61]. Here we give briefly the main aspects of the model. The theory can be divided into two main parts: a microscopic derivation of a collective Hamiltonian, and a numerical solution of the Hamiltonian. The microscopic Hamiltonian is composed of a demoralized Nilsson-type single particle plus pairing and has the form:

$$H = H_{av} + V_{res} \dots \dots \dots (2-32)$$

Where

$$H_{av} = \frac{p^2}{2M} + \frac{1}{2} M \sum_{k=1}^3 \omega_k^2 \chi_k^2 + \hbar \omega_0 [\nu_{ls} l \cdot s + \nu_{ll} (l^2 - \langle l^2 \rangle_N)] \dots \dots \dots (2-33)$$

Combining all the various contributions together, the potential energy is written as:

$$V_{coll} = V_{DM} + \delta U + \delta V_{proj} + \delta E_{pair} \dots \dots \dots (2-34)$$

where δV_{proj} is a nine-dimensional projection correction introduced by Kumar [61]. The generalized cranking method is employed to derive the general expression for mass parameters $B_{\mu\nu}(\beta, \gamma)$ as used in the collective kinetic energy which can be written as:

$$T_{coll} = \frac{1}{2} \sum_{\mu\nu} B_{\mu\nu} \alpha'_\mu \alpha_\nu^* \dots \dots \dots (2-35)$$

This kinetic energy function is quantized by Pauli method.

The DDM code used for our calculation is a modified version of the latest DDM code which was developed for super-heavy nuclei. The single particle levels and the configuration space ($n = 0$ to 8) employed in the present calculation, as well as the deformation definition, are identical to those of Kumar *et al.*, [59]. The main virtues of the above approach (restoration of symmetries, unified treatment of spherical-transitional-deformed nuclei) have recently been combined with the main virtues of the Nilsson-

Strutinsky approach (large configuration space, no effective charges, applicability to fission isomers and barriers) in the Dynamic Deformation Model (**DDM**).

The GCM (general coordinate motion) wave function is written as [62]:

$$\Psi_{\alpha,I}(q) = \int \Phi_{\alpha}(q, \beta) f_{\alpha,I}(\beta) d\beta \dots \dots \dots (2-36)$$

where I is total nuclear angular momentum, α distinguishes states with the same I , q represents *all* the nucleonic variables, and β represents *all* the collective variables. The expectation value of the nuclear Hamiltonian H is then given by

$$\langle \alpha I | H | \alpha I \rangle = \iint d\beta' f_{\alpha}(\beta') h(\beta, \beta') f_{\alpha,I}(\beta) d\beta \dots \dots \dots (2-37)$$

where $h(\beta, \beta')$ is the expectation value of H with respect to the nucleonic variables. The "double" integral of Eq. (2-37) is replaced in the DDM by a "single" integral. The function $h(\beta, \beta')$ is expanded in the non-locality with respect to deformation,

$$h(\beta', \beta) = h_0(\beta) \delta(\beta' - \beta) + h_1(\beta) \delta''(\beta' - \beta) + h_2(\beta) \delta''(\beta' - \beta) + \dots \dots \dots (2-38)$$

The formal derivation has been given by Giraud and Grammaticos [63]. Although a complete derivation of the formalism used in the PPQ model or the DDM (or the cranking method combined with the Bohr Hamiltonian method) is not claimed, the conceptual connection is quite clear and precise, and is briefly the following: The h_0 term of Eq. (2-38) leads to the potential energy V of the collective Hamiltonian. The h_1 term vanishes because of the symmetry requirements. The h_2 term leads to the kinetic energy, $T = (1/2) \beta^{\bullet} \cdot B \cdot \beta$ of the collective Hamiltonian, where B is the mass-parameter-matrix. This matrix is given by:

$$B_{\mu,\nu} = \partial^2 T / (\partial \beta_{\mu}^{\bullet} \partial \beta_{\nu}^{\bullet}) = \partial^2 H / (\partial \beta_{\mu}^{\bullet} \partial \beta_{\nu}^{\bullet}) \dots \dots \dots (2-39)$$

The collective velocities β_{μ}^{\bullet} may represent β -vibrations, γ -vibrations, pair fluctuations, or rotational frequencies. The original cranking method of Inglis dealt with only one of these, the frequency of rotation around an axis perpendicular to the assumed symmetry axis or the nuclear spheroid. Then, the connection between the time-dependent Schrodinger equations in the laboratory system and in the intrinsic system gives the ω -dependence of the Hamiltonian, $H' = H - \omega J_x$. We generalize this to obtain [64]:

$$H' = H - \frac{\hbar}{i} \sum_{\mu} \beta_{\mu}^{\bullet} \frac{\partial}{\partial \beta_{\mu}} \dots \dots \dots (2-40)$$

Then, the second-order time-dependent perturbation theory gives the 'cranking' type of formulae for the mass-parameter-matrix $B_{\mu,\nu}$. Note that the following constraint conditions are satisfied automatically up to second order in β_{μ}^{\bullet} [62]:

$$\frac{\hbar}{i} \left\langle \frac{\partial}{\partial \beta_\mu} \right\rangle = \sum_\nu B_{\mu\nu} \dot{\beta}_\nu \dots \dots \dots (2-41)$$

These conditions include the traditional 'cranking' constraint, $\langle J_x \rangle = \Theta \omega$, as a special case.

In the current version of the DDM, the adiabatic approximation is made that the collective velocities/frequencies are small compared to those of the single-particle motion, that is [62]

$$\hbar \omega_{rot} \ll \hbar \omega_{sp} = 41A^{-1/3} \text{MeV} \dots \dots \dots (2-42)$$

$$\hbar \omega_{vib} \ll \hbar \omega_{sp} = 41A^{-1/3} \text{MeV} \dots \dots \dots (2-43)$$

However, this adiabatic approximation is far superior to that of the rotational model where some additional approximations are made ($\omega_{rot} \ll \omega_{vib}$, harmonic vibrations with amplitudes much smaller than the equilibrium deformation value). The rotation-vibration coupling is treated exactly in the DDM by avoiding any expansions around the equilibrium shapes, by calculating the potential and inertial functions microscopically for each point of a $\beta - \gamma$ mesh, and by solving the collective Schrodinger equation by numerical method [65,66,67].

2.2.4. Other Microscopic Models

In addition to the approaches discussed here, there have been many other attempts at understanding the microscopic structure of nuclear excitations away from closed shells. This section will briefly summarize some of these.

Bes and coworkers [68,69] have described the macroscopic β -and γ -vibrations in terms of the Nilsson excitations that generate them. Their method employs the BCS theory as described earlier, as well as the standard technique of the Random Phase Approximation (RPA) [70], to generate the energy spectrum and wave functions. An alternate description, in which a Woods-Saxon potential was employed, of these same excitations, as well as of the ground state wave functions, has been performed by Soloviev and collaborators [71].

Large scale numerical calculations have recently been performed by Kishimoto and Tamura [72,73]. They investigate the collective excitations that result from a boson expansion.

Calculations of energy spectra and transition probabilities for several nuclei, including ^{194}Pt , are presented in Ref. [46].

Obviously, not all microscopic models can be presented here. The summary has been restricted to those models which have had the most relevance to the Hf-W deformed nuclei. The end of the next section, which presents a new approach to understanding collective structures in nuclei, will describe an alternate means of understanding the microscopic foundations of collective excitations.

2.3. PHENOMENOLOGICAL MODEL

2.3.1. GROUP THEORETICAL MODEL -THE INTERACTING BOSON MODEL (IBM)

F. Iachello and A. Arima [74-79] have proposed a model which attempts to describe the collective structure of all nuclei with $A \geq 100$, except those near closed shells. The particles outside of closed shells are treated as bosons, or pairs of particles, which can

occupy one of two levels: a ground state with angular momentum equal to zero (called s-bosons) and an excited state with two units of angular momentum (called d-bosons) The d-bosons have energy ε_d , the s-bosons ε_s ; one can define a boson energy $\varepsilon = \varepsilon_d - \varepsilon_s$. Unlike the more familiar bosons, these bosons may interact with each other. Thus, the model has been called the Interacting Boson Model (IBM) . The total number of bosons, equal to the number of d-bosons plus the number of s-bosons, $N = n_d + n_s$, is a constant in the IBM prescription as for a given nucleus. N is the number of pairs of neutrons plus the number of pairs of protons, outside their respective nearest closed shells, without distinguishing between the particle or hole character of the pairs. For example, ${}^{130}_{56}\text{Ba}_{74}$ is characterized by $N = 7$, due to the 6 protons (3 proton pairs) + 8 neutrons (4 neutron pairs) away from the closed shell ${}^{208}_{82}\text{Pb}_{126}$. Alternatively, ${}^{164}\text{Er}$ would correspond to $N = 14$, because of the 14 neutron particles away from the 82 neutron closed shell and 14 proton holes away from the 82 proton closed shell.

As stated earlier, interactions between the s-and d-bosons, and among the s- or d-bosons themselves, may occur. Therefore, in the simplest terms, the Hamiltonian of the system can be written as [80]:

$$H = \varepsilon_s s^+ s + \varepsilon_d \sum_m d_m^+ d_m + V \dots\dots\dots(2-44)$$

where ε_s and ε_d , are the s-and d-boson energies, s^+ (s) is the creation (annihilation) operator for s-bosons, d^+ (d) is the creation (annihilation) operator for d-bosons, the sum is taken over the 5 ($2(L=2) + 1$) components of the d-boson state, and V is the interaction(s) between the bosons.

In this description three natural limits occur. The first [74,78] occurs when $\varepsilon = \varepsilon_d - \varepsilon_s \gg V$, so that the energy spectrum is simply given by $E = \varepsilon n_d$, the ground state being a C_L zero d-boson state. This first limit is similar to the harmonic oscillator of the geometrical picture described in section (2.1.1) of this chapter. The IBM interpretation will be discussed later . The other two limits occur when $V \gg \varepsilon$, and correspond to specific interboson interactions. If V is a quadrupole-quadrupole interaction [75,79] between bosons, the system obtained is very similar to a certain kind of deformed rotor. The IBM version will be presented in section (2.1.2). The third limit arises when a repulsive pairing interaction [76] exists between the bosons. As will be seen in the discussion of section (2.1.3), this limit is very-similar to the geometrical description of the γ -unstable oscillator of Wilets and Jean [44].

The most general form of the IBM Hamiltonian, in which all possible boson-boson interactions up to second order are explicitly included, is given by [78]:

$$\begin{aligned}
H = & \varepsilon_s s^+ s + \varepsilon_d \sum_m d_m^+ d_m + \sum_{J=0,2,4} \frac{1}{2} (2J+1)^{\frac{1}{2}} c_J [(d^+ d^+)^{(J)} d d^{(J)}]^{(0)} \\
& + \frac{1}{2} \frac{1}{2} v_2 [(d^+ \times d^+)^{(2)} \cdot (d \times s)^{(2)} + (s^+ \times d^+)^{(2)} \cdot (d \times d)^{(2)}]^{(0)} \\
& + \frac{1}{2} v_0 [(d^+ \times d^+)^{(0)} \cdot (s \times s)^{(0)} + (s^+ \times s^+)^{(0)} \cdot (d \times d)^{(0)}]^{(0)} \dots\dots\dots(2-45) \\
& + \frac{1}{2} u_2 [(d^+ \times s^+)^{(2)} \cdot (d \times s)^{(2)}]^{(0)} + \frac{1}{2} u_0 [(s^+ \times s^+)^{(0)} \cdot (s \times s)^{(0)}]^{(0)}
\end{aligned}$$

where d^+ , d , s^+ , s , are as described for Eq.(2-44) and the parentheses denote angular momentum couplings. The parameters C_J , V_J , u_J are related to the two-body matrix elements by [78]:

$$\begin{aligned}
 C_J &= \langle d^2 J | V | d^2 J \rangle \\
 v_2 &= \langle ds 2 | V | d^2 2 \rangle (5/2)^{1/2} \\
 v_0 &= \langle d^2 0 | V | s^2 0 \rangle (1/2)^{1/2} \dots\dots\dots(2-46) \\
 u_2 &= \langle ds 2 | V | ds 2 \rangle 5^{1/2} \\
 u_0 &= \langle s^2 0 | V | s^2 0 \rangle
 \end{aligned}$$

The IBM-1 Hamiltonian (Eq. (2-45) can be written in general form as [79] :

$$H^\wedge = \varepsilon(n_s^\wedge + n_d^\wedge) + a_0 P^\wedge . P^\wedge + a_1 L^\wedge . L^\wedge + a_2 Q^\wedge . Q^\wedge + a_3 T_3^\wedge . T_3^\wedge + a_4 T_4^\wedge . T_4^\wedge \dots\dots\dots(2-47)$$

where ε is the boson energy, and the operators are:

$$\begin{aligned}
 n_s^\wedge &= s^{\wedge+} . s^{\wedge-} \quad , \quad n_d^\wedge = d^{\wedge+} . d^{\wedge-} \quad , \quad P^\wedge = \frac{1}{2}(d^{\wedge-} . d^{\wedge+}) - \frac{1}{2}(s^{\wedge+} . s^{\wedge-}) \\
 L^\wedge &= \sqrt{10}[d^{\wedge+} \times d^{\wedge-}]^{(1)} \quad , \quad Q^\wedge = \sqrt{5}[(d^{\wedge+} \times s^{\wedge-}) + (s^{\wedge+} \times d^{\wedge-})]^{(2)} + \chi[d^{\wedge+} \times d^{\wedge-}] \\
 T_3^\wedge &= [d^{\wedge+} \times d^{\wedge-}]^{(3)} \quad , \quad T_4^\wedge = [d^{\wedge+} \times d^{\wedge-}]^{(4)} \dots\dots\dots(2-48)
 \end{aligned}$$

The phenomenological parameters $a_0, a_1, (a_2, \chi), a_3, a_4$, represents the strengths of the pairing angular momentum, quadrupole, octupole and hexadecapole interaction between bosons, respectively.

Eq.(2-45) appears formidable, especially given the explicit form of the parameters, as introduced in Eq. (2-46). However, the terms correspond to one of four types:

- 1) $\varepsilon_s s^+ s + \varepsilon_d \sum d_m^+ d_m$ - simply counts the number of s-and d-bosons, respectively, and multiplies this number by the appropriate energy;
- 2) the terms with coefficients C_J , u_2 and u_0 represent interactions in which the total number of d-bosons and s-bosons, separately, are conserved, i.e., n_d , is not changed;
- 3) a term (with coefficient v_2) in which n_d , is changed by unity;
- 4) a term (with coefficient v_0) in which n_d is changed by two units.

Returning to the three limits alluded to earlier, the vibrational limit will correspond to a Hamiltonian with only n_d - conserving terms, the rotational limit to a situation with one and two d-boson number changing terms, and the " γ -unstable" limit

will represent the situation with two d-boson number changing terms included.

An alternate form, in which the general Hamiltonian may be frequently written, is in terms of the specific interactions between the bosons. In these cases [78,80]:

$$H = \varepsilon \sum_m d_m^+ d_m - \kappa \sum_{ij} \vec{Q}_i \cdot \vec{Q}_j - \kappa' \sum_{i<j} L_{ij} - \kappa'' \sum_{i<j} P_{ij} \dots\dots\dots(2-49)$$

where \vec{Q}_i is the quadrupole moment of the i^{th} boson, $L_{ij} = 2\vec{\ell}_i \cdot \vec{\ell}_j$ with $\vec{\ell}_i, \vec{\ell}_j$ being the angular momenta of the i^{th} and j^{th} boson, respectively, P_{ij} is the pairing operator, between bosons, and $\kappa, \kappa', \kappa''$ are the respective strengths of the different interactions. For simplicity, was set equal to zero, so that only $\varepsilon = \varepsilon_d - \varepsilon_s = \varepsilon_d$ appears in Eq.(2-49).

Associated with the collective states calculated with the IBM are transition operators. In the most general form, the E0, M1, E2, M3, E4 transition operators are, to leading order, given [78,79,81]:

$$T_m^{(\ell)} = \alpha_\ell \delta_{\ell 2} (d^+ s + s^+ d)_m^{(2)} + \beta_\ell (d^+ d)_m^{(\ell)} + \gamma_{10} \delta_{10} \delta_{m0} (s^+ s)_0^{(0)} \dots\dots\dots(2-50)$$

where l denotes the multipolarity with projection m , and α, β, γ are the coefficients of the different terms of the operator. In particular, for E2 transitions [78,79,81]:

$$T_m(E2) = \alpha_2 (d^+ s + s^+ d)_m^{(2)} + \beta_2 (d^+ d)_m^{(2)} \dots\dots\dots(2-51)$$

This operator has two parts: which satisfies the selection rule, and which satisfies the selection rule. The coefficients and depend on the limit involved or the appropriate intermediate structure. The form of the operator that corresponds to the various limiting symmetries will be discussed later.

Exact forms of the E0, M3, and E4 operators exist. It should be noted that *no M1 transitions can occur* in first order [78,79,81]. The reasons lie in the form of the M1 operator [78,79,81]:

$$T_m(M1) = \beta_1 (d^+ d)_m^{(1)} \dots\dots\dots(2-52)$$

As discussed in references [51,52,54], the operator $(d^+ d)^{(1)}$ proportional to the boson angular momentum operator; therefore, Eq.(2-52) may be rewritten as

$$T_m(M1) = g_B I_m^{(1)} \dots\dots\dots(2-53)$$

where g_B is the effective boson g -factor. This form of the operator has no off-diagonal matrix elements, implying that in this approximation M1 transitions are forbidden [78,79,81]. Some of the transition probabilities obtained from perturbation theory are further discussed in Refs. [78] and [79].

The solution of the Hamiltonian, in either the Eq.(2-45) or the Eq.(2-53) form, may be attempted either analytically or numerically. Arima and Iachello [74,75,76] have been able to solve the Hamiltonian analytically in the three -limiting situations described earlier by utilizing the underlying group theoretic aspects of this system. As discussed in Ref. [78], the five components of the $L = 2$ d-boson state and the single component of the $L = 0$ s-boson state span a linear vector space which provides a basis for the totally symmetric representations of the group $SU(6)$, the special unitary group in six dimensions. The group $SU(6)$ is partitioned, with each totally symmetric representation labeled by $[N]$. For a situation where all boson states are degenerate and no boson-boson interaction exists, all states belonging to a particular partition $[N]$ are degenerate. However, given the energy

difference $\varepsilon = \varepsilon_d - \varepsilon_s$ and an interaction between the bosons, a definite energy level spectrum will exist. The group $SU(6)$ is characterized by nine parameters which will correspond to the parameters of Eq.(2-45), i.e., N , ε , and the coefficients $C_J (J = 0, 2, 4), v_2, v_0, u_2, u_0$.

The E0 operator can be written directly as:

$$T^\wedge(E0) = \beta_0(d^+d^-) + \gamma_0(s^+s^-) \dots \dots \dots (2-54)$$

where β_0 and γ_0 are free parameters and the superscript notation indicates spherical tensor coupling. Eq. (2-54) can be expressed in terms of the boson number operators n_s^\wedge ; n_d^\wedge and $N^\wedge = (n_s^\wedge + n_d^\wedge)$ as [78]:

$$T^\wedge(E0) = \beta_0^\sim n_d^\wedge + \gamma_0 n_s^\wedge = \gamma_0 N^\wedge + \beta_0^\sim n_d^\wedge = \beta_0' N^\wedge + \gamma_0' n_s^\wedge \dots \dots \dots (2-55)$$

where

$$\beta_0' = \frac{\beta_0}{\sqrt{5}}, \quad \beta_0^\sim = \beta_0' - \gamma_0, \quad \gamma_0^\sim = \gamma_0 - \beta_0' \dots \dots \dots (2-56)$$

The IBM-1 possesses simple limiting dynamical symmetries which lead to closed form expressions for the matrix elements of $T^\wedge(E0)$ and, consequently, to selection rules [78]. We deal with the three limiting cases, $U(5)$, $SU(3)$, and $O(6)$, separately.

The isomer shift, $\delta < r^2 >$ is measure in r^2 between the first 2^+ state and the ground state,

$$\delta < r^2 > = \beta_0^\sim \left[\langle n_d^\wedge \rangle_{2^+}^{(N)} - \langle n_d^\wedge \rangle_0^{(N)} \right] \dots \dots \dots (2-57)$$

The isotope (isotone) shifts $\Delta < r^2 >$, are measure of difference in radii between nuclei one neutron (or proton) pair (one boson) away from each other,

$$\Delta < r^2 >^{(N)} = \langle r^2 \rangle_{0^+}^{(N+1)} - \langle r^2 \rangle_{0^+}^{(N)}$$

$$\Delta < r^2 >^{(N)} = \gamma_0^\sim + \beta_0^\sim \left[\langle r^2 \rangle_{0^+}^{(N+1)} - \langle r^2 \rangle_{0^+}^{(N)} \right] \dots \dots \dots (2-58)$$

If one can find a subgroup $G \subset SU(6)$ under which the Hamiltonian is invariant, then the diagonalization problem is simplified. In particular, Arima and Iachello have observed that there are three such groups, namely $SU(5)$ [74,78], $SU(3)$ [75,79], and $O(6)$ [76], the special unitary groups in five and three dimensions, and the orthogonal group in six dimensions. The solutions obtained correspond to the same three limits mentioned earlier, the vibrational, rotational, and " γ -unstable" limits, respectively.

Frequently, when the subgroup G under which the Hamiltonian is invariant has been identified, the problem may be written in terms of the forces as given in Eq. (2-45). Then the eigenvalue problem is reduced to finding the expectation value of the forces. This method of solution in the different limits will be discussed in their separate subsections.

An alternative approach to the eigenvalue problem presented in Eq. (3-45) or Eq. (2-49) is to solve the Hamiltonian numerically. This has advantages in that the entire Hamiltonian may be solved, not only in the limits for which analytic solutions are readily

obtainable, but also in the intermediate cases. To this end, O. Scholten has written a computer code *PHINT* [82] which solves the entire IBM Hamiltonian in the Eq. (2-45) or Eq. (2-47) parameterization, or a convenient mixture of the two forms.

The computer code presents the wave functions in the basis $J^\pi |n_d n_\beta n_\Delta\rangle$ where J^π is spin-parity, n_d is the number of d-bosons. n_β is the number of pairs of d-bosons coupled to angular momentum zero, and n_Δ is the number of triplets of bosons coupled to angular momentum zero. For example, the 2 d-boson 0^+ state would be denoted $0^+|210\rangle$; the 3 d-boson 0^+ state would be $0^+|310\rangle$; the 3 d-boson 2^+ state would be $2^+|310\rangle$, because the parentage of this state is the $2^+|210\rangle$.

Calculations have been performed with this code to reproduce a number of different situations:

- 1) calculations of the three limiting symmetries which reproduce the analytic solutions;
- 2) calculations of systematic deviations from these limiting cases;
- 3) calculations of, not necessarily physical, situations to understand the operation and interplay of the different parameters contained in the IBM.

The first case will be discussed in subsections (2.3.2.1), (2.3.2.2) and (2.3.2.3). However, since an understanding of the effect of the parameters is essential to the later discussions, the third aspect will be discussed here.

It is more convenient to discuss the forces of the IBM in terms of the parameterization of Eq.(2-49), where the variables are ε , the boson energy, and the strengths of the quadrupole- quadrupole, $\vec{\ell}_i \cdot \vec{\ell}_f$, and pairing interactions between the bosons.

To summarize this section, the IBM model developed by Iachello and Arima aims to predict the structure of collective states of heavy even-even nuclei. This model can be analytically solved for the case of three limiting symmetries; these will be discussed in the next three sections. The model can also be solved numerically with the computer code *PHINT* [82]. A discussion of the transition between the limits will be presented in next section.

2.3.1.1- The Vibrational $SU(5)$ Symmetry

The first limiting symmetry of the IBM to be discussed was the vibrational limit [74,78]. As described in the last section, a very simple spectrum of collective states, presented in **Figure (2. 1)**, arises from a system characterized by a boson energy ε . This limit corresponds to the $O(5)$, orthogonal group in 5 dimensions, symmetry. However, the IBM Hamiltonian can also be solved analytically for the $SU(5)$ representation [74,78].

The form of the Hamiltonian in this limit is given by [74,78]:

$$H = \varepsilon \sum_m d_m^\dagger d_m + \sum_J \frac{1}{2} (2J+1)^{\frac{1}{2}} C_J \left[(d^\dagger d^\dagger)^{(J)} \cdot (dd)^{(J)} \right]^{(0)} \dots\dots\dots(2-59)$$

where the C_J 's are given in Eq. (2-46). An analytic solution to this Hamiltonian is presented in detail in Ref. [78]. For the reader's information, the arguments of Arima and Iachello will be repeated here.

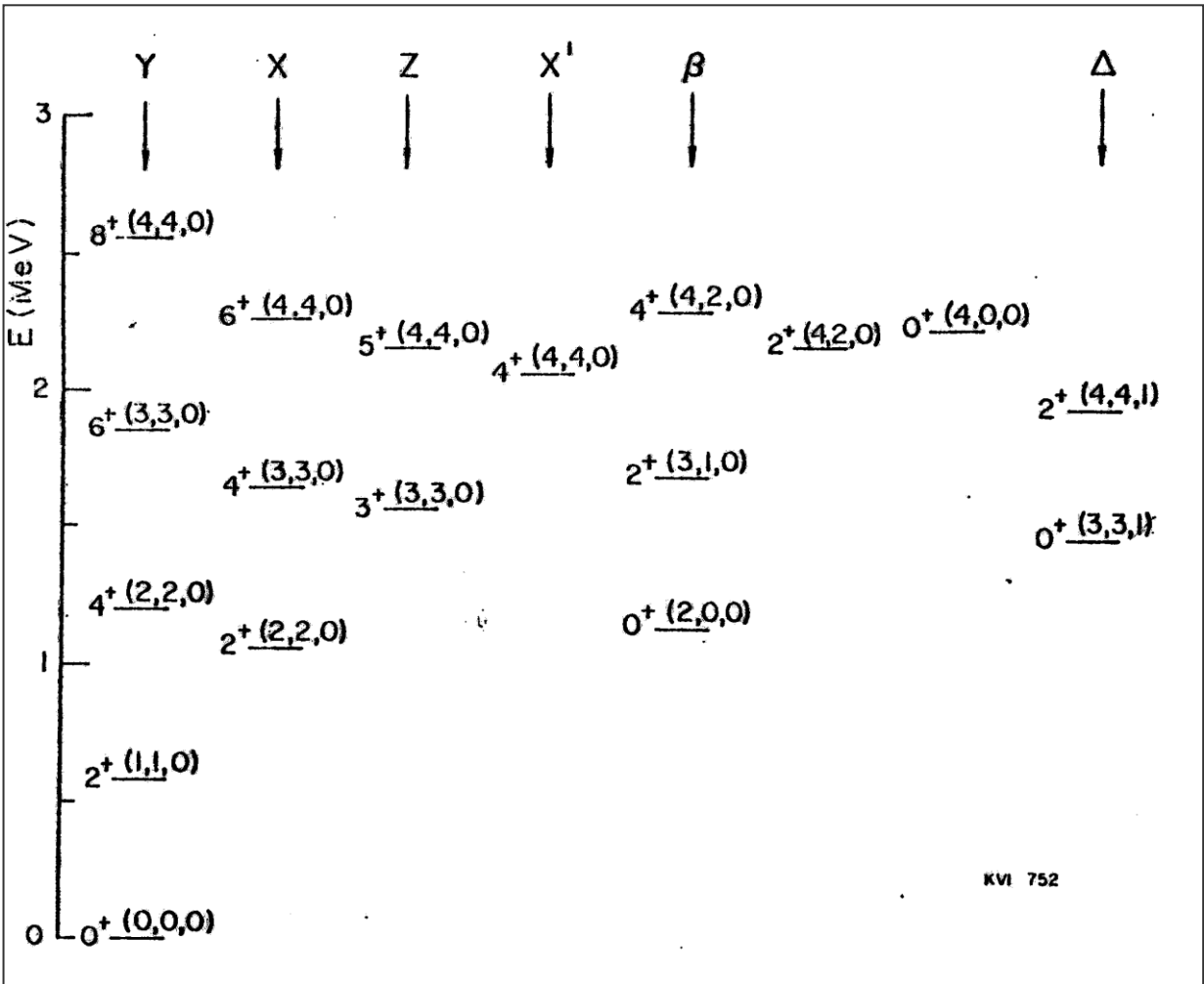


Figure (2.2) Typical spectrum of a nucleus exhibiting the SU(5) symmetry. The states are labeled by the quantum numbers $J^\pi(n_d, \nu, n_A)$. The spectrum is broken up into a number of bands [78]

The eigenvalue equation may be expressed as

$$H|n_d \nu n_A JM\rangle = E|n_d \nu n_A JM\rangle \dots\dots\dots(2-60)$$

where H is given by Eq.(2-59) and the states are labelled by the quantum numbers n_d, ν, n_A, J, M . The number of d-bosons, n_d , the angular momentum J and its projection M are already familiar; n_d , as discussed earlier, is the number of d-boson triplets coupled to angular momentum zero, and ν is the seniority, which counts the number of d-bosons not coupled to angular momentum zero. An alternate representation involves the quantum number n_β , which counts the number of d-boson pairs coupled to angular momentum zero; ν and n_β are related by $\nu = n_d - 2n_\beta$. The total number of bosons is partitioned as [78]:

$$n_d = 2n_\beta + 3n_\Delta + \lambda \dots\dots\dots(2-61)$$

where λ is the excess bosons and determines the angular momentum range [78]:

$$J = 2\lambda, 2\lambda - 2, 2\lambda - 3, \dots, \lambda + 1, \lambda \dots\dots\dots(2-62)$$

The angular momentum $J = 2\lambda - 1$ is absent because of the requirement that bosons may only be coupled to form symmetric states [37].

An alternate method of solving the Hamiltonian in Eq. (2-59) is to rewrite it in terms of the forces presented earlier in Eq. (2-49). Only three parameters are necessary to describe the interaction between two d -bosons because only three angular momentum couplings can occur [37]: $J = 0, 2, 4$. Therefore, the coefficients $C_J (J = 0, 2, 4)$ in Eq. (2-59), or three alternate parameters α, β, γ , are necessary. Iachello and Arima have expressed the interaction as [78]:

$$V = \sum_{i < j} V_{ij} = \sum_{i < j} (\alpha l_{ij} + \beta P_{ij} + \gamma L_{ij}) \dots\dots\dots(2-63)$$

where l_{ij} is the unit operator, and P_{ij} and L_{ij} are the pairing and L interactions discussed earlier in section 1. The expectation values of these operators, as given in Ref. [78], are:

$$\begin{aligned} \langle 1 \rangle &= \frac{1}{2} n_d (n_d - 1) && \dots\dots\dots(2-64) \\ \langle L \rangle &= J(J + 1) - 6n_d \\ \langle P \rangle &= (n_d - \nu)(n_d + \nu + 3) \end{aligned}$$

Therefore, the eigenvalue of interacting d -boson Hamiltonian are [74,78]:

$$\begin{aligned} E([N], n_d, \nu, n_\Delta, J, M) &= \epsilon n_d + \alpha \frac{1}{2} n_d (n_d - 1) \\ &+ \beta (n_d - \nu)(n_d + \nu + 3) && \dots\dots\dots(2-65) \\ &+ \gamma [J(J + 1) - 6n_d] \end{aligned}$$

A typical spectrum in the vibrational limit is presented in **Figure (2.1)**. The spectrum may be divided into several "bands"; this terminology is valid since large E2 matrix elements exist between adjacent members of the same band. The states in **Figure (2.1)** are labelled by the quantum numbers n_d, ν, n_Δ . The "bands" are very reminiscent of those occurring in rotational nuclei. The Y -band corresponds to the ground band, X and Z to a γ -vibrational band, β to a β -vibrational band and Δ to a 2-phonon γ -vibrational band. The energies of states in some of these bands are given by [78]:

$$\begin{aligned} \mathbf{Y\ band} \quad E_Y(n_d, n_d, 0, J = 2n_d, M) &= \epsilon n_d + \frac{1}{2} C_4 n_d (n_d - 1) \\ \mathbf{X\ band} \quad E_X(n_d, n_d, 0, J = 2n_d - 2, M) &= \epsilon n_d + \frac{C_4}{2} n_d (n_d - 1) - \gamma(8n_d - 2) \\ \mathbf{Z\ band} \quad E_Z(n_d, n_d, 0, J = 2n_d - 3, M) &= \epsilon n_d + \frac{C_4}{2} n_d (n_d - 1) - \gamma(12n_d - 6) \\ \mathbf{\beta\ band} \quad E_\beta(n_d, n_d - 2, 0, J = 2n_d - 4, M) &= \epsilon n_d + \frac{C_4}{2} n_d (n_d - 1) + \gamma(12n_d - 16n_d) + \beta(4n_d + 1) \\ \mathbf{\Delta\ band} \quad E_\Delta(n_d, n_d, 1, J = 2n_d - 6, M) &= \epsilon n_d + \frac{C_4}{2} n_d (n_d - 1) - 6\gamma(4n_d - 5) \dots\dots\dots(2-66) \end{aligned}$$

The general form of the electric quadrupole transition operator $T(E2)$ was given in Eq. (2-51). In the limits for which analytic solutions are obtainable, Arima and Iachello require the transition operator to be a generator of the underlying group. For the limit characterized by $SU(5)$, $T(E2)$ is given by [78]:

$$T_m(E2) = \alpha (d^+ s + s^+ d)_m^{(2)} \dots \dots \dots (2-67)$$

for $\alpha = \langle d \| \bar{Q} \| s \rangle (\frac{1}{5})^{(2)}$, where \bar{Q} is the quadrupole operator. This form of the operator leads to the selection rule $\Delta n_d = \pm 1$.

2.3.1.2- The Rotational SU(3) Symmetry

The second limit of the IBM model is based on the $SU(3)$ group and gives rise to nuclear structures similar to a certain form of the symmetric rotor. This symmetry occurs when there is a dominant quadrupole-quadrupole interaction between bosons, as described in subsection (2.1.1). The most general form of the interboson interaction will also include a term of the form $L = l_i^{\rightarrow} \cdot l_j^{\rightarrow}$.

In Eq. (2-44), the entire IBM Hamiltonian was presented. Many years ago Elliott [83] showed that if a Hamiltonian could be expressed in terms of the generators of a group, in particular $SU(3)$, the special unitary group in three dimension, the eigenvalue problem [79, 82]:

$$H = -\kappa \sum Q_i^{\rightarrow} \cdot Q_j^{\rightarrow} \dots \dots \dots (2-68)$$

where \bar{Q}_i is the quadrupole operator of particle i and κ is the strength of the quadrupole-quadrupole interaction.

The solution of Eq. (2-68) is presented in Ref. [79]. Some of the results will be repeated here. The eigenvalue equation becomes [79]:

$$H|[N](\lambda, \mu)KJM\rangle = E|[N](\lambda, \mu)KJM\rangle \dots \dots \dots (2-69)$$

where $[N]$ labels the totally symmetric representations of $SU(6)$; (λ, μ) are two quantum numbers which label the representations of $SU(3)$; and J, M are the angular momentum and its projection along the z-axis, respectively. The additional quantum number K labels states having the same λ, μ, J . In this basis, the eigenvalues can be written [79]:

$$E([N](\lambda, \mu)KJM) = K(J(J+1) - C(\lambda, \mu)) \dots \dots \dots (2-70)$$

where $C(\lambda, \mu)$ is quadratic Casimir operator of $SU(3)$ [79]:

$$C(\lambda, \mu) = \lambda^2 + \mu^2 + \lambda\mu + 3(\lambda + \mu) \dots \dots \dots (2-71)$$

As mentioned earlier, the addition of the L interaction does not change the diagonalization problem. Therefore, in its most general form, the Hamiltonian becomes [79]:

$$H = -\kappa \sum_{i,j} \bar{Q}_i \cdot \bar{Q}_j - \kappa' \sum_{i,j} \bar{\ell}_i \cdot \bar{\ell}_j \dots \dots \dots (2-72)$$

with the eigenvalues [79]:

$$E([N](\lambda, \mu)KJM) = \alpha J(J+1) - \beta C(\lambda, \mu) \dots \dots \dots (2-73)$$

$$\alpha = \frac{3}{4} \kappa - \kappa', \beta = \kappa$$

Due to their importance in predicting the level spacings of deformed nuclei, the parameters (λ, μ) will be discussed here in terms of the Young Tableaux [37] they represent. Each particle can be represented by a box; boxes may be coupled to form symmetric or antisymmetric states. Examples of the different symmetries are in Refs. [84,85]: For bosons, the antisymmetric couplings are not permitted. An N boson state will be of the form

The spectrum is divided into a number of bands according to the (λ, μ) value. The angular momenta J which may occur in each (λ, μ) group are given by [78]:

$$J = K, (K+1), \dots, (K + \max\{\lambda, \mu\}) \dots \dots \dots (2-74)$$

where $K = \text{integer} = \min\{\lambda, \mu\}, \min\{\lambda, \mu\} - 2, \dots, 1$ or 0 unless $K = 0$. For $K = 0$, the allowed angular momentum values are [78]:

$$J = \max\{\lambda, \mu\}, \max\{\lambda, \mu\} - 2, \dots, 1 \text{ or } 0 \dots \dots \dots (2-75)$$

The quantum number K is analogous to the K quantum number of a symmetric rotor, namely the projection of the angular momentum J along the nuclear symmetry axis. Therefore, the $K = 0$ and $K = 2$ bands of the $(N-4, 2)$ representation would correspond to the β and γ bands, respectively, in the geometrical rotor description of section A. However, in this limit of the IBM, states with the same angular momentum and (λ, μ) representation are required to be degenerate; eg., the 2^+_{β} and 2^+_{γ} states. Also, the transition probabilities between bands are considerably altered, as will be discussed below.

The most general form of the $E2$ transition operator $T(E2)$ was presented in Eq. (2-51). As for the earlier SU(5) symmetry, Arima and Iachello require this operator to be a generator of the underlying group symmetry. For the case of the SU(3) symmetry, since the operators of Eq. (2-51), namely d^+s and d^+d are already generators of the group [78], the requirement reduces to fixing the values, of the coefficients α_2 and β_2 in Eq. (2-51). The resulting $E2$ operator in the SU(3) symmetry is [78]:

$$T_m(E2) = \alpha_2 \left[(d^+s + s^+d)_m^{(2)} - \frac{1}{2} \sqrt{7} (d^+d)_m^{(2)} \right] \dots \dots \dots (2-76)$$

where α_2 is the effective E2 charge; β_2 of Eq. (2-51) became $-\frac{1}{2} \sqrt{7} \alpha_2$.

Due to the form of the $E2$ operator $T(E2)$ in Eq.(2-76) does not connect states with different (λ, μ) representations [79]. Thus, transitions between the γ -band or β -band and the ground band are **forbidden**. Conversely, transitions between states of the same

representation are allowed. Therefore, unlike the predictions of the geometrical rotational model, the 2^+_γ state will preferentially decay to the 0^+_β state rather than to the 0^+_g state.

A number of regions of the periodic table have shown evidence of exhibiting a rotational structure characterized by a $J(J+1)$ level sequence. However, the requirement of degenerate β - and γ -vibrations tends to limit the regions of $SU(3)$ symmetry to those where the onset of prolate deformation is occurring, such as the Gd isotopes.

$$B(E2; J+2 \rightarrow 2) = \alpha_2^2 \frac{3}{4} \frac{(J+2)(J+1)}{(2J+3)(2J+5)} (2N-J)(2N+J+3) \dots \dots \dots (2-77)$$

Eq. (2-77) shows that all transition probabilities depend explicitly upon the number of valence nucleons. Now that two limiting symmetries have been presented, the $SU(5)$ and $SU(3)$ limits, it would be interesting to investigate the transition between these two regions. Such work has recently been conducted by F. Iachello, O. Scholten, and A. Arima. In this investigation, they considered a simpler form of the IBM Hamiltonian in Eq. (2-45), namely [86]:

$$H = \epsilon n_d - \kappa \sum_{i,j} \bar{Q}_i \cdot \bar{Q}_j - \kappa' \sum_{i < j} L_{ij} \dots \dots \dots (2-78)$$

where ϵ , the boson energy, and the quadrupole-quadrupole and L interactions are as previously described. To study a transitional region, they fixed κ and κ' , allowing to linearly decrease as a function of the number of bosons [86]:

$$\epsilon = \epsilon_c - \theta N_v \dots \dots \dots (2-79)$$

where ϵ_c is a constant and N_v is the number of neutron bosons. This will simulate the transition, since, near $SU(5)$, ϵ is much greater than any interboson interaction, while, near $SU(3)$, the quadrupole-quadrupole interaction dominates the boson energy.

2.3.1.3- The Gamma Unstable $O(6)$ Symmetry

A third limiting symmetry of the IBM model will occur when the interboson interaction is dominated by a pairing force [76].

Analogous to the $SU(5)$ and $SU(3)$ symmetries, Iachello and Arima have diagonalized the IBM Hamiltonian, generated by $SU(6)$ (Eq. (2-45), by identifying a subgroup of $SU(6)$ under which the Hamiltonian is invariant. In this case, the subgroup is $O(6)$ which also contains the subgroups $O(5)$ and $O(3)$. By using the group chain, $SU(6) \supset O(6) \supset O(5) \supset O(3)$, the IBM Hamiltonian in the $O(6)$ limit can be written as:

$$H = AP_6 + BC_5 + CC_3 \dots \dots \dots (2-80)$$

where P_6 is the pairing operator in $O(6)$ and C_5 and C_3 are the Casimir operators of $O(5)$ and $O(3)$, respectively. A , B , and C are the strengths of the various components. In terms of the IBM Hamiltonian of Eq. (2-45), corresponds to the term:

$$v_0 \left[(d^+ d)^{(0)} (ss)^{(0)} + (s^+ s^+)^{(0)} (dd)^{(0)} \right]^{(0)} \dots \dots \dots (2-81)$$

while C_5 and C_3 and correspond to the terms

$$\varepsilon \sum_m d_m^+ d_m + \sum_{J=0,2,4} \frac{1}{2} (2J+1)^{\frac{1}{2}} C_J \left[(d^+ d^+)^{(J)} (dd)^{(J)} \right]^{(0)} \dots\dots\dots(2-82)$$

The symmetric irreducible representations of $O(6)$ are labelled by a quantum number σ where [76]:

$$\sigma = N, N-2, N-4, \dots, 0 \text{ or } 1 \text{ for } N = \text{even or odd} \dots\dots\dots(2-83)$$

expectation value of the $O(6)$ pairing operator, P_6 , can be written in terms of σ as [76]:

$$\langle P_6 \rangle = \frac{1}{4} (N - \sigma)(N + \sigma + 4) \dots\dots\dots(2-84)$$

As stated in Ref. [76], the quantum number τ is chosen to characterize the representations of $O(5)$ where

$$\tau = \sigma, \sigma-1, \dots, 0 \dots\dots\dots(2-85)$$

The expectation value of C_5 in the τ representation of $O(5)$ is given by [76]:

$$\langle C_5 \rangle = \frac{1}{6} \tau(\tau + 3) \dots\dots\dots(2-86)$$

Therefore, the eigenvalues of states corresponding to the Hamiltonian in Eq. (2-80) are [76]:

$$E([N] \sigma \tau \nu_\Delta JM) = \frac{A}{4} (N - \sigma)(N + \sigma + 4) + B \tau(\tau + 3) + C J(J + 1) \dots\dots\dots(2-87)$$

where the $1/6$ in Eq. (2-86) has been incorporated into the constant B. The quantum number ν_Δ is useful in labelling the states: it is related to n_Δ , which counts the number of boson triplets coupled to angular momentum zero. The quantum numbers τ and ν_Δ are related by $\tau = 3\nu_\Delta + \lambda$ for $\nu_\Delta = 0, 1, \dots$. The value of λ determines the angular momentum of states via [76]:

$$J = 2\lambda, 2\lambda-2, 2\lambda-3, \dots, \lambda+1, \lambda \dots\dots\dots(2-88)$$

Arima and Iachello have also succeeded in obtaining analytic expressions for transition probabilities [76]. As in the $SU(5)$ and $SU(3)$ symmetries, they require the $E2$ transition operator, $T(E2)$, to be a generator of the underlying group structure, in this case

O(6). The form of T(E2) satisfying this requirement is [76]:

$$T(E2) = \alpha(d^+s + s^+d)^{(2)} \dots\dots\dots(2-89)$$

Since T(E2) is a generator of O(6), it cannot connect states from different representations; therefore, one selection rule is $\Delta\sigma = 0$. Also, due to the O(5) structure contained in O(6), the O(5) selection rule $\Delta\tau = \pm 1$ still holds. Several closed form expressions for B(E2) values for transitions within the $\sigma = \sigma_{\max} = N$ group are presented in Table 5. Some useful max branching ratios are given in Table 3. In particular, it should be noted that, as in all IBM B(E2) values, the finite dimensionality of the system is automatically included. Due to the form of the transition operator, branching ratios occurring in the O(6) limit are independent of the parameters A, B, and C.

Within each σ grouping itself, the level spacing somewhat resembles that of a vibrational model, as described in section A, but with an energy spacing proportional to $\tau(\tau + 3)$ rather than simply to τ . This will give rise to the energy ratio $E(4_1^+)/E(2_1^+) = 2.5$ rather than 2, as expected in the vibrational picture; also, as τ increases even larger energy differences will occur between states of different τ . Further, the degeneracies of the geometrical vibrational phonon model are explicitly eliminated by the $J(J + 1)$ term and certain states, e.g., the 0^+ state of the two-phonon triplet, do not occur. As described earlier in subsection 1, the state which would correspond to this 0^+ state is "repelled" by the ground state and is raised in energy due to the repulsive pairing force which characterizes this limit. Branching ratios and absolute B(E2) values also differ significantly from the geometrical prescription.

The O(6) limit (especially for large N) seems to resemble most closely the γ -unstable model described by Wilets and Jean [44].

In such a geometrical description, as shown in Figure Id, the levels follow a $\tau(\tau + 3)$ energy dependence. Also, the same levels and level spacings that occur in the γ -unstable $n_\beta = 0$ group are repeated for the higher-lying $n_\beta \neq 0$ groups. In this sense, the role of n_β is analogous to that of the different values.

However, in the O(6) scheme, the level degeneracies are no longer maintained, and there are spin cutoffs, and a specific number of different σ groupings. It is reasonable that the O(6) description may correspond to the γ -unstable geometrical model, in analogy to the SU(5)-vibrator and SU(3)-symmetric rotor correspondences. As described in section A, the Hamiltonian of a γ -unstable oscillator is characterized by a potential energy which is independent of γ , although γ -dependent terms are included in the kinetic energy. A correspondence exists between the coordinates of the Bohr-Mottelson picture and the

operators of the IBM. Arima has suggested the result that the γ -unstable potential corresponding to the $O(6)$ limit of the IBM would be of the form:

$$V = -c\beta^2 + d\beta^4 \dots\dots\dots(2-90)$$

where β is the deformation parameter and c and d are arbitrary constants. This form of potential arises from the zero d-boson and two d-boson number changing terms of the $O(6)$ Hamiltonian. A γ -dependent term in the potential would be of the form $\beta^3 \cos 3\gamma$, which corresponds to one d-boson number changing terms that are not included in this symmetry [86]. Currently, attempts to understand more explicitly the analogy between the $O(6)$ symmetry and relevant geometrical models are being pursued. A convenient basis in which to describe the $O(6)$ level wave functions is that of the vibrational limit, given by $J^\pi |n_d n_\beta n_\Delta\rangle$, where $n_d n_\beta n_\Delta$ are, as usual, the number of d-bosons, number of d-boson pairs coupled to angular momentum zero, and the number of d-boson triplets coupled to angular momentum zero, respectively. Although the wave functions are not pure in this basis, they can be described in a simple manner as a linear combination of basis states differing in the n_d and n_β quantum numbers. For example, in the vibrational limit, the ground state is a pure $0^+|000\rangle$ state; in $O(6)$, the ground state, with $\sigma = \sigma_{\max}$ would be characterized by the 0^+ wave function A convenient basis in which to describe the $O(6)$ level wave functions is that of the vibrational limit, given by $J^\pi |n_d n_\beta n_\Delta\rangle$, where $n_d n_\beta n_\Delta$ are, as usual, the number of d-bosons, number of d-boson pairs coupled to angular momentum zero, and the number of d-boson triplets coupled to angular momentum zero, respectively. Although the wave functions are not pure in this basis, they can be described in a simple manner as a linear combination of basis states differing in the n_d and n_β quantum numbers. For example, in the vibrational limit, the ground state is a pure $0^+|000\rangle$ state; in $O(6)$, the ground state, with $\sigma = \sigma_{\max}$ would be characterized by the 0^+ wave function $\alpha|000\rangle + \beta|210\rangle + \gamma|420\rangle + \dots\dots\dots\varepsilon|NN/20\rangle$.

Two types of perturbations may be added to the exact results of the $O(6)$ limit: one which does not change the forces of the symmetry, and one which introduces a force from outside the limit. The former type can be accomplished, for example, by changing the boson energy from the value determined by B . This will alter the amplitudes of the non-zero components of all wave- functions, but will not add new components. The result will be to break the selection rule $\Delta\sigma = 0$, but to preserve the $\Delta\tau = \pm 1$ E2 selection rule. The second type of perturbation can be accomplished, for example, by the introduction of a quadrupole-quadrupole interboson force. Since such an interaction contains one d-boson changing terms, all wave function components would be non-zero, though perhaps small, and the effect would be to break both $O(6)$ E2 selection rules, as well as to alter all E2 branching ratios.

The interferences between these three dynamical symmetries give three transitional regions. These regions are as follows **SU(3) → SU(5)** : This transitional region can be treated by breaking SU(3) symmetry in the direction of SU(5) by adding $H^\wedge = \varepsilon(n_s^\wedge + n_d^\wedge) + a_3 T_3^\wedge T_3^\wedge + a_4 T_4^\wedge T_4^\wedge$ terms. The Hamiltonian of this region can be written as:

$$H^{\wedge} = \varepsilon(n_s^{\wedge} + n_d^{\wedge}) + a_1 L^{\wedge} . L^{\wedge} + a_2 Q^{\wedge} . Q^{\wedge} + a_3 T_3^{\wedge} . T_3^{\wedge} + a_4 T_4^{\wedge} . T_4^{\wedge} \dots\dots\dots(2-91)$$

SU(3) → O(6) : The nuclei in this transitional region can be treated by breaking SU(3) symmetry in the direction of O(6) by adding $P^{\wedge} . P^{\wedge}, a_3 T_3^{\wedge} . T_3^{\wedge}$ terms. The Hamiltonian of this region can be written as:

$$H^{\wedge} = a_0 P^{\wedge} . P^{\wedge} + a_1 L^{\wedge} . L^{\wedge} + a_2 Q^{\wedge} . Q^{\wedge} + a_3 T_3^{\wedge} . T_3^{\wedge} \dots\dots\dots(2-92)$$

O(6) → SU(5): The nuclei in this transitional region can be treated by a Hamiltonian containing $\varepsilon(n_s^{\wedge} + n_d^{\wedge})$ and $a_0 P^{\wedge} . P^{\wedge}$ terms as :

$$H^{\wedge} = \varepsilon(n_s^{\wedge} + n_d^{\wedge}) + a_0 P^{\wedge} . P^{\wedge} + a_1 L^{\wedge} . L^{\wedge} + a_3 T_3^{\wedge} . T_3^{\wedge} + a_4 T_4^{\wedge} . T_4^{\wedge} \dots\dots\dots(2-93)$$

The O(6) limit of the IBM-1 possesses N as a good quantum number together with the conventional O(6) quantum numbers $\sigma; \tau$ but n_d is not a good quantum number [52]. The E0 transition operator possesses the selection rules $\Delta\sigma = 0; +2; \Delta\tau = 0$. Thus, the E0 matrix elements that connect to the 0^+ ground-state level $|[N], \sigma = N, \tau = 0, L = 0\rangle$ originate in the $\sigma = N - 2$ multiplet, i.e.. $|[N], \sigma = N - 2, \tau = 0, L = 0\rangle$

2.3.1.4- The Potential Energy Surface (PES)

All deformed nuclei have quadrupole moments in their states. The changing in the shape which depends on the direction of motion with the symmetric axis is classified into oblate or prolate type. The potential energy surface function $V(N, \beta, \gamma)$ depends on the shape variables β and γ , where β is the magnitude of nuclear deformation and γ gives the turn way from axis symmetry (a symmetry angle), and they are different for different states of nucleus. The $V(N, \beta, \gamma)$ and their contour lines are very important because the geometrical collective properties can make more sensitive test than the phenomenological.

The potential energy surface can be leads to the knowledge of nuclear deformation shape. This deformation shape depends on two parameters (β, γ) for a given total number of boson (N) as the following. When the value of deformation parameter ($\beta = 0-2.4$) is approach to zero, the shape of nuclei will be spherical, and when these values are grater than zero the deformation of nuclei is dominant.

When the value of γ parameter equal to 0° this lead to triplet symmetric from prolate type, and when the value of γ equal to 60° the distortion will be triplet symmetric from oblate type. The Hamiltonian matrix diagonalized in order to determine the Eigen values and eigenvectors. The Hamiltonian (potential) of the numerical values of potential at each point of (β, γ) mesh, is unknown (or variation parameter), and used directly and no assumptions are made about these function. The most commonly general equation for potential energy surface as a function of geometrical variables β and γ is given by [87]:

$$V(N, \beta, \gamma) = \frac{N(\varepsilon_s + \varepsilon_d \beta^2)}{1 + \beta^2} + \frac{N(N-1)}{1 + \beta^2} (f_1 \beta^4 + f_2 \beta^3 \cos 3\gamma + f_3 \beta^2 + f^4) \dots\dots\dots(2-94)$$

The variables f_1, f_2, f_3, f_4 are related to the parameter c_L, N_L and u_L in Hamiltonian equation which can be written in Eq. (2-45). The relationship between the variables f parameters and these parameters has been expressed [88]:

$$f_1 = \frac{c_0}{10} + \frac{c_2}{7} + \frac{9c_4}{35}, \quad f_2 = \sqrt{\frac{8}{35}}v_2, \quad f_3 = \frac{v_0 + v_2}{\sqrt{5}}, \quad f_4 = u_0 \dots \dots \dots (2-95)$$

One must take into account that the asymmetry angle accurse only in the term $(\cos 3\gamma)$. Thus the energy surface has minima only at $\gamma = 0^\circ$ and $\gamma = 60^\circ$, the energy in their limits, can display the essential dependence β and γ .

2.3.2 Interacting Boson Model-2 (IBM-2)

In the IBM-2 model the neutrons and protons degrees of freedom are taken into account explicitly. Thus the Hamiltonian [89,90] can be written as,

$$H = H_\pi + H_\nu + V_{\pi\nu} \dots \dots \dots (2-96)$$

$$H = \varepsilon_\pi d_\pi^+ d_\pi^- + \varepsilon_\nu d_\nu^+ d_\nu^- + V_{\pi\pi} + V_{\nu\nu} + \kappa Q_\pi \cdot Q_\nu + M_{\pi\nu} \dots \dots \dots (2-97)$$

Here ε is the d -boson energy, κ is the strength of the quadrupole interaction between neutron and proton bosons.

In the IBM-2 model, the quadrupole moment operator is given by:

$$Q_{\rho\rho} = (s^+ d^- + d^+ s^-)_\rho^{(2)} + \kappa_\rho (d^+ d^-)_\rho^{(2)} \dots \dots \dots (2-98)$$

where $\rho = \pi$ or ν , $Q_{\rho\rho}$ is the quadrupole deformation parameter for neutrons ($\rho = \nu$) and protons ($\rho = \pi$). Where the terms $V_{\nu\nu}$ and $V_{\pi\pi}$ are the neutron-neutron and proton-proton d -boson interactions only and given by:

$$V_{\rho\rho} = \sum_{J=0,2,4} \frac{1}{2} C_{L\rho} (2J+1)^{1/2} \left[(d^+ d^+)_\rho^{(2)} \left(\tilde{d} \tilde{d} \right)_\rho^{(2)} \right]^{(0)} \dots \dots \dots (2-99)$$

The last term $M_{\pi\nu}$ is the Majorana interaction, which accounts for the symmetry energy and shifts the states with mixed proton-neutron symmetry with respect to the totally symmetric ones, which affects only the relative location of the states with mixed symmetry with respect to the fully symmetric states. Since little experimental information is known about such states with mixed symmetry, which has the form:

$$M_{\pi\nu} = - \sum_{k=1,3} 2\xi_k (d_\pi^+ d_\pi^+)^{(k)} (d_\nu^- d_\nu^-)^{(k)} + \xi_2 (d_\pi^+ s_\nu^+ - s_\pi^- d_\nu^-)^{(2)} (d_\pi^- s_\nu^- - s_\pi^- d_\nu^-)^{(2)} \dots \dots \dots (2-100)$$

Electromagnetic Transitions and Quadrupole Moments in IBM-2

The general one-body E2 transition operator in the IBM-2 is

$$T(l) = T_\pi(l) + T_\nu(l) \dots\dots\dots(2-101)$$

$$T(E2) = e_\pi \left[(s^+ d^- + d^+ s^-)_\pi^{(2)} + \chi_\pi (d^+ d^-)_\pi^{(2)} \right] + e_\nu \left[(s^+ d^- + d^+ s^-)_\nu^{(2)} + \chi_\nu (d^+ d^-)_\nu^{(2)} \right]$$

$$T(E2) = e_\pi Q_\pi + e_\nu Q_\nu \dots\dots\dots(2-102)$$

where Q_ρ is in the form of Eq.(2-98). For simplicity, the χ_ρ has the same value as in the Hamiltonian. This is also suggested by the single j -shell microscopy. In general, the E2 transition results are not sensitive to the choice of e_ν and e_π , whether $e_\pi = e_\nu$ or not. Thus, the reduced electric quadrupole transition rates between $J_i \rightarrow J_f$ states are given by:

$$B(E2; J_i^+ \rightarrow J_f^+) = \frac{1}{2J_i + 1} \left| \langle J_f^+ \| T(E2) \| J_i^+ \rangle \right|^2 \dots\dots\dots(2-103)$$

The electric quadrupole moment in IBM-2 is given:

$$Q_l = \left[\frac{16\pi}{5} \right]^{1/2} \begin{bmatrix} J & 2 & J \\ -J & 0 & J \end{bmatrix} \langle J \| T(E2) \| J \rangle \dots\dots\dots(2-104)$$

In the IBM-2, the M1 transition operator up to the one-body term ($l=1$) is

$$T(M1) = \left[\frac{3}{4\pi} \right]^{1/2} (g_\pi L_\pi^{(1)} + g_\nu L_\nu^{(1)}) \dots\dots\dots(2-105)$$

where $L_\rho^{(1)} = \sqrt{10} (d^+ \tilde{d})_\rho$ and $L^{(1)} = L_\pi^{(1)} + L_\nu^{(1)}$. The g_π and g_ν are the boson g-factors (gyromagnetic factors) in unit μ_n that depends on the nuclear configuration. They should be different for different nuclei.

$$T(M1) = \left[\frac{3}{4\pi} \right]^{1/2} \left[\frac{1}{2} (g_\pi + g_\nu) (L_\pi^{(1)} + L_\nu^{(1)}) + \frac{1}{2} (g_\pi - g_\nu) (L_\pi^{(1)} - L_\nu^{(1)}) \right] \dots\dots\dots(2-106)$$

The magnetic dipole moment operator is given by:

$$T(M1) = 0.77 \left[(d^+ d^-)_\pi - (d^+ d^-)_\nu \right]^{(1)} (g_\pi - g_\nu) \dots\dots\dots(2-107)$$

the reduced magnetic dipole transition rates between $J_i \rightarrow J_f$ states are given by:

$$B(M1, J_i^+ \rightarrow J_f^+) = \frac{1}{2J_i + 1} \left| \langle J_f^+ \| T(M1) \| J_i^+ \rangle \right|^2 \dots\dots\dots(2-108)$$

The reduced E2 and M1 matrix elements were combined in the calculation of the mixing ratio $\delta(E2/M1)$ using the relation [91]:

$$\delta(E2/M1; J_i^+ \rightarrow J_f^+) = 0.835 E_\gamma (MeV) \frac{\langle J_f^+ \| T(E2) \| J_i^+ \rangle}{\langle J_f^+ \| T(M1) \| J_i^+ \rangle} \dots\dots\dots(2-109)$$

The $E0$ reduced transition probability is written [92]

$$B(E0; J_i \rightarrow J_f) = e^2 R_0^4 \rho^2(E0) \quad J_i = J_f \dots\dots\dots(2-110)$$

where e is the electron effective charge, $R_0 = 1.25A^{1/3} fm$ is the nuclear radius and $\rho(E0)$ is the monopole transition matrix elements. There are only limited cases of $\rho(E0)$ that can be measured directly. The electric monopole transition operator is

$$T(E0) = \beta_{0\rho} (d^+ \times d^-)_\rho^{(0)} + \gamma_{0\rho} (s^+ \times s^-)_\rho^{(0)} \dots\dots\dots(2-111)$$

$$N_\rho = \sqrt{5} (d^+ \times d^-)_\rho^{(0)} + (s^+ \times s^-)_\rho^{(0)} \dots\dots\dots(2-112)$$

$$T(E0) = \beta_{0\rho} (d^+ \times d^-)_\rho^{(0)} + \gamma_{0\rho} N_{op} \dots\dots\dots(2-113)$$

$$\beta'_{0\rho} = \beta_{0\rho} / \sqrt{5} - \gamma_{0\rho}$$

The monopole matrix element is given by:

$$\rho_{if}(E0) = \frac{Z}{R_0^2} \sum \beta'_{0\rho} \langle f | d_\rho^+ \times d_\rho^- | i \rangle \dots\dots\dots(2-114)$$

The two parameters $\beta_{0\pi}$, $\beta_{0\nu}$ in equation (2-114) must be estimated. In most cases we have to determine the intensity ratio of $E0$ to the competing $E2$ transition, $X(E0/E2)$ [92]

$$X(E0/E2; J_i^+ \rightarrow J_f^+) = e^2 R_0^4 \rho^2(E0; J_i^+ \rightarrow J_f^+) / B(E2; J_i^+ \rightarrow J_f^+) \dots\dots\dots(2-115)$$

where $J_f = J_f'$ for $J_i = J_i' = 0$, and $J_f' = 2$ for $J_i = J_i' = 0$. The two parameters $\beta_{0\pi}$ and $\beta_{0\nu}$ in Eq. (2-112) may be estimated by fitting the isotope shift, which is different in the mean square radius between neighboring isotopes in their ground state. They are given by *Bijker et al.*, [93]:

$$\begin{aligned} \Delta \langle r^2 \rangle &= \langle 0_1 | r^2 | 0_1 \rangle_A - \langle 0_1 | r^2 | 0_1 \rangle_{A+1} \\ \Delta \langle r^2 \rangle &= \beta_{0\pi}^- [\langle 0_1 | d_\pi^+ d_\pi^- | 0_1 \rangle_{N_\nu} - \langle 0_1 | d_\pi^+ d_\pi^- | 0_1 \rangle_{N_\nu}] \\ &+ \beta_{0\nu}^- [\langle 0_1 | d_\nu^+ d_\nu^- | 0_1 \rangle_{N_\nu} - \langle 0_1 | d_\nu^+ d_\nu^- | 0_1 \rangle_{N_\nu}] - \gamma_{0\nu} \\ &\dots\dots\dots(2-116) \end{aligned}$$

The isomer shift, which is the difference between the mean square radius $\delta \langle r^2 \rangle$ of an excited state and the ground state in a given nucleus [93]:

$$\delta \langle r^2 \rangle = \langle r^2 \rangle_{e.s} - \langle r^2 \rangle_{g.s}$$

$$\delta \langle r^2 \rangle = \langle 2_1 | r^2 | 2_1 \rangle - \langle 0_1 | r^2 | 0_1 \rangle$$

$$\delta \langle r^2 \rangle = \beta_{0\pi}^- [\langle 2_1 | d_\pi^+ d_\pi^- | 2_1 \rangle - \langle 0_1 | d_\pi^+ d_\pi^- | 0_1 \rangle] + \beta_{0\nu}^- [\langle 2_1 | d_\nu^+ d_\nu^- | 2_1 \rangle - \langle 0_1 | d_\nu^+ d_\nu^- | 0_1 \rangle] \dots (2-117)$$

The IBM-2 Basis States

The calculation of IBM-2 energy eigenvalues and eigenfunctions is usually done numerically using the computer code **NPBOS** [94]. The resulting eigenvectors can then be used to calculate transition rates and related properties using the computer code **NPBTRN** [94]. The relationship between the parameters of Eq. (2-97).

The basis states used in the calculations are products of neutron and proton basis states. The latter are $U(5)$ basis states for neutron bosons and proton bosons, as given in expression (2.20).

The complete IBM-2 basis state can be as .

$$\begin{aligned} |\Psi JM\rangle &= \left[[N = N_\nu + N_\pi] n_{d\nu}, v_\nu, n_{\Delta\nu}, L_\nu, M_\nu; n_{d\pi}, v_\pi, n_{\Delta\pi}, L_\pi, M_\pi; JM \right] \\ &= \left[[N] n_d, v, n_\Delta, L, M \right]_\nu \left[[N] n_d, v, n_\Delta, L, M \right]_\pi \dots (118) \end{aligned}$$

The basis states can be found by choosing states that transform as the representations of the chain of algebras that can be derived from the $U(6)$ algebra formed by the bilinear pair of boson creation and annihilation operators. In the IBM-2, the bilinear pairs of proton and neutron creation and annihilation operators respectively form the algebras $U_\pi(6)$ and $U_\nu(6)$. There are several ways decompose and combine the two algebras into a chain of subalgebras and each way will determine the basis. As in the IBM-1, the requirement for the chain is the inclusion of the $SO_{\pi+\nu}(3)$ algebra as it is related to a good total angular momentum quantum number. The algebra $SO_{\pi+\nu}(3)$ is created from the sum of generators of the algebras $SO_\pi(3)$ and $SO_\nu(3)$.

As an example, one may take the two chains of algebras for protons and neutron,

$$U_\pi(6) \supset U_\pi(5) \supset SO_\pi(5) \supset SO_\pi(3) \supset SO_\pi(2)$$

$$U_\nu(6) \supset U_\nu(5) \supset SO_\nu(5) \supset SO_\nu(3) \supset SO_\nu(2)$$

These two chains can be combined at any point up except at $SO_{\pi+\nu}(2)$ since the combined algebra $SO_{\pi+\nu}(3)$ is needed. One of the possibilities is:

$$U_\pi(6) \supset U_\pi(5) \supset SO_\pi(5) \supset SO_\pi(3)$$

$$\begin{array}{cccc} N_\pi & n_{d\pi} & v_\pi, n_{\Delta\pi} & L_\pi & SO_{\pi+\nu}(3) \supset SO_{\pi+\nu}(2) \\ U_\nu(6) \supset U_\nu(5) \supset SO_\nu(5) \supset SO_\nu(3) & & & & L \quad M \end{array}$$

N_ν $n_{d\nu}$ $\nu_\nu, n_{\nu\Delta}$ L_ν

where the quantum numbers are labelled beneath the corresponding algebra. This is the basis that is used in the *IBM-2* program *NPBOS*.

Another set of bases can be obtained if one combines the algebras at a different point such as:

$$\begin{aligned}
 &U_\pi(6) \\
 &U_{\pi+\nu}(6) \supset U_{\pi+\nu}(5) \supset SO_{\pi+\nu}(5) \supset SO_{\pi+\nu}(3) \supset SO_{\pi+\nu}(2) \\
 &U_\nu(6)
 \end{aligned}$$

In general there are three chains that can be combined at $U_{\pi+\nu}(6)$ to give three different bases. In these chains, the proton and neutron bosons exhibit a symmetry and this is the subject of the following section.

2.3.2.1 Mixed-Symmetry States

The low-energy spectrum of even-even nuclei is dominated by simple collective excitation modes [95]. These correlations in the nucleon motion are induced by the long-range quadrupole component of the nuclear force. In spherical nuclei with few valence nucleons, surface vibrations evolve which can be described as bosons, so-called phonons. In an ideal case the excitation spectrum of a vibrator nucleus is a harmonic oscillator with equidistant level spacings $\hbar\omega$, where phonons can couple to multiphonon states with different angular momenta and parities. For large numbers of the valence nucleons an elliptically deformed equilibrium state becomes energetically more favorable. Its vibrational modes can be divided into vibrations of the deformation parameter β (β -vibrations) and the form parameter γ (γ -vibrations).

Multiphonon excitations of atomic nuclei are interesting collective structures of the nuclear many-body system. Their existence enables us to judge the capability of the corresponding phonon modes to act as building blocks of nuclear structure. Possible deviations from harmonic phonon coupling occur due to the microscopic structure of the underlying phonon modes and serve as a sensitive source of information on the formation of collectivity in the nuclear many-body system. The proton-neutron interaction in the nuclear valence shell has been known for a long time as the driving force for the evolution of the low-energy nuclear structure. This has been discussed in many ways, e.g. in terms of the evolution of collectivity in heavy nuclei as a function of the product of valence proton and neutron numbers $N_\pi N_\nu$ [96]. More recently Otsuka *et al.* have identified the proton-neutron interaction as being responsible for the evolution of shell structure [97]. Therefore, it is interesting to study those nuclear excitations that are most sensitive to the proton-neutron interaction in the valence shell. One class of states are collective isovector valence

shell excitations that are frequently called mixed-symmetry states (*MSSs*) in the terminology of the interacting boson model.

The first observation of a nuclear *MSS* was made in electron scattering experiments [98] on the deformed nucleus ^{156}Gd . A strong *MI* excitation to a 1^+ state close to 3 MeV excitation energy, the scissors mode, was observed. The scissors mode has subsequently been studied mainly in electron and photon scattering experiments on deformed nuclei. Data are available for many nuclei in the rareearth mass region and interpretations of the systematic of the centroid and the total strength as a function of deformation have been put forward [99].

***F*-spin**

The *F*-spin formalism is analogous to the isospin formalism of nucleons. Proton bosons and neutron bosons have $F = 1/2$ and the z -projection is $F_z = +1/2$ for protons and $F_z = -1/2$ for neutrons. For a system of N_π proton bosons and N_ν neutron bosons, the maximum *F*-spin is $F = F_{max} = (N_\pi + N_\nu)/2$ and

$$F_z = \frac{|N_\pi - N_\nu|}{2} \leq F_{max} \leq \frac{N_\pi + N_\nu}{2} \dots\dots\dots(2-119)$$

In the *F*-spin space, one can also define the creation and annihilation operators F_+ and F_- by

$$F_+ = s_\pi^+ s_\nu + \sum_\mu d_{\pi,\mu}^+ d_{\nu,\mu} \dots\dots\dots(2-120)$$

$$F_- = s_\nu^+ s_\pi + \sum_\mu d_{\nu,\mu}^+ d_{\pi,\mu} \dots\dots\dots(2-121)$$

The projection operator F_z is given by

$$F_z = \frac{1}{2} \left[s_\pi^+ s_\nu + \sum_\mu d_{\pi,\mu}^+ d_{\nu,\mu} + s_\nu^+ s_\pi + \sum_\mu d_{\nu,\mu}^+ d_{\pi,\mu} \right] \dots\dots\dots(2-122)$$

A state composed by N_π proton bosons and N_ν neutron bosons with *F*-spin quantum number $F = F_{max}$ can be transformed by the successive action of the *F*-spin raising operator F_+ into a state that consists of proton bosons only. This state has still a total *F*-spin quantum number $F = F_{max}$ since the raising operator does not change the total *F*-spin quantum number. This new state has only proton bosons and obviously stays unchanged under a pair wise exchange of proton and neutron labels. Therefore, *IBM-2* states with $F = F_{max}$ are called **Full Symmetry States (FSSs)**. These states corresponds actually to the *IBM-1* states which are all symmetric. All others states with *F*-spin quantum numbers $F < F_{max}$ contain pairs (at least one) of proton and neutron bosons that are anti-symmetric under a pairwise exchange of protons and neutrons labels. They are called **Mixed-Symmetry States (MSSs)**.

A comprehensive review of the *F*-spin symmetry of the *IBM-2* has been given by Van Isacker *et al.* [100]. One important result of the *F*-spin formalism is given by the proton-neutron contribution to the matrix elements of any one-body operator between *FSSs*:

$$\langle F_{\max}, \alpha \| b_{\rho, \beta}^+ b_{\rho, \beta} \| F_{\max}, \alpha' \rangle = N_{\rho} c_{\alpha, \alpha', \beta, \beta'} \dots \dots \dots (2-123)$$

where $\alpha, \alpha', \beta, \beta'$ are additional quantum numbers and $c_{\alpha, \alpha', \beta, \beta'}$ is independent of ρ . This major result tells us that there are no $M1$ transition between FSSs.

Both operators $E2$ and $M1$ can be divided into F -scalar (denoted by s) and F -vector (denoted by v) parts

$$T(M1)_s = \frac{g_{\pi} + g_{\nu}}{2} (L_{\pi} + L_{\nu}) \dots \dots \dots (2-124)$$

$$T(M1)_v = \frac{g_{\pi} - g_{\nu}}{2} (L_{\pi} - L_{\nu}) \dots \dots \dots (2-125)$$

$$T(E2)_s = \frac{e_{\pi} + e_{\nu}}{2} (Q_{\pi}^{\chi_s} + Q_{\nu}^{\chi_s}) \dots \dots \dots (2-126)$$

$$T(E2)_v = \frac{e_{\pi} - e_{\nu}}{2} (Q_{\pi}^{\chi_v} - Q_{\nu}^{\chi_v}) \dots \dots \dots (2-127)$$

with

$$\chi^s = \frac{e_{\pi} \chi_{\pi} + e_{\nu} \chi_{\nu}}{e_{\pi} + e_{\nu}} \dots \dots \dots (2-128)$$

$$\chi^v = \frac{e_{\pi} \chi_{\pi} - e_{\nu} \chi_{\nu}}{e_{\pi} - e_{\nu}} \dots \dots \dots (2-129)$$

From the previous discussion concerning the $E2$ and $M1$ decays of full symmetric states and the mixed-symmetry states (here discussed in near vibrational nuclei), we expect following signatures for mixed-symmetry one-phonon and two phonon excitations for vibrational and transitional nuclei:

First: The one-quadrupole-phonon $2_{1,MS}^+$ state is the lowest-lying MSS in vibrational nuclei.

Second: The $2_{1,MS}^+$ state decays to the 2_1^+ state by a strong $M1$ transition

$$\langle 2_{1,MS}^+ \| T(M1) \| 2_1^+ \rangle \approx 1 \mu_N^2$$

Third: A weakly collective $E2$ transition strength of a few $e^2 b^2$ for the $2_{1,MS}^+ \rightarrow 0_1^+$ transition.

In the IBM-1, geometrical shapes can be assigned to the algebras of the three possible chains, which correspond directly to the description of nuclear shapes by Bohr and Mottelson's shape variables [32,101]. In the IBM-2, the mixed-symmetry states correspond to a quadrupole vibration where the protons and neutrons oscillate out of phase. For deformed nuclei, the protons and neutrons oscillate with respect to one another as the nucleus as a whole rotates. Because of this type of motion, the mixed-symmetry states for deformed nuclei are also known as the scissors mode.

Mixed-symmetry states can be identified by their unique signature, namely a collective $M1$ decay to a fully-symmetric state. $M1$ transitions are forbidden between fully-symmetric states and between mixed-symmetry states in the F -spin basis.

CHAPTER THREE RESULTS AND DISCUSSION

3-1 IBM-1 Results

3-1-1 Energy Spectra

Even-even Ba isotopes with $Z = 54$ and $64 \leq N \leq 94$ have a collective quadrupole excitation strongly dependant on the number of nucleons outside the closed shells 50 and 82, and the neutron- proton interaction is known to have a great influence on nuclear properties. These isotopes are part of an interesting region including Te, Xe and Ce isotopes, which has and is likely to attract many theoretical works [9, 102, 103, 104].

The energy of the positive states of barium series of isotopes are calculated using computer code *PHINT* [82]. A comparison between the experimental spectra [105] and our calculations, using values of the model parameters given in Table (3-1) for the ground state band are illustrated in Figs. (3-1) to (3-14). The agreement between the calculated levels energy and their correspondence experimental values for all isotopes are slightly higher especially for the higher excited states. We believe this is due to the change of the projection of the angular momentum which is due mainly to band crossing.

The Table (3-1) contain the IBM-1 Hamiltonians' parameters (in MeV units) used in the present study to calculate the energies of the positive parity low-lying levels of $^{120-148}\text{Ba}$ isotopes. Number of bosons ($N = N_\pi + N_\nu$) changes from 10 for ^{120}Ba and 11 for ^{122}Ba to 4 for ^{140}Ba and finally varies from 5 to 9 for $^{144-148}\text{Ba}$. The Hamiltonian parameter values of IBM-1 were estimated by fitting to the experimental energy levels and it was made by allowing one parameter to vary while keeping the others constant. This procedure was carried out iteratively until an overall fit was achieved.

Table (3-1): Parameters used in IBM-1 Hamiltonian for $^{120-148}\text{Ba}$ nuclei (all in MeV)

Isotopes	N	EPS	ELL	QQ	CHQ	OCT	HEX
$Ba - 120$	10	0.531	0.0280	-0.00220	-0.2900	-0.0011	-0.0072
$Ba - 122$	11	0.524	0.0300	-0.00260	-0.3100	-0.0011	-0.0072
$Ba - 124$	10	0.515	0.0097	-0.00390	-0.5000	-0.0011	-0.0072
$Ba - 126$	9	0.495	0.0082	-0.00760	-0.5420	-0.0011	-0.0072
$Ba - 128$	8	0.493	0.0083	-0.00795	-0.5970	-0.0011	-0.0072
$Ba - 130$	7	0.542	0.0083	-0.00530	-0.6010	-0.0011	-0.0072
$Ba - 132$	6	0.895	-0.0790	-0.05700	-0.6010	-0.0032	-0.0072
$Ba - 134$	5	0.993	-0.0800	-0.05500	-0.6010	-0.0033	-0.0072
$Ba - 136$	4	0.900	0.0200	-0.05500	-0.6010	-0.0027	-0.0072
$Ba - 140$	4	0.892	0.0220	-0.05300	-0.6010	-0.0027	-0.0072
$Ba - 142$	5	0.823	0.0210	-0.05400	-0.6010	-0.0028	-0.0072
$Ba - 144$	6	0.801	0.0220	-0.05400	-0.6010	-0.0028	-0.0072
$Ba - 146$	7	0.711	0.0220	-0.05500	-0.6010	-0.0029	-0.0072
$Ba - 148$	8	0.696	0.0220	-0.05500	-0.6010	-0.0029	-0.0072

The comparisons between calculated and experimental values of energy levels for each Ba isotopes [105] are shown in Figs. (3-1) to (3-14), respectively. In general, the agreement is good, especially for the ground-state band levels and gamma band levels. However, there exist some discrepancies. The main reason is that the mix of many bands is not considered.

In figures we see the increased smoothly of the $E(2_1^+)$ energy of $^{120-140}\text{Ba}$ isotopes with neutron number, while the isotopes $^{142-148}\text{Ba}$ decrease rapidly with increasing the neutron number ($N = 86$ to $N = 92$).

The behavior of the ratio of the energies of the $R = E(4_1^+)/E(2_1^+)$ states is a good criterion for the shape transition (see Table (3-2)). The energy ratio decreases smoothly with increasing the N for $^{120-140}\text{Ba}$ isotopes. for all $^{120-140}\text{Ba}$ isotopes and it means that these structure seems to be verifying gamma soft rotor to vibrator nuclei (O(6) to SU(5)). The energy spectrum of the $^{126-136}\text{Ba}$ isotopes lie between vibrator and rotational limit. The general features of the transition between U(5) in ^{140}Ba isotope near the beginning of the closed shell and SU(3) in ^{148}Ba isotope with moderate deformation are well reproduced by the IBM-1. In Table (3-2), we have introduced the experimental and theoretical values of the ratios $E(4_1^+)/E(2_1^+)$, $E(6_1^+)/E(2_1^+)$, $E(2_2^+)/E(2_1^+)$, $E(0_2^+)/E(4_1^+)$ and $E(0_2^+)/E(2_1^+)$ together with the values of IBM limits.

From Table (3-2) and Figs. (3-1) to (3-14), we see the phase transition of shape in light $^{120-140}\text{Ba}$ isotopes (with $N < 82$) with increasing neutron number N is of current interest. The triplet phonon states $J_i^+ = 4_1^+, 2_2^+$ and 0_2^+ and a quintuplet of states (only 3 states shown). Near mid shell at ^{122}Ba , the state $J_i^+ = 4_1^+$ lies pretty low, signifying the prolate deformation in $^{122-126}\text{Ba}$. Also the state $J_i^+ = 0_2^+$ rises high, which is akin to O(6) pattern.

In the quintuplet, the state $J_i^+ = 3_1^+$ touches $J_i^+ = 4_2^+$ at ^{128}Ba , and then separates on either side. So one says that ^{128}Ba is O(6) on account of the degenerate $J_i^+ = 3_1^+$ and $J_i^+ = 4_2^+$. Like the triplet phonon states, in the quintuplet also there is bunching of states near $N=72$ (^{128}Ba isotope).

At higher neutron number ($N= 72$ and $N = 74$) the state $J_i^+ = 2_2^+$ descends below the state $J_i^+ = 4_1^+$, but this property is reflected in $^{136-148}\text{Ba}$ isotopes the state $J_i^+ = 4_1^+$ descends below $J_i^+ = 2_2^+$.

The energy of the $J_i^+ = 2_1^+$ at fast rate compared to the energy of $J_i^+ = 2_2^+$, which is even increasing at ^{128}Ba isotope ($N = 72$) to ^{134}Ba isotope ($N = 78$). The pattern of spectrum here indicates a continuous phase transition from near SU(3) (rotational limit) to γ -soft rotor. Here we focus on $E(2_2^+) - E(4_1^+)$, respective measures of deformation, γ -triaxiality and prolate oblate potential energy difference (V_{PO}). All the three important indicators of level structure are reproduced in our calculation.

Table (3-2)

نسب الطاقة

The energy ratio $E(4_1^+)/E(2_1^+)$ is falling (see Table (3-2)) with increasing neutron number and $E(2_2^+)/E(2_1^+)$ ratio is falling from about 4.284 for ^{120}Ba isotope to 3.835 for ^{140}Ba isotope corresponding to the increase of triaxiality parameter γ^0 from 20° to 30° [107], and this ratio increased from 3.835 for ^{142}Ba isotope to 6.858 for ^{148}Ba isotope.

From the energy ratio $E(4_1^+)/E(2_1^+)$ shows a nuclear structure is spherical (near harmonic vibrator), ^{122}Ba being a transitional nucleus (O(6) limit)). As it is seen from the calculated and experimental energy values for ^{122}Ba isotope are very close to X(5) predictions. Around $N = 66$, the positions of the excited 0^+ states are also close to the X(5) prediction and we note that the spacings in the excited sequence follow the expected behavior. It is regarded as a transitional nucleus, since it exhibits both the features of vibrational nuclei, like a two phonon triplet at approximately twice the excitation energy of 2_1^+ as well as the features of rotational nuclei, like an intrinsic quadrupole moment and an enhanced $B(E2)$ value of the 2_1^+ state. For X(5) critical point symmetry these signatures are listed below [108]:

- 1- The energy ratio $E(4_1^+)/E(2_1^+)$ should be approximately 2.91.
- 2- The position of the first excited collective 0_2^+ state is approximately 5.67 times the energy of the 2_1^+ .

The most basic structural signature of the E(5) symmetry is a value of the ratio $E(4_1^+)/E(2_1^+) = 2.20$. This value is intermediate between the values for spherical nuclei (2.00) and gamma-soft rotor (2.50). However there are large number of nuclei in the mass region $A \sim 130$ having the value for this ratio in the desired range. Thus, an interpretation based only on the $R_{4/2}$ can be ambiguous and additional signatures need to be considered. Often, the decay properties of the lowest excited 0^+ states are used as an additional signature of the E(5) structure. In the case of ^{134}Ba isotope the $R_{4/2}$ value is 2.316 for experimental data and 2.321 for IBM-1 results (see table (3-2)) therefore this isotope lies very close to the ideal value for the E(5) symmetry indicating that it lies more towards the SU(5) side.

It has been observed that the positioning of the 0^+ states plays a crucial role in determining the behavior of the nucleus near the critical symmetry. This can be seen from the Fig. (3-8). This figure show the changes in positioning of the levels as the neutron number changes for ^{134}Ba isotope respectively. It is clear from the figure that the variation of the levels other than the 0_2^+ level is smooth, where as there are abrupt changes in the positioning of these two levels.

Our data and our analysis have emphasized the significance of the ordering of the excited 0_3^+ and 0_2^+ configurations for assigning the structure of a nucleus near the E(5) critical point. Therefore, it is interesting to examine the behavior of the observable $\Delta_{0^+} = [E(0_2^+) - (0_3^+)]/E(2_1^+)$. It takes the values -1 (harmonic vibrator), -0.880 (E(5)), 0 at the crossing point of the $0_{3,2}^+$ configurations and becomes positive towards the O(6) limit. Along the chain of ^{134}Ba isotope we consider the

experimental energies of the first and the second excited 0^+ states with dominant 0_3^+ or 0_2^+ assignment.

In general, the ground bands are fitted very well, The fitting in the gamma bands are slightly worse but are still better than those for the beta bands. The fitting in beta bands are not so good as those in the ground bands and gamma bands. Also it is in the beta bands that IBM-1 show the most distinct improvements become smaller as we go to lighter isotopes. This suggest that the interactions between unlike bosons are relatively more important in system which are closer to the closed shells.

The light $^{120-126}\text{Ba}$ isotopes are known to belong to a transitional region between spherical and axially deformed nuclei, as shown in Tale (3-2), where the ratios $E(4_1^+)/E(2_1^+)$ for $N = 62-70$ isotones are reported.

The ^{122}Ba isotope was proposed by Fransen *et al.* [109] as a rather good X(5) candidate on the basis of the agreement observed between experimental and theoretical level energies. In ^{122}Ba isotope the ratio $R_{4/2}$ attains the near X(5) value of 2.90 [110], and decreases sharply to the $O(6)$ limit value of 2.5 up to $N = 74$ in ^{130}Ba , indicating a shape change from the β -soft deformed to the γ -soft or $O(6)$ with increasing N . ^{132}Ba isotope lies near the $O(6)$ limit towards $U(5)$. The ^{134}Ba isotope lies close to the $E(5)$ symmetry (the value of the energy ration $R_{4/2} \approx 2.1$).

Here we focus on the energy ratios $R_{4/2}$, R_γ ($R_\gamma = E(2_2^+)/E(2_1^+)$) and $\Delta E = [E(2_2) - E(4_1)]$, the respective measures of the deformation, the γ -triaxiality and the energy difference ΔE related to the prolate-oblate potential energy difference V_{PO} in the potential energy surface (PES) for the intrinsic structure of the nuclei calculated in the microscopic theory [32]. All the three important indicators of the level structure formation are well reproduced in our IBM calculation. The ratio $R_{4/2}$ varies with N as in experiment. The ratio R_γ , which determines the triaxiality or the degree of γ -softness, is also well reproduced. The movement of 2_2^+ below 4_1^+ at ^{130}Ba is reproduced. Finally, the variation of the energy difference $\Delta E = [E(2_2) - E(4_1)]$ is well given in our calculation, including its sign change at ^{130}Ba isotope (see table (3-3)). This difference ΔE decreases with increasing N and changes sign at ^{130}Ba isotope. The variation in V_{PO} corresponds to the variation in ΔE , as suggested in ref. [111].

The variation of their energies with neutrons number is interesting and is at variance with ground-band energies and with the 2_2^+ band energies. The state 0_2^+ falls up to $N = 72$ and then rises up to $N = 78$. The state 0_3^+ varies in a different way. The value for $N = 74$ ^{130}Ba isotope is not yet known, but is likely to be the minimum. In the physical view, it implies the shape transition at $N = 74$ and $N = 74$.

A characteristic feature of the γ -unstable limit of the IBM-1 is a bunching of γ -band states according to 2^+ , $(3^+, 4^+)$, $(5^+, 6^+)$,. . . , that is, 3^+ and 4^+ are close in energy, etc. This even-odd staggering is observed in certain $\text{SO}(6)$ nuclei but not in all and in some it is, in fact, replaced by the opposite bunching $(2^+, 3^+)$, $(4^+, 5^+)$,. . . which is typical of a rigid triaxial rotor [112]. From these qualitative observations it is

Table (3-3)

clear that the even-odd γ -band staggering is governed by the γ -degree of freedom (i.e., triaxiality) as it changes character in the transition from a γ -soft vibrator to a rigid triaxial rotor.

The root mean square deviation (**RMSD**) [113]:

$$RMSD = \left[\frac{1}{N} \sum (E_{cal.} - E_{exp.})^2 \right]^{1/2} \dots\dots\dots(3-1)$$

(where N is the number of energy levels)
 is used to compare the experimental and theoretical energy levels. Tale (3-4) given the **RMSD** between experimental and theoretical energy levels. In this table we see the ground state levels the best agreement was found in ^{126}Ba isotope where the smallest value of **RMSD** is equal 0.0031 and equal 0.011 for gamma band in ^{124}Ba isotope. However **RMSD** = 0.012 for beta band in ^{148}Ba isotope.

Table (3-4) : The root mean square deviations (RMSD**) between experimental and calculated energy levels for Ba isotopes.**

Isotopes	root mean square deviations (RMSD)								
	ground state band			β - band			γ - band		
	IBM-1	IBM-2	DDM	IBM-1	IBM-2	DDM	IBM-1	IBM-2	DDM
<i>Ba</i> - 120	0.0041	0.0040	-	0.062	0.055	-	0.016	0.015	-
<i>Ba</i> - 122	0.0046	0.0044	0.0450	0.063	0.052	0.0480	0.033	0.027	0.104
<i>Ba</i> - 124	0.0040	0.0047	0.0114	0.058	0.0034	0.0405	0.011	0.010	0.152
<i>Ba</i> - 126	0.0031	0.0033	0.0161	0.055	0.023	0.1234	0.014	0.013	0.019
<i>Ba</i> - 128	0.0046	0.0042	0.0519	0.046	0.0023	0.123	0.022	0.021	0.0581
<i>Ba</i> - 130	0.033	0.0039	0.0191	0.047	0.0033	0.125	0.013	0.012	0.0.31
<i>Ba</i> - 132	0.036	0.0036	0.0319	0.043	0.0045	0.104	0.020	0.019	0.054
<i>Ba</i> - 134	0.032	0.0038	0.1268	0.052	0.0047	0.1452	0.023	0.022	0.0325
<i>Ba</i> - 136	0.031	0.0030	0.0227	0.051	0.0024	0.1287	0.026	0.021	0.191
<i>Ba</i> - 140	0.030	0.040	-	0.048	0.0034	-	0.028	0.025	-
<i>Ba</i> - 142	0.034	0.051	-	0.046	0.0057	-	0.034	0.029	-
<i>Ba</i> - 144	0.035	0.0056	-	0.016	0.024	-	0.023	0.024	-
<i>Ba</i> - 146	0.0042	0.0039	-	0.018	0.056	-	0.017	0.018	-
<i>Ba</i> - 148	0.0048	0.0023	-	0.012	0.011	-	0.019	0.017	-

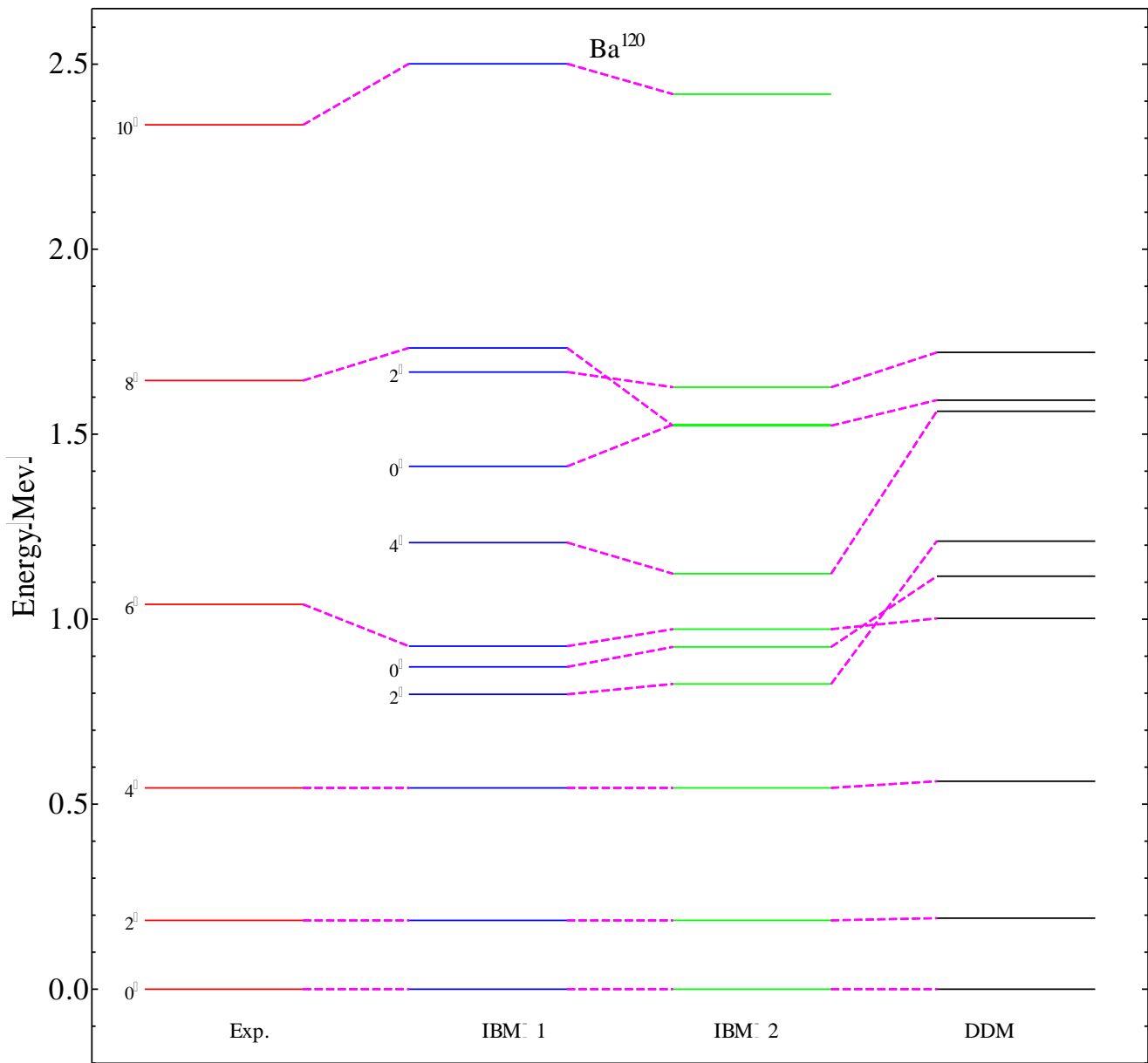


Fig. (3.1): Comparison between experimental data [105,114], IBM-1, IBM-2 and DDM calculated energy levels for ^{120}Ba .

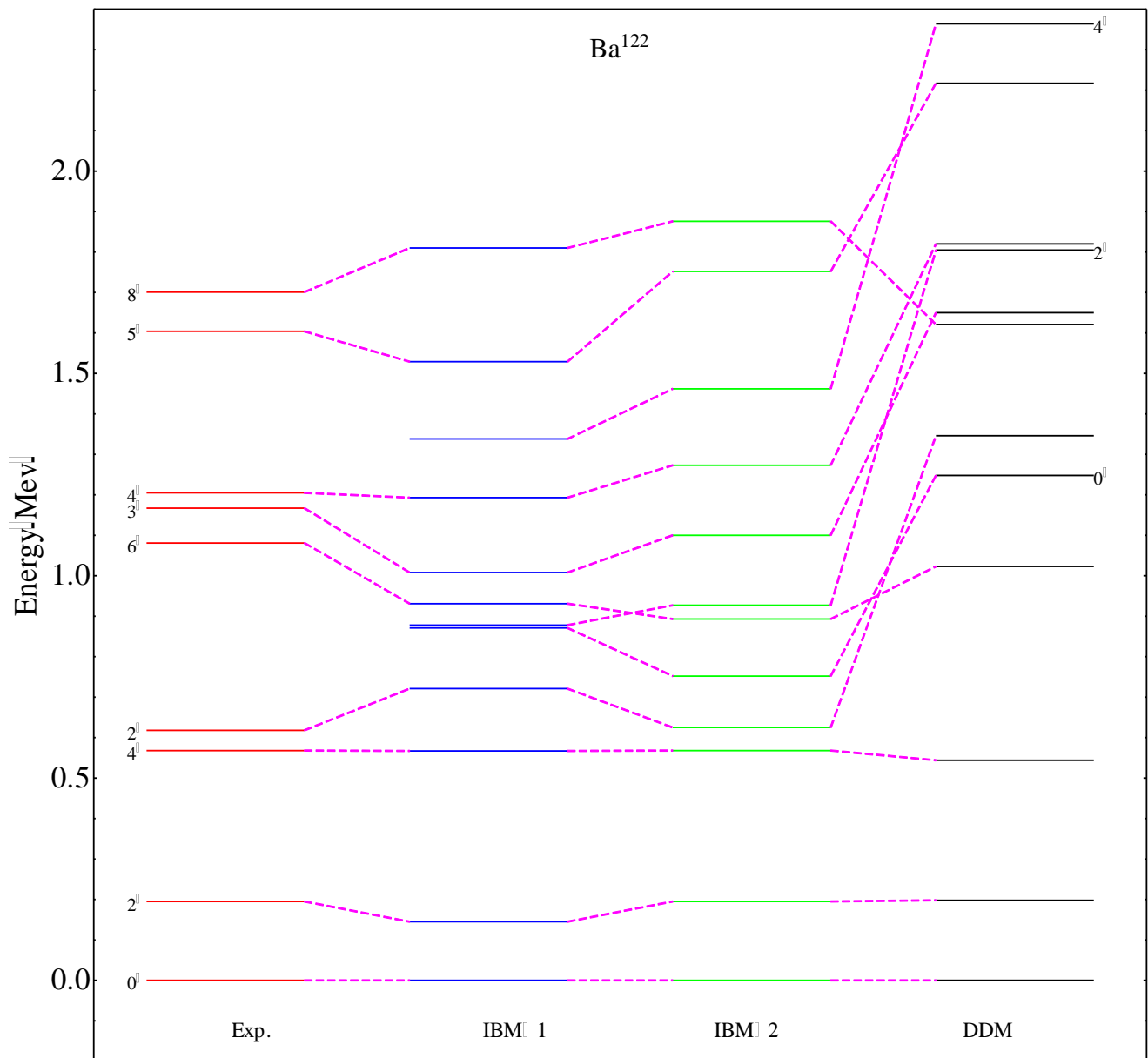


Fig. (3.2): Comparison between experimental data [105,114], IBM-1, IBM-2 and DDM calculated energy levels for ^{122}Ba .

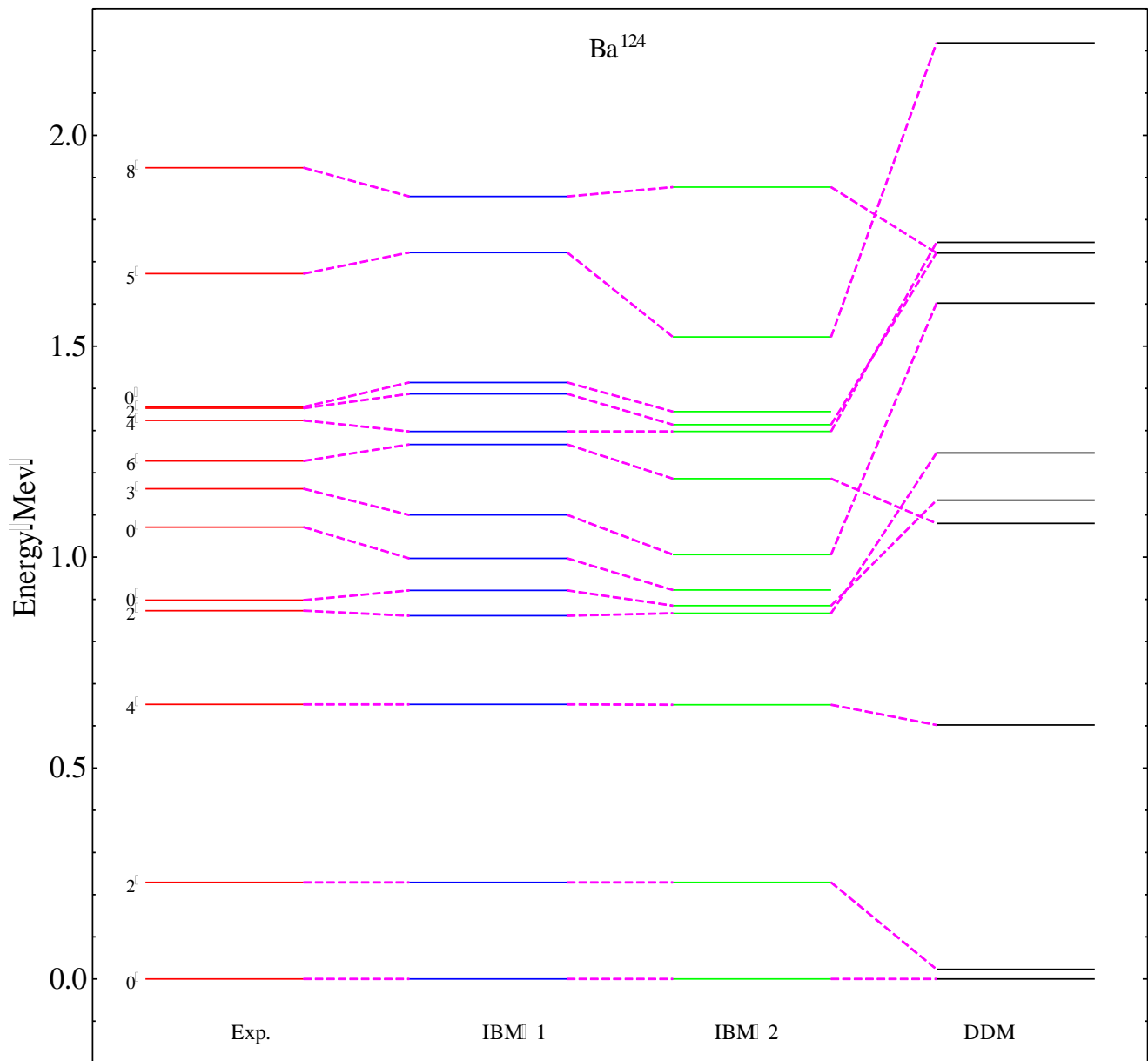


Fig. (3.3): Comparison between experimental data [105,114], IBM-1, IBM-2 and DDM calculated energy levels for ^{124}Ba .

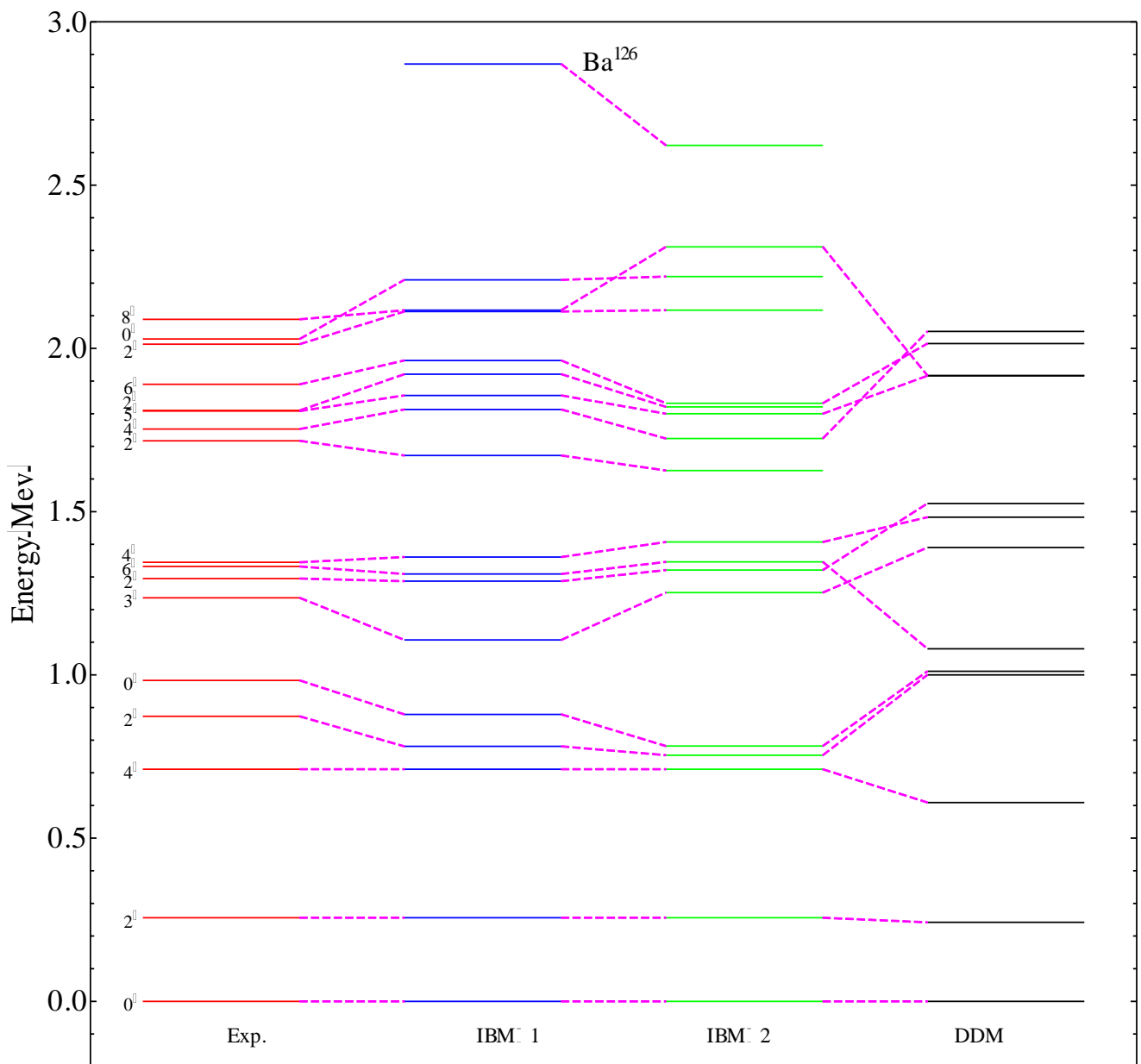


Fig. (3.4): Comparison between experimental data [105,114], IBM-1, IBM-2 and DDM calculated energy levels for ^{126}Ba .

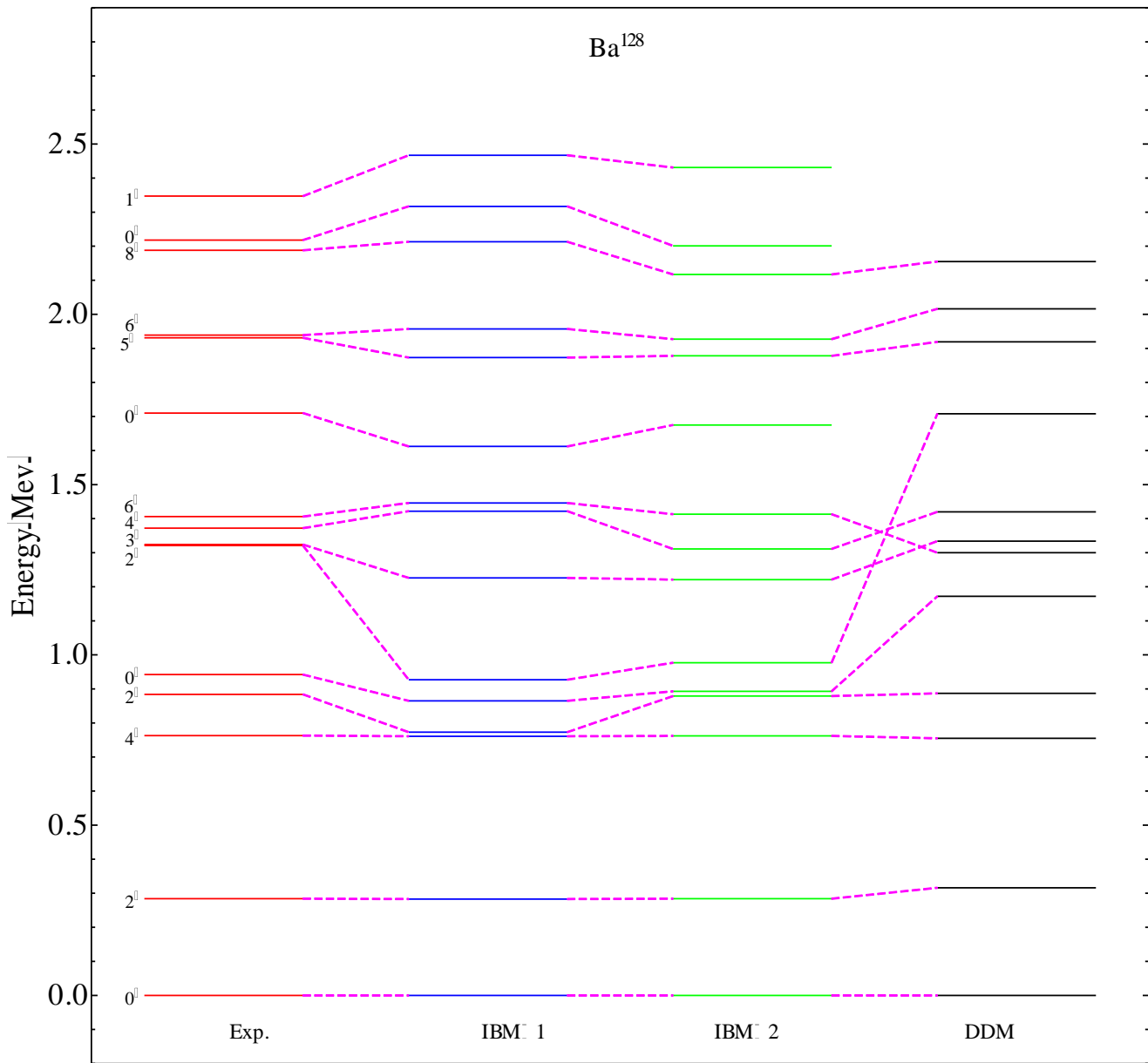


Fig. (3.5): Comparison between experimental data [105,114], IBM-1, IBM-2 and DDM calculated energy levels for ^{128}Ba .

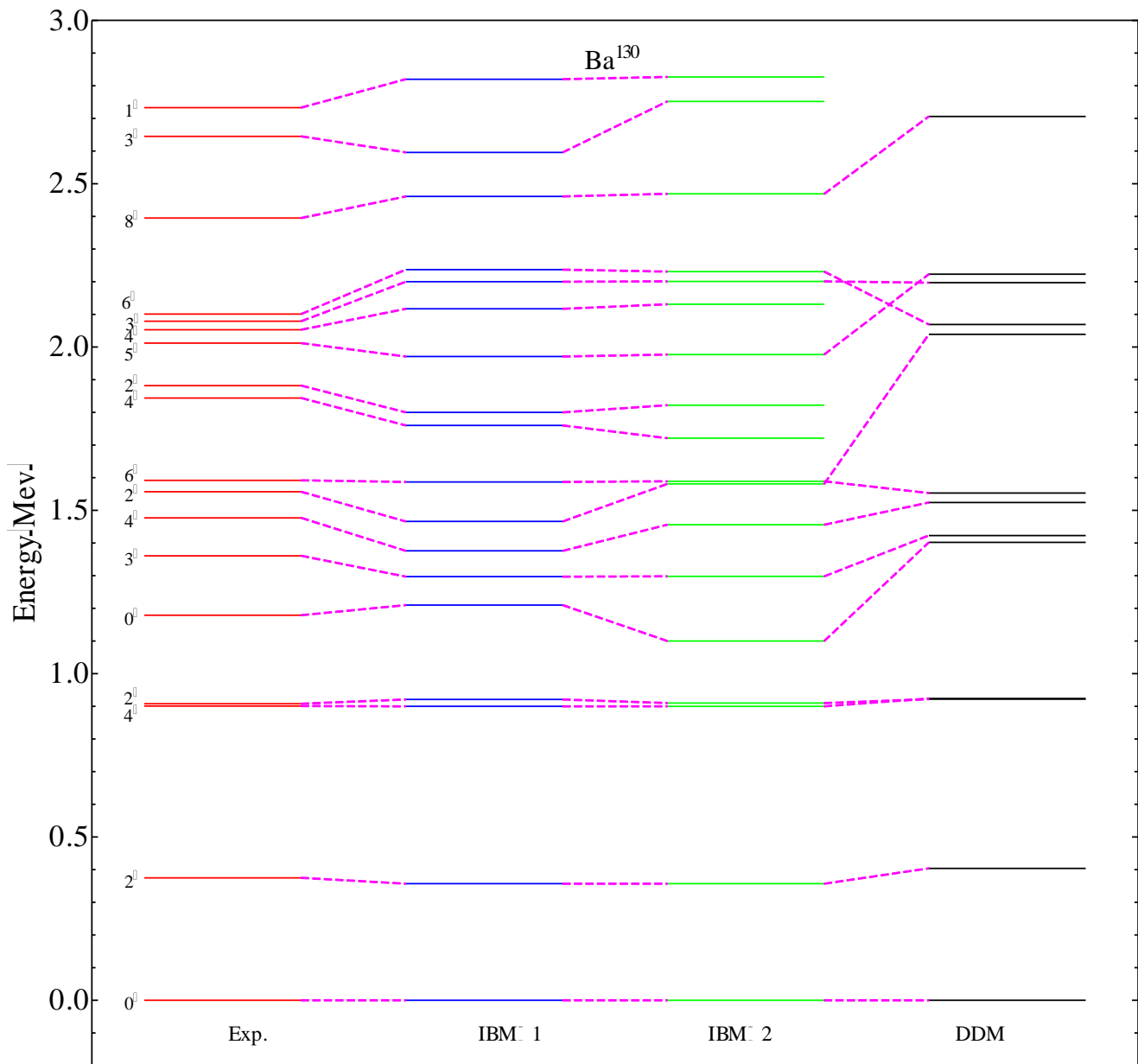


Fig. (3.6): Comparison between experimental data [105,114], IBM-1, IBM-2 and DDM calculated energy levels for ¹³⁰Ba .

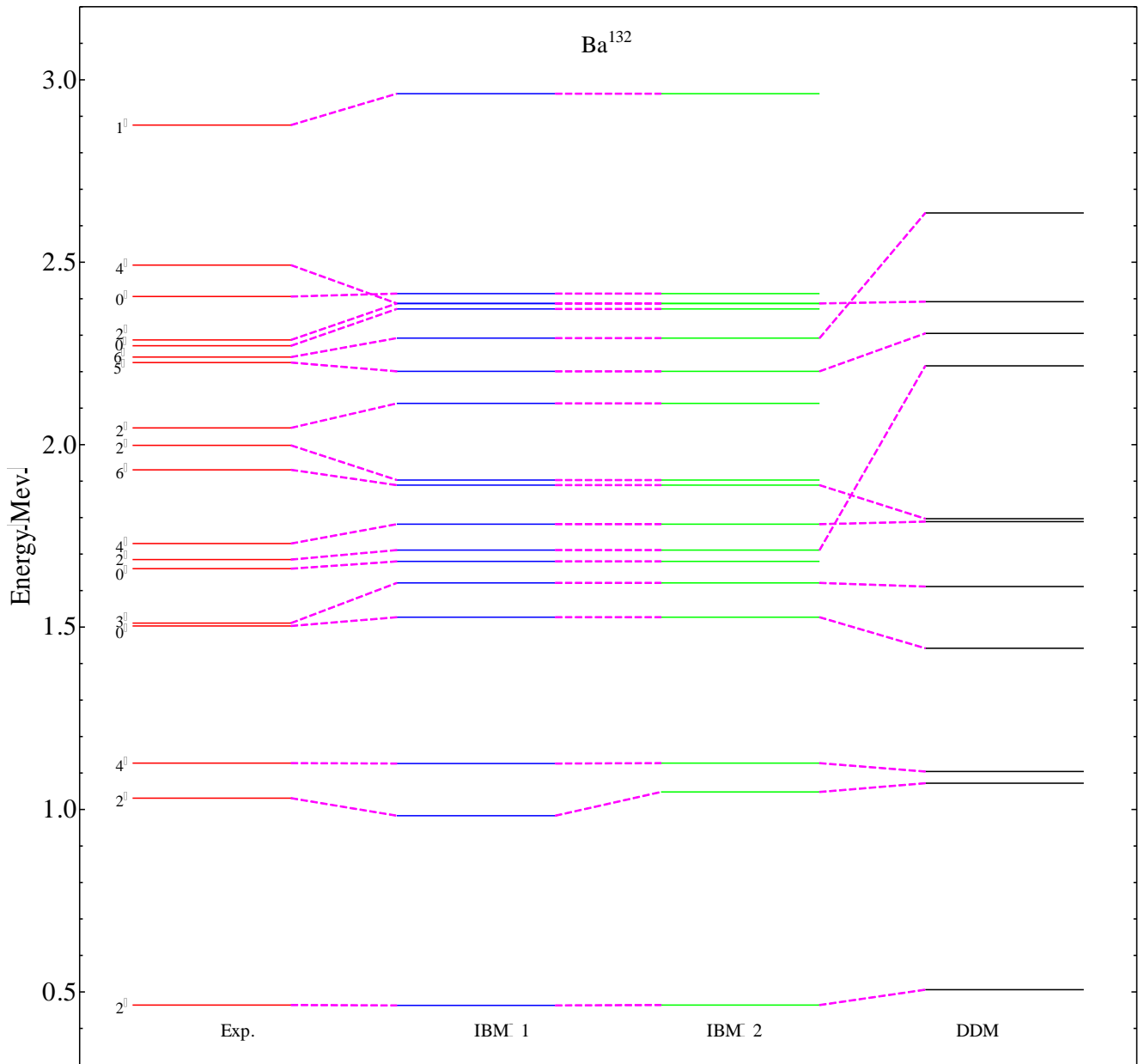


Fig. (3.7): Comparison between experimental data [105,114], IBM-1, IBM-2 and DDM calculated energy levels for ^{132}Ba .

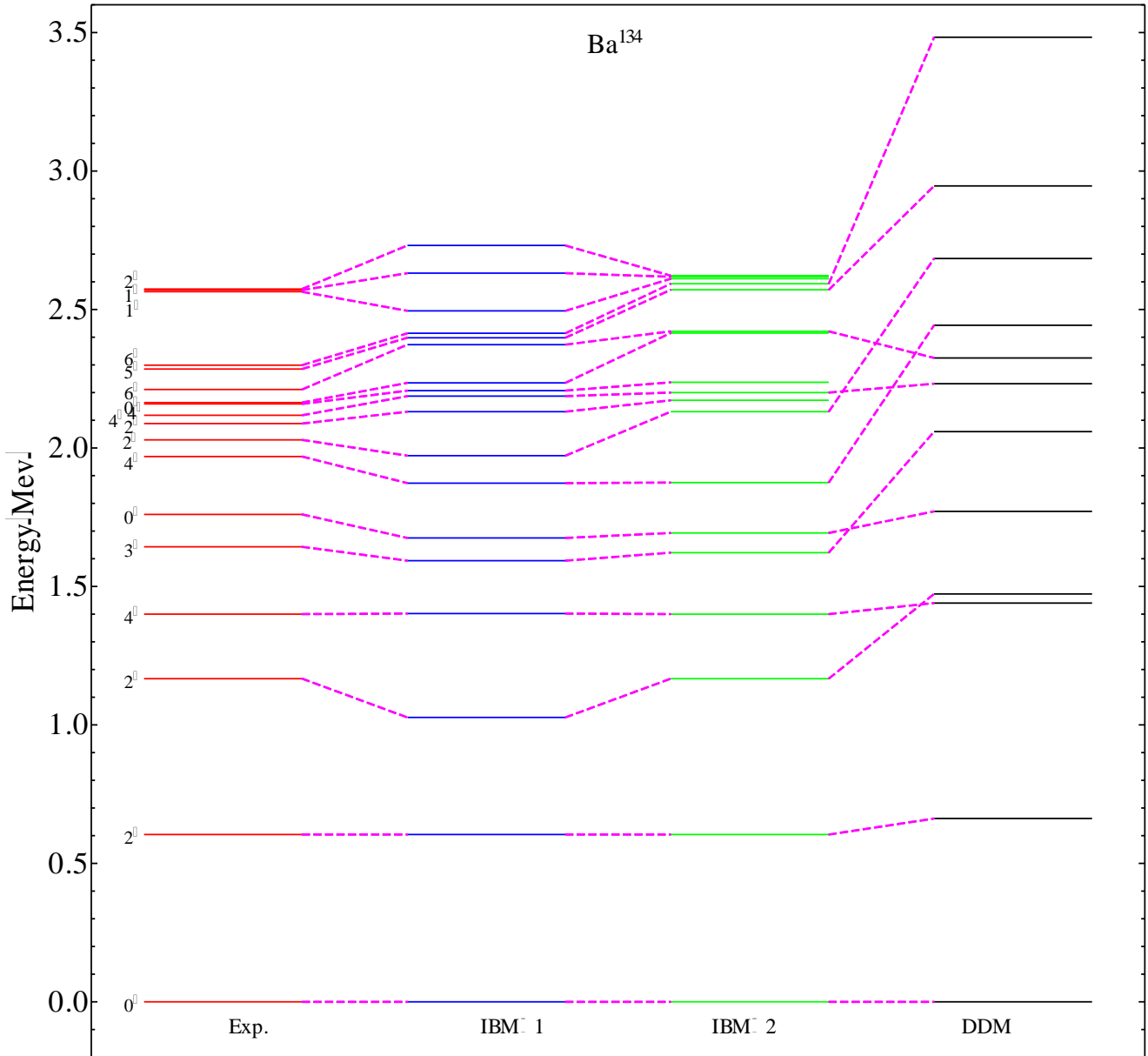


Fig. (3.8): Comparison between experimental data [105,114], IBM-1, IBM-2 and DDM calculated energy levels for ^{134}Ba .

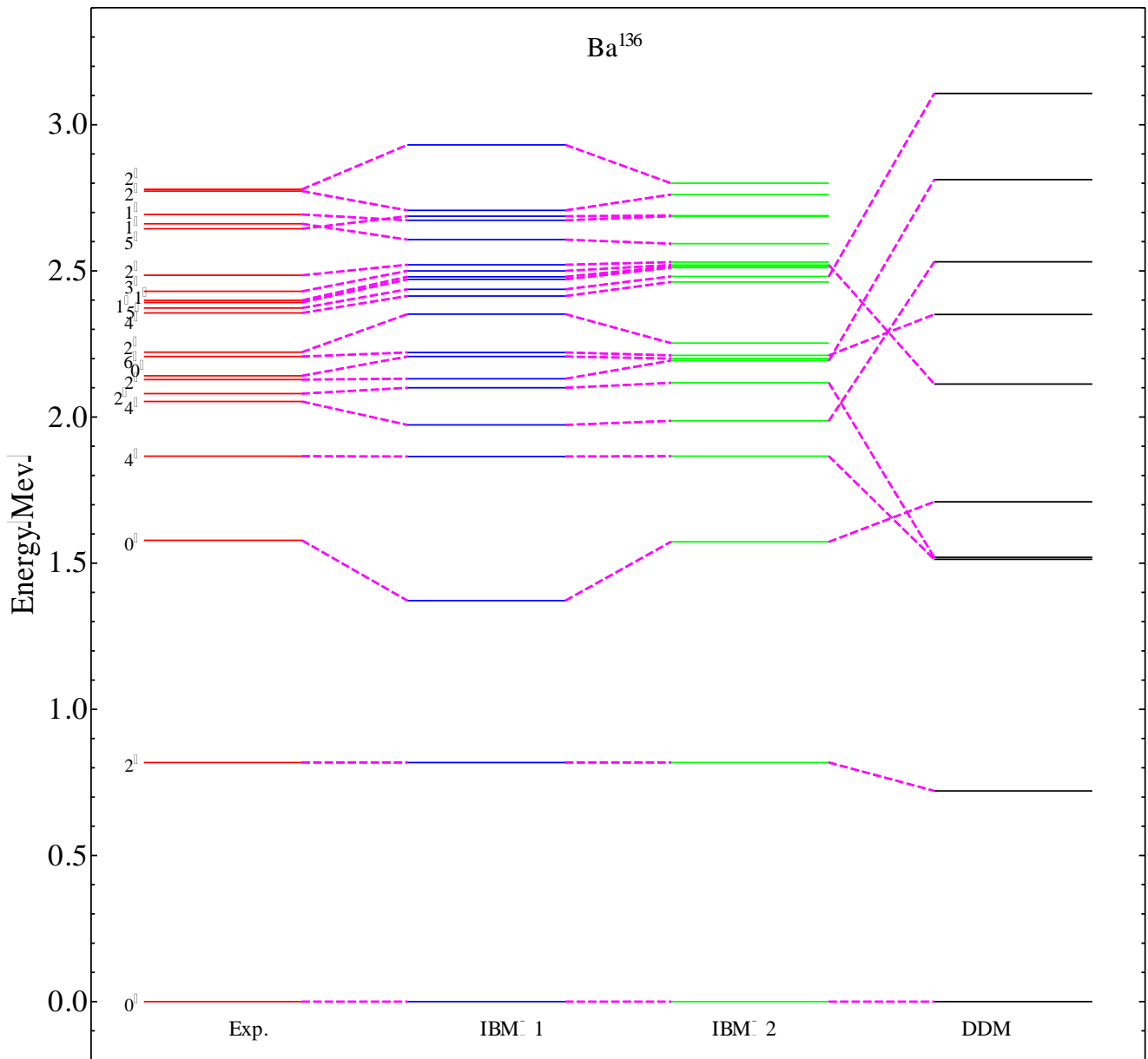


Fig. (3.9): Comparison between experimental data [105,114], IBM-1, IBM-2 and DDM calculated energy levels for ^{136}Ba .

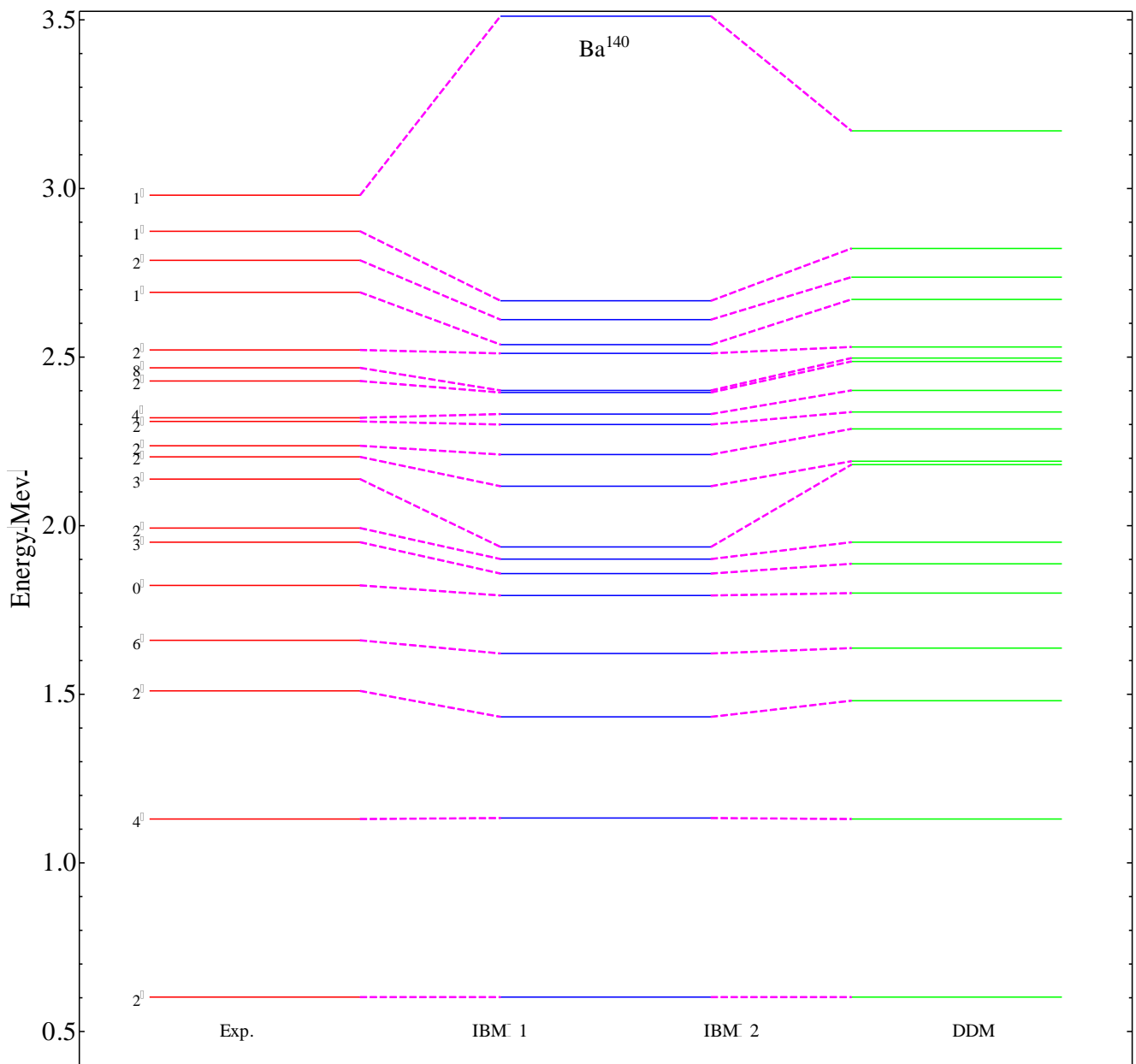


Fig. (3.10): Comparison between experimental data [105,114], IBM-1, IBM-2 and DDM calculated energy levels for ^{140}Ba .

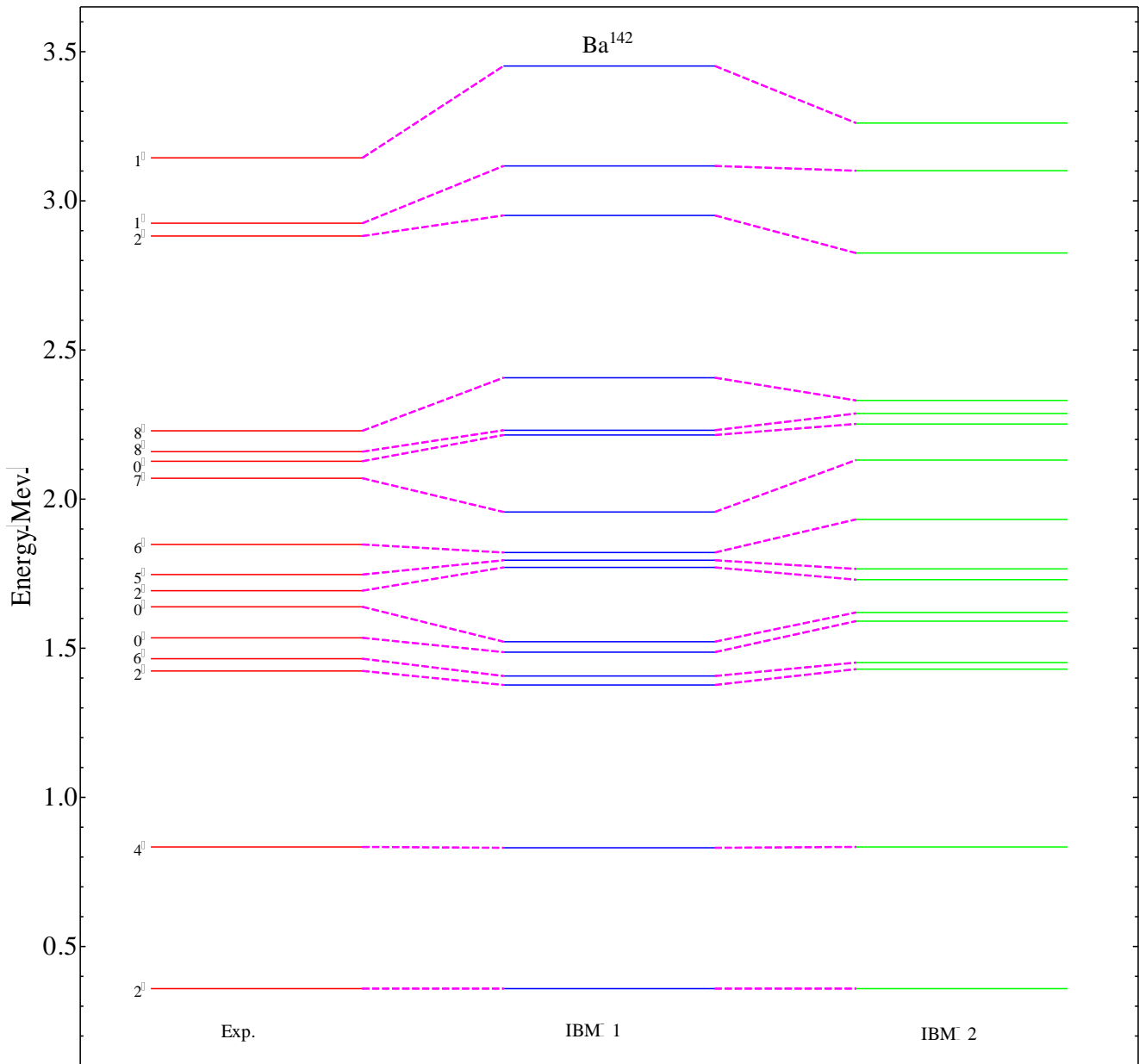


Fig. (3.11): Comparison between experimental data [105,114], IBM-1 and IBM-2 calculated energy levels for ^{142}Ba .

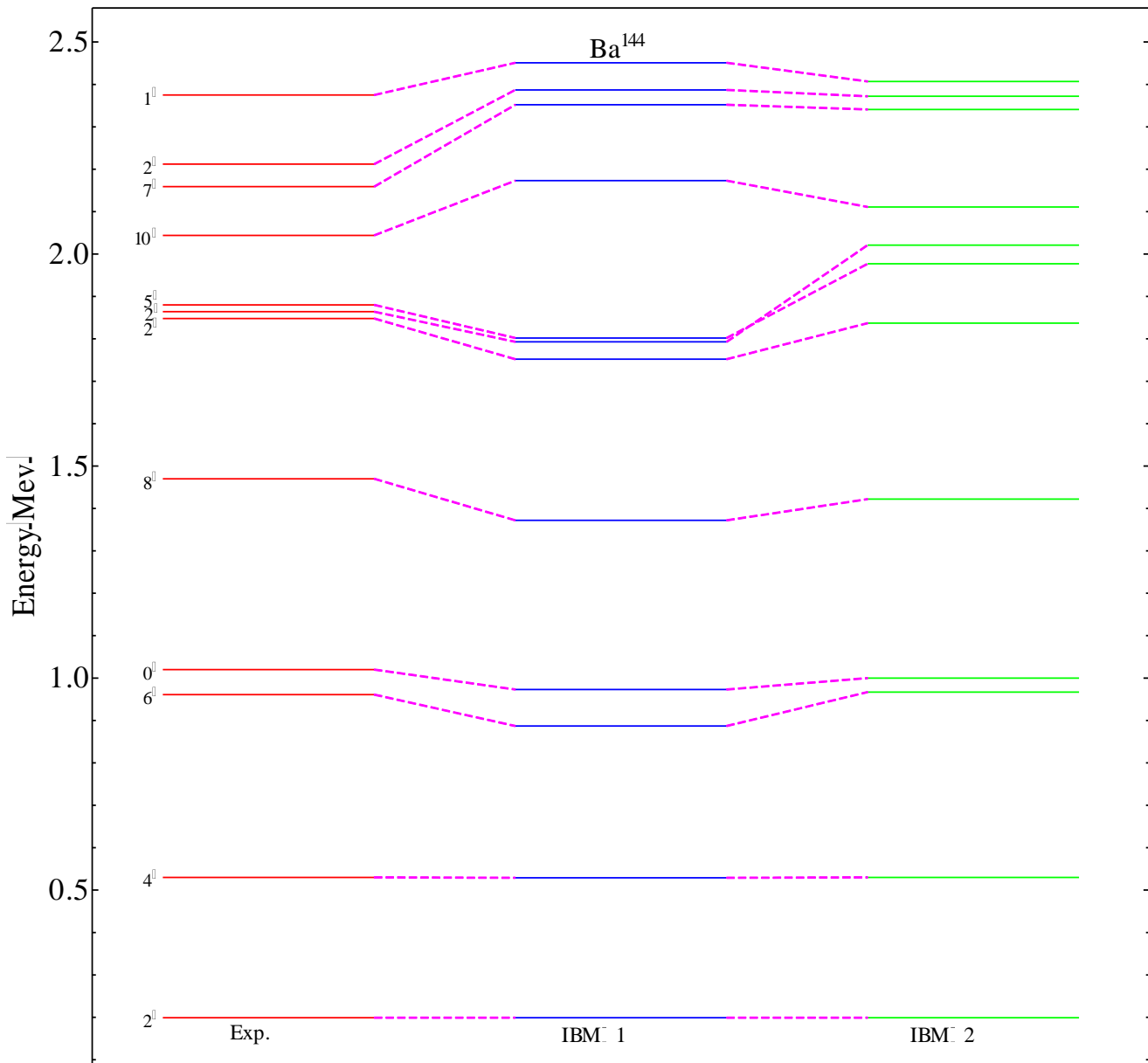


Fig. (3.12): Comparison between experimental data [105,114], IBM-1 and IBM-2 calculated energy levels for ^{144}Ba .

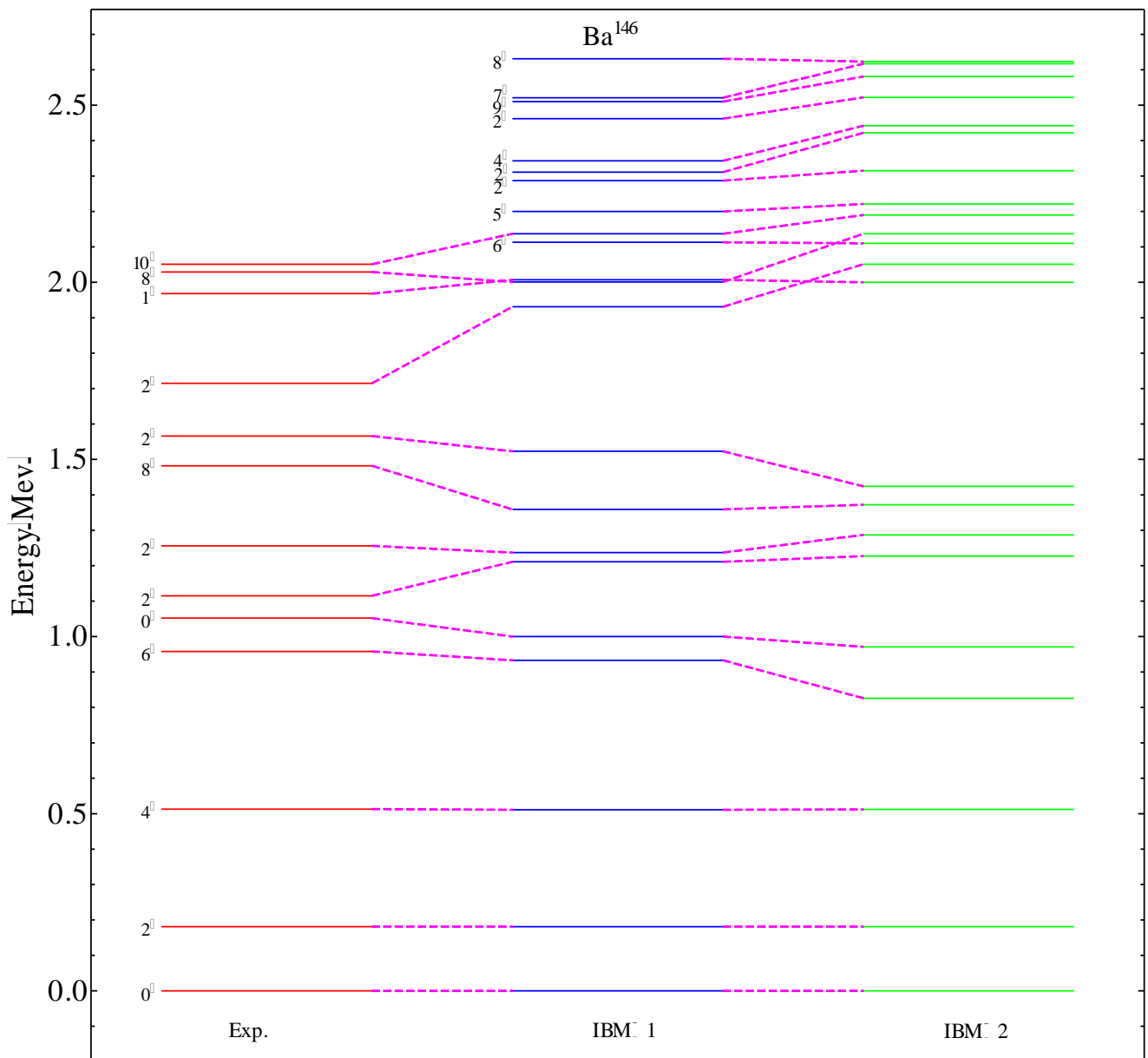


Fig. (3.13): Comparison between experimental data [105,114], IBM-1 and IBM-2 calculated energy levels for ^{146}Ba .

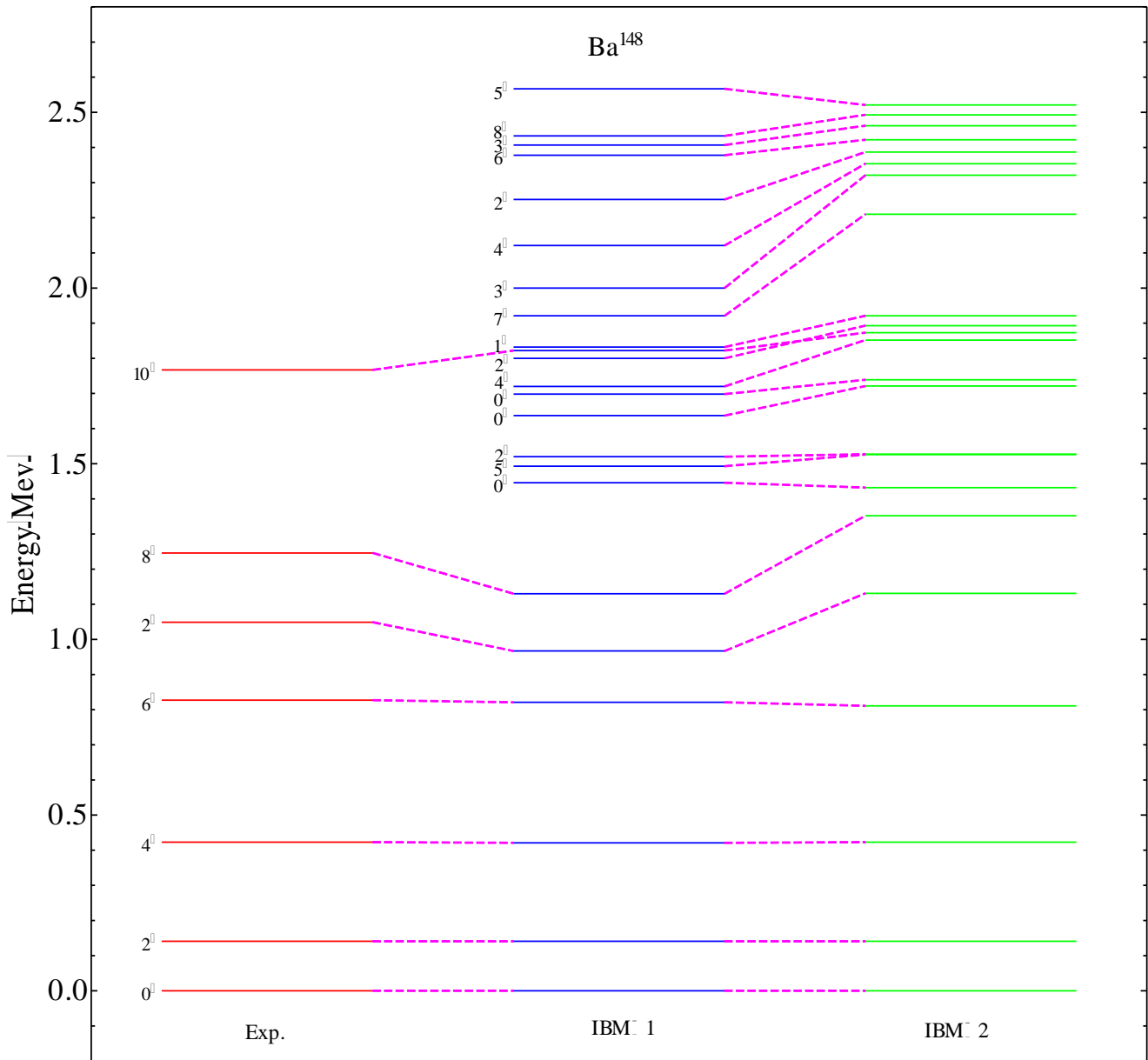


Fig. (3.14): Comparison between experimental data [105,114], IBM-1 and IBM-2 calculated energy levels for ^{148}Ba .

3-1-2 Potential Energy Surface

The potential energy surfaces, for barium isotopes as a function of the deformation parameters β and γ have been calculated using the Eq. (2-94). The calculated difference between prolate and oblate potential energy surfaces for Ba series of isotopes presented in Table (3-3), show that IBM-1 calculated the values of the PES for $^{122-134}\text{Ba}$ isotopes and obtained the V_{PO} (is the energy difference of the prolate and oblate minima in the potential energy curve) values of $^{120-140}\text{Ba}$ isotopes (see table (3-3)), which correspond to the PES. A flat PES at β_{min} for ^{122}Ba isotope. The finite V_{PO} for ^{122}Ba isotope accounts for the dynamics of the nuclear structure. The important requirement of the valid critical symmetries is that they represent the shape transition point in the shape variation with N or Z . In the physical view, it implies the shape transition at ^{128}Ba isotope to ^{130}Ba isotope in the (β, γ) variables.

In general, we obtain deeper prolate minima and shallower secondary oblate minima in all cases, both decreasing in depth with increasing neutron number. At ^{122}Ba , the prolate minimum is 3.14 MeV deep and the oblate minimum is 0.7 MeV deep and lies at lesser β value ($< \beta_{\text{min}}$). The same feature continues with increasing N . At ^{132}Ba isotope ($N = 76$) we get a very shallow prolate minimum and at $N = 78$ ^{134}Ba isotope a very shallow oblate minimum.

The difference in the depth of prolate and oblate minima, V_{PO} , is decreasing with increasing neutron number in our calculation. We obtain the prolate shape for the light Ba isotopes as in experimental data. At in $^{134-140}\text{Ba}$ isotopes $N = 78, 80$ and 84 V_{PO} is negative but we obtain almost vanishing prolate and oblate minima, or the predicted shape is not a permanently deformed one. In fact the predicted potential well at $N = 76, 78$ corresponds to the spherical shape anharmonic oscillator with flat bottom. The V_{PO} values obtained in Table (3-3) are rather small and its sign varies irregularly.

3-1-3 Electric Transition Probability B(E2)

The E2 transitions provide more stringent test of the IBM-1. The general E2 transition operator is given by the Eq. (2-6). The coefficient α_2 called the boson effective charge is an over all scaling factor for all B(E2) values which is determined from the fit to the $B(E2; 2_1^+ \rightarrow 0_1^+)$ value. The coefficient β_2 may be determined from the quadrupole moment $Q(2_1^+)$. The ratio $\beta_2 / \alpha_2 = \chi = -1.32$ in the SU(3) limit and is reduced to zero in the O(6) limit. In the “**FBEM**” program [82] the corresponding parameters are $\alpha_2 = (E2SD)$ and $\beta_2 = (1/\sqrt{5})(E2DD)$. The used parameters in T(E2) matrix element of $^{120-148}\text{Ba}$ isotopes are given in Table (3-5).

Table (3-5): The effective boson charges used in IBM-1 for the calculation of B(E2) transition probabilities for $^{120-148}\text{Ba}$ isotopes.

Isotopes	$E2SD (e.b)$	$E2DD (e.b)$
$Ba - 120$	0.112	-0.861
$Ba - 122$	0.104	-0.878
$Ba - 124$	0.105	-0.890
$Ba - 126$	0.110	-0.661
$Ba - 128$	0.110	-0.560
$Ba - 130$	0.125	-0.890
$Ba - 132$	0.143	-0.890
$Ba - 134$	0.145	-0.890
$Ba - 136$	0.130	-0.890
$Ba - 140$	0.132	-0.890
$Ba - 142$	0.133	-0.890
$Ba - 144$	0.135	-0.890
$Ba - 146$	0.137	-0.890
$Ba - 148$	0.138	-0.890

The reduced transition probability $B(E2; 2_1^+ \rightarrow 0_1^+)$ decreases gradually with increasing neutron number (N), which is well reproduced in IBM-1 (see Table (3-6)). The χ coefficient of the $(d^+d)^{(2)}$ term in reduced matrix element $T(E2)$ is kept at -1.215 .

In Table (3-6) the experimental absolute reduced transition probability $B(E2)$ values for the transitions from gamma band to ground state band ($\gamma \rightarrow g$) are few available. So we compare the IBM-1 values with the experimental data in Table (3-6). $B(E2; 2_2^+ \rightarrow 0_1^+)$ decreases with increasing neutron number (N) as expected for decreasing β (and increasing γ).

In Table (3-6) which shows that the electric transition probability for $\beta \rightarrow g$ and $\gamma \rightarrow g$ are smaller than the electric transition probabilities between $g \rightarrow g$ band, and in this table shows also that, in general, there is a good agreement between the experimental and theoretical $B(E2)$ values in ground state band in $^{120-148}\text{Ba}$ isotopes. The $B(E2; 6_1^+ \rightarrow 4_1^+)$ in $^{120-148}\text{Ba}$ isotopes, where the experimental and IBM-1 results of this transitions are weak in agreement. The experimental and IBM-1 $B(E2)$ calculations between beta and ground band and between gamma band in general are weakly in agreement except the transition $2_2^+ \rightarrow 0_1^+$ in some Ba isotopes and $2_3^+ \rightarrow 0_1^+$ also in some Ba isotopes which gave a good agreement.

For the transitions $B(E2; 3_1^+ \rightarrow 2_1^+)$ and $B(E2; 3_2^+ \rightarrow 2_1^+)$ seem to get weaker with increasing neutron number, because this transitions between different bands. The values of the transition $B(E2; 0_2^+ \rightarrow 2_1^+)$ is very small but the maximum value at ^{142}Ba isotope. The $B(E2)$ values of Ba isotopes as well as those in ref. [121] decrease smoothly as neutron number approaches $N = 80$ ^{136}Ba isotope, as can be seen in the Table (3-6).

Table (3-6)

Continued to Table (3-6)

Isotopes	$B(E2; 2_2^+ \rightarrow 2_1^+)$	$B(E2; 3_1^+ \rightarrow 2_2^+)$
----------	----------------------------------	----------------------------------

	Exp.	IBM-1	IBM-2	DDM	Exp.	IBM-1	IBM-2	DDM
¹²⁰ Ba	-	0.067	0.072	-	-	0.065	0.0700	0.0267
¹²² Ba	-	0.057	0.063	0.086	-	0.044	0.0540	0.0347
¹²⁴ Ba	-	0.158	0.166	0.117	-	0.0121	0.1270	0.0321
¹²⁶ Ba	0.13 (5)	0.141	0.136	0.146	-	0.073	0.0681	0.0265
¹²⁸ Ba	0.28(4)	0.310	0.264	0.248	-	0.028	0.025	0.017
¹³⁰ Ba	0.195	0.184	0.200	0.331	-	0.021	0.023	0.0059
¹³² Ba	0.141(41)	0.158	0.158	0.251	-	0.026	0.029	0.0023
¹³⁴ Ba	0.015	0.020	0.023	0.187	0.018(5)	0.022	0.0021	0.0017
¹³⁶ Ba	≥ 0.0022	0.0031	0.042	0.164	-	0.019	0.021	0.00134
¹⁴⁰ Ba	0.13 (5)	0.015	0.161	0.181	-	0.017	0.0188	0.0012
¹⁴² Ba	-	0.110	0.143	-	-	0.015	0.0169	-
¹⁴⁴ Ba	-	0.091	0.095	-	-	0.012	0.0145	-
¹⁴⁶ Ba	-	0.088	0.075	-	-	0.098	0.085	-
¹⁴⁸ Ba	-	0.0751	0.064	-	-	0.087	0.073	-

Experimental data are taken from refs. [105, 115, 116, 117, 118, 119, 120]

In the initial two-body Hamiltonian the E2 transition rates depend strongly on the value of χ parameter in the quadrupole operator. It is expected that this is still the case when cubic terms are added to the Hamiltonian as long as these do not substantially alter its eigen-states. In several of the Ba isotopes many B(E2) values between the low-lying states are known and these allow a test of the wave function in the calculation. The results are shown in Table (3-6). Generally a good agreement between experimental and calculated B(E2) values is obtained. One notable discrepancy is the $B(E2; 2_2^+ \rightarrow 0_1^+)$ transition in ¹³²Ba isotope with a calculated B(E2) value which is an order of magnitude too small. This value is equally small in the IBM-1 calculation without cubic interaction and is due to an accidental cancellation of terms with the Hamiltonian.

Calculation of the electromagnetic transition matrix elements, the high sensitivity of the results on the signs of the matrix elements of the transitions had to be addressed. The B(E2) branching ratios for Ba isotopes, we use the Alaga rule was utilized to evaluate the branching ratio. Using it in its square rooted version [25]:

$$\text{sgn} \left(\frac{\langle J_f \| T(E) \| J_i \rangle}{\langle J_f \| T(E2) \| J_i \rangle} \right) = \text{sgn} \left(\frac{\langle J_i K_i 2\Delta K | J_f K_f \rangle}{\langle J_i K_i 2\Delta K | J_f' K_f' \rangle} \right) \dots \dots \dots (3-2)$$

it can be used to deduce the relative signs of inter-band transitions from a state J_i, K_i into different states J_{f, K_f}^π and $J_{f', K'}^\pi$ of the same band with $K_f = K_{f'}$. In Eq. (3-2), the coefficients in angle brackets on the right-hand side denote **Clebsch-Gordan coefficients**. The ground state transition matrix elements of each state have been

chosen to be positive, the relative signs of the other decay matrix elements have been deduced from (3-2).

Table (3-7) given the $B(E2)$ branching ratios for $^{120-148}\text{Ba}$ isotopes. In the IBM-1 calculation, this variation is reproduced fairly well. The branching ratios $B(E2;2_2^+ \rightarrow 0_1^+)/B(E2;2_2^+ \rightarrow 2_1^+)$, $B(E2;3_1^+ \rightarrow 2_1^+)/B(E2;3_1^+ \rightarrow 2_2^+)$ and $B(E2;3_1^+ \rightarrow 2_1^+)/B(E2;3_1^+ \rightarrow 4_1^+)$ falling with increasing neutron number are also reproduced in IBM-1. The $B(E2;4_2^+ \rightarrow 2_1^+)/B(E2;4_2^+ \rightarrow 2_2^+)$ increased ratio increases with increasing neutron number in experimental data as in our calculation in IBM-1. While $B(E2;4_2^+ \rightarrow 4_1^+)/B(E2;4_2^+ \rightarrow 2_2^+)$, values decrease with increasing N , also $B(E2;0_2^+ \rightarrow 2_1^+)/B(E2;0_2^+ \rightarrow 2_2^+)$ and $B(E2;2_3^+ \rightarrow 2_2^+)/B(E2;2_3^+ \rightarrow 2_1^+)$ decreased with increasing neutron number, because the transitions between different bands.

The interband $B(E2)$ branching ratios provide valuable information on band mixings and the nature of the bands. In light Ba isotopes, even at mid shell ^{122}Ba the experimental $B(E2)$ ratio is = 0.2, way off the experimental value of $B(E2;3_1^+ \rightarrow 2_1^+)/B(E2;3_1^+ \rightarrow 4_1^+)$. At ^{128}Ba ($N = 72$) it falls to 0.1 and at ^{130}Ba isotope ($N = 74$) to 0.05 (Table (3-7)). In general up to $N = 70$, the IBM-1 values agree with experiment, but for $N > 70$, IBM-1 values decrease much more than experiment.

The IBM-1 values for $^{130-138}\text{Ba}$ isotopes are better but the slight variation with neutron number is opposite to the experimental trend.

The calculated absolute magnitude of quadrupole moment $Q(2_1^+)$ decreases smoothly with increasing neutron number N (see Table (3-4)). The same trend was predicted in experimental data. The negative sign signifies prolate shape in $^{120-140}\text{Ba}$ isotopes.

Table (3-7)

contained to Table (3-7)

continued to Table (3-7)

3-1-4 Magnetic Transition Probability $B(M1)$ and Mixing Ratio $\delta(E2/M1)$

To evaluate the magnetic transition probability $B(M1)$, we depend on Eq. (2-53), where the effective boson g -factor is estimated using the fact $g = Z/A$ is. The form (2-53) of the operator has no off-diagonal matrix elements, implying that in this approximation M1 transitions are forbidden [78, 79, 81]. Some of the transition probabilities obtained from perturbation theory are further discussed in refs. [78, 79].

The results shows that the transitions between low-lying collective states are weak. This is because of the increase of antisymmetric component in the wave functions. The magnitude of M1 values increase with increasing spin for $\gamma \rightarrow g$ and $\gamma \rightarrow \gamma$ transitions, see Table (3-8).

The $E2/M1$ multiple mixing ratios for $^{120-148}\text{Ba}$ isotopes, $\delta(E2/M1)$, were calculated for some selected transitions between states of $\Delta J = 0$. The sign of the mixing ratio must be chosen according to the sign of the reduced matrix elements. The equations used are (2-7) for M1 transitions and (2-109) for the mixing ratios. The results are listed in Table (3-9). The agreement with available experimental data [105, 124, 126, 127] is more than good especially in the sign of the mixing ratio. However, there is a large disagreement in the mixing ratios of $3^+ \rightarrow 2^+$, due to the small value of M1 matrix elements.

The IBM-1 formalism predicts essentially the same spin dependence for M1 transitions in $^{120-148}\text{Ba}$ isotopes as does a geometrical approach, and is thus capable of giving at least an equally good description of the data. In addition, the IBM-1 model yields the simple prediction that $\Delta(E2/M1)$ values of $\gamma \rightarrow \gamma$ and $\gamma \rightarrow g$ transitions should be equal for the same initial and final spins, and this prediction seems to be borne out empirically. It has been shown that different signs for $\beta \rightarrow g$ and $\gamma \rightarrow g$ $\Delta(E2/M1)$ values can be reproduced by the IBM-1 model.

Table (3-8)

Table (3-9)

continued to Table (3-9)

3-2 IBM-2 Results

3-2-1 Energy Spectra

In the phenomenological calculations the parameters appearing in the Hamiltonian ((Eq.(2-97)) may in general depend both on proton (N_π) and neutron (N_ν) boson number. Guided by the microscopic theory as "discussed in the Chapter Two we have assumed that only ε and κ , depend on N_π and N_ν i.e., $\varepsilon(N_\pi, N_\nu)$, $\kappa(N_\pi, N_\nu)$ while χ_ν depends only on N_ν and χ_π on N_π , i.e., $\chi_\nu(N_\nu)$, $\chi_\pi(N_\pi)$. Thus a set of isotopes, (constant N_ν) have the same value of χ_ν , while a set of isotones, (constant N_π), have the same value of χ_π . This parametrization allows one to correlate a large number of experimental data. Similarly, when a proton-proton $V_{\pi\pi}$ and neutron-neutron $V_{\nu\nu}$, interaction is added, the coefficients C_L are taken as $C_{L\pi}(N_\pi)$ and $C_{L\nu}(N_\nu)$, i.e. the proton boson interaction will only depend on N_π , and the neutron boson on N_ν . Since there is no information on the location of the states with mixed neutron-proton symmetry we kept the coefficients appearing in the Majorana force $M_{\pi\nu}$ (see table (3-10)).

The isotopes chosen in this work are $A = 120$ to 148 due to the presents of experimental data for the energy levels. We have $N_\pi = 3$ (6 protons outside the closed shell 50), and N_ν varies from 11 for ^{122}Ba to 4 for ^{140}Ba and increased from, 5 for ^{142}Ba to 8 for ^{148}Ba measured from the closed shell at 82. While the parameters ε , κ , χ_ρ , $C_{L\pi}$, $C_{2\nu}$ and $C_{4\nu}$ as well as the Majorana parameters ξ_k , with $k=1,2,3$, were treated as free parameters and their values were estimated by fitting with the available experimental values. The procedure was made by selecting the traditional value of the parameters and allowing one parameter to vary while keeping the others constant until the best fit with the experimental obtained. The parameters in the work of Subber [21,23] and the parameters of Turkan [19] have been used as starting parameters, with slight modification to fit the experimental data. This was carried out until one overall fit was obtained. The best values for the Hamiltonian parameters are given in Table (3-10).

The calculated energy levels are obtained by diagonalizing the Hamiltonian in Eq. (2-97) using the **NPBOS** code [94] that contains many free parameters; one has to estimate them to obtain better agreement with the experimental data. The parameter κ always has negative sign, and it represents the quadrupole interaction strengths and also depends on the d-boson numbers. The parameter χ_ν has positive values for $^{120-136}\text{Ba}$ isotopes and negative sign for $^{140-148}\text{Ba}$ isotopes and the parameter χ_π has a negative values for all Ba isotopes, the both parameters χ_ρ have an influence on the excitation energy and an important one on electromagnetic properties, so they are adjusted to reproduce the experimental data for transition probability.

Table (3-10): Parameters used in IBM-2 Hamiltonian for $^{120-148}\text{Ba}$ nuclei (all in MeV except χ_ν and χ_π are dimensionless)

Isotopes	ε	κ	χ_ν	χ_π	ξ_2	$\xi_1 = \xi_3$	$C_{2\nu}$	$C_{4\nu}$	$C_{0\pi}$	$C_{2\pi}$	$C_{4\pi}$
<i>Ba</i> – 120	0.631	-0.181	0.80	-1.20	0.121	1.22	0.0	0.0	0.0	0.0	0.0
<i>Ba</i> – 122	0.622	-0.193	0.80	-1.20	0.127	1.27	0.0	0.0	0.0	0.0	0.0
<i>Ba</i> – 124	0.611	-0.121	0.81	-1.20	0.135	1.35	0.0	0.0	0.0	0.0	0.0
<i>Ba</i> – 126	0.603	-0.121	0.78	-1.20	0.182	1.92	0.0	0.0	0.0	0.0	0.0
<i>Ba</i> – 128	0.602	-0.088	0.62	-1.20	0.190	2.28	0.0	0.0	0.0	0.0	0.0
<i>Ba</i> – 130	0.618	-0.088	0.55	-1.20	0.210	2.46	0.0	0.0	0.0	0.0	0.0
<i>Ba</i> – 132	0.688	-0.092	0.54	-1.20	0.236	2.78	-0.01	0.0	0.0	0.0	0.0
<i>Ba</i> – 134	0.810	-0.092	0.53	-1.20	0.241	2.88	-0.03	-0.03	0.0	0.0	0.0
<i>Ba</i> – 136	0.828	-0.088	0.52	-1.20	0.252	3.11	-0.035	-0.035	0.0	0.0	0.0
<i>Ba</i> – 140	0.770	-0.311	-0.18	-0.11	0.260	0.321	-0.06	-0.04	0.20	0.20	-0.40
<i>Ba</i> – 142	0.650	-0.300	-0.40	-0.29	-0.041	0.510	-0.11	-0.04	-0.10	0.20	-0.30
<i>Ba</i> – 144	0.341	-0.300	-0.40	-0.32	-0.061	0.510	-0.11	-0.04	-0.10	0.20	-0.50
<i>Ba</i> – 146	0.205	-0.280	-0.58	-0.34	-0.191	0.222	-0.16	-0.03	-0.10	0.20	-0.55
<i>Ba</i> – 148	0.252	-0.220	-0.68	-0.39	-0.042	0.222	-0.26	-0.01	-0.10	0.20	-0.10

$$C_{0\nu} = 0.0\text{MeV}$$

The parameters $C_{L\pi}$ are varying from isotope to another smoothly, this parameters is very important to reproduce the sequences of the ground state levels and the $0_{2,3}^+$ states .

The Majorana parameters $\xi_{1,2,3}$ is very important to study the mixed symmetry states, in the Table (3-10), the values $\xi_1 = \xi_3$ and ξ_3 changed gradually and smoothly from isotopes to another.

The energy level results of IBM-2 and experimental data are given in Figs. (3-1) to (3-14). The agreement between the theoretical and the experimental energy levels is, in general, good except for some cases of the high spin states, such as 0_2^+ , 0_3^+ , $2_{3,4}^+$ states; this indicates that these states is outside the IBM-2 space, which is the ‘intruder state’.

The energy ratios are given in Table (3-2), from this table we see the ratio $E(4_1^+)/E(2_1^+)$ is decreased smoothly from ^{120}Ba isotope to ^{140}Ba isotope at $N = 84$ because approach to the major shell ($N = 82$). This ratio equal 1.877 in ^{140}Ba isotope ($N = 84$) and increased again for ^{142}Ba isotope to ^{148}Ba isotope equal 3. In general the energy ratio decreases smoothly with increasing the N for $^{120-140}\text{Ba}$ isotopes, for all $^{120-140}\text{Ba}$ isotopes and it means that these structure seems to be verifying gamma soft rotor to vibrator nuclei (O(6) to SU(5)). The energy spectrum of the $^{126-136}\text{Ba}$ isotopes lie between vibrator (U(5) limit) and rotational (SU(3)) limit. The general features of the transition between U(5) in ^{140}Ba isotope near the beginning of the closed shell and SU(3) in ^{148}Ba isotope with moderate deformation are well reproduced by the IBM-1. In Table (3-2), we have introduced the experimental and IBM-2 values of the ratios,

$E(6_1^+)/E(2_1^+)$, $E(2_2^+)/E(2_1^+)$, $E(0_2^+)/E(4_1^+)$ and $E(0_2^+)/E(2_1^+)$ together with the values of IBM limits.

From Figs. (3-1) to (3-14), the energy states 0_2^+ (two phonon states) for example, ^{124}Ba isotope, the energy of 0_2^+ is equal to 0.898 MeV and 0.885 MeV in IBM-2 and is in good agreement with the experimental ones at 0.983 MeV and 0.872 MeV, in ^{126}Ba isotope, in the other hand in ^{134}Ba isotope the IBM-2 value 1.693 MeV and 1.760 MeV in experimental data which means that the experimental 0_2^+ at 1.760 MeV is the intruder state. It is interesting to note that our calculation reproduces the available experimental data well for all the low-lying levels in $^{140,148}\text{Ba}$ isotopes, except for the 0_2^+ state. The calculations show that the energy of the 0_2^+ state is predicted in a good agreement with the experimental data. The pedagogical calculations [128] with the $Z = 64$ shell assumption yield the correct energy ratios, and suggest that this sub-shell is still effective concerning the structure of these isotopes, especially for $N > 88$ [21].

The root mean square deviation (*RMSD*) [113], is used to compare the experimental and theoretical energy levels. Table (3-4) given the *RMSD* between experimental and IBM-2 energy levels. In this table we see the ground state levels the best agreement was found in ^{148}Ba isotope where the smallest value of *RMSD* is equal 0.0023 and equal 0.010 for gamma band in ^{124}Ba isotope. However *RMSD* = 0.0023 for beta band in ^{128}Ba isotope.

In general the IBM-2 calculations agree with the experimental data very well. The IBM-2 energy level values and experimental values do show some of degrees of staggering in the calculations a very small. In $^{126-140}\text{Ba}$ isotopes, the staggering is almost completely removed. The values of $J_i^+ = 0_2^+$, 0_3^+ states are too higher compared with experimental data in some Ba isotopes. These higher states in bands, most of them with angular momentum $J^\pi = 0^+$ may be the mixing states of bosons configurations and intruder configuration.

In order to investigate the effect of Majorana interaction parameters which is given in Table (3-10) on the energies of 2_2^+ , 3_1^+ and 2_3^+ states, the calculated energy is plotted in the as a function of Majorana parameters ξ_2 and $\xi_1 = \xi_3$ all the other parameters were kept at their best-fit values,. One can see from Figs. (3-1) to (3-14) that the energies of 2_2^+ , 3_1^+ , 2_3^+ and 2_4^+ states exhibit rapid response to the changes in the parameters compared to the others. This means that these states are good candidates for mixed symmetry states [129]. However, there are effects on the energies of these states as can be seen from the **Table (3-11)**. This is a good search method to clarify the mixed symmetry states. As hinted in **Table (3-11)**, we were unable to find one value of this parameter that fitted all the experimental values [21,23]. In rotational nuclei we see the 1_1^+ is a mixed symmetry states.

Table (3-11): Variation of the 2_2^+ , 3_1^+ , 2_3^+ , 4_2^+ and 4_3^+ energies as a function of Majorana parameters ξ_2 .

Isotopes	ξ_2	2_2^+	3_1^+	2_3^+	4_2^+	2_4^+
<i>Ba</i> – 120	0.121	0.825	-	1.627	1.123	-
<i>Ba</i> – 122	0.127	1.160	0.625	0.927	1.273	-
<i>Ba</i> – 124	0.135	0.867	1.006	1.314	1.298	-
<i>Ba</i> – 126	0.182	0.754	1.257	1.321	1.407	1.626
<i>Ba</i> – 128	0.190	0.879	1.221	0.977	1.311	1.822
<i>Ba</i> – 130	0.210	0.910	1.298	1.581	1.721	1.903
<i>Ba</i> – 132	0.236	1.084	1.621	1.711	1.782	2.172
<i>Ba</i> – 134	0.241	1.167	1.622	2.131	1.400	2.253
<i>Ba</i> – 136	0.252	2.117	2.250	2.193	1.987	2.191
<i>Ba</i> – 140	0.260	1.481	1.887	2.931	2.401	2.827
<i>Ba</i> – 142	-0.041	1.430	-	1.730	-	2.825
<i>Ba</i> – 144	-0.061	1.837	-	2.021	-	2.372
<i>Ba</i> – 146	-0.191	1.227	-	1.287	2.422	1.424
<i>Ba</i> – 148	-0.042	1.131	2.321	1.893	1.852	1.893

3-2-1 Electric Transition Probability B(E2)

Calculations of electromagnetic properties give us a good test of the nuclear models prediction. The electromagnetic matrix elements between eigenstates were calculated using the program *NPBTRN* for IBM-2 model.

From Eq.(2-102) we note that an E2 transition mainly depends on identifying proton and neutron bosons effective charges e_π and e_ν . These isotopes lying in region between U(5) limit (vibrational nuclei) and SU(3) limit (rotational nuclei), therefore, the relationship between (e_π, e_ν) and the reduced transition probability B(E2) for vibrational limit U(5) and rotational limit SU(3) is given in the form [11, 130, 131]:

$$B(E2; 2_1^+ \rightarrow 0_1^+) = \frac{(e_\pi N_\pi + e_\nu N_\nu)}{N} \dots\dots\dots(3-3) \quad \text{For SU(5) limit}$$

$$B(E2; 2_1^+ \rightarrow 0_1^+) = \frac{(2N + 3)(e_\pi N_\pi + e_\nu N_\nu)}{5N} \dots\dots\dots(3-4) \quad \text{For SU(3) limit}$$

where $B(E2; 2_1^+ \rightarrow 0_1^+)$ is the experimental reduced transition probability from the first excited states (2_1^+) to the ground state (0_1^+), N is the total number of bosons.

The relations (3-3) and (3-4), was used to estimate the effective boson charges for proton and neutron bosons (e_π, e_ν). In this calculations, we use the following criteria to determine the effective charges. $e_\pi = 0.2032 e.b$ is a constant throughout the whole isotopic chain and the e_ν changes with neutron number. This is true if the neutron (proton) interaction does not depend on the proton (neutron) configurations.

The values of e_π and e_ν are determined by fitting to the five $B(E2;2_1^+ \rightarrow 0_1^+)$ and $B(E2;2_2^+ \rightarrow 2_1^+)$ in ^{124}Ba and ^{140}Ba isotopes. They are given in Table (3-12).

Table (3-12): Effective charge used in E2 transition calculations ($e_\pi = 0.2032 e.b$).

Isotopes	^{120}Ba	^{122}Ba	^{126}Ba	^{128}Ba	^{130}Ba	^{132}Ba	^{134}Ba	^{136}Ba	^{140}Ba	^{142}Ba	^{144}Ba	^{146}Ba	^{148}Ba
e_ν (eb)	0.521	0.501	0.362	0.363	0.330	0.341	0.342	0.301	0.298	0.295	0.275	0.252	0.201

It is well known that absolute gamma ray transition probabilities offer the possibility of a very sensitive test of nuclear models and the majority of the information on the nature of the ground state has come from studies of the energy level spacing. The transition probability values of the excited state in the ground state band constitute another source of nuclear information. Yrast levels of even-even nuclei ($J_i = 2, 4, 6, \dots$) usually decay by $E2$ transition to the lower lying yrast level with $J_f = J_i - 2$.

In Table (3-6) we show the $B(E2;2_1^+ \rightarrow 0_1^+)$, $B(E2;4_1^+ \rightarrow 2_1^+)$ and $B(E2;6_1^+ \rightarrow 4_1^+)$ values, which are of the same order of magnitude and display a typical decrease towards the middle of the shell.

As a consequence of possible $M1$ admixture the $B(E2;3_1^+ \rightarrow 2_1^+)$ quantity is rather difficult to measure. There is no experimental data to compare the values of IBM-2. For ^{134}Ba isotope, we give the agreement with experimental value, from these values seems to decrease for $^{120-134}\text{Ba}$ isotopes and increased for $^{136-148}\text{Ba}$ isotopes.

In the Table (3-6), we show $B(E2;2_2^+ \rightarrow 0_1^+)$ values. Experimentally the results are radically different for the Ba isotopes. In the some Ba isotopes the value seems to increased towards the middle of the shell, whereas in another Ba isotopes is decreased. Our calculations could not reproduce these contradictory features simultaneously. The results for $B(E2;2_2^+ \rightarrow 0_1^+)$ values are shown in Table (3-6). This quantity is rather small since this transition is forbidden in all three limits of the IBM-1 [78, 79] as discussed in Chapter Two.

The quantity $B(E2;0_2^+ \rightarrow 2_1^+)$, which is shown in Table (3-6), provides a second clue for identifying intruder 0_2^+ states. If the experimental $B(E2;0_2^+ \rightarrow 2_1^+)$ value small largely deviates from the results of our calculation, it is very likely the observed 0_2^+ states does not correspond to the collective state, but it is rather an intruder state.

In ^{146}Ba isotope, there is a good agreement between experimental and calculated $B(E2;0_2^+ \rightarrow 2_1^+)$ value. This confirm our earlier statement about the nature of the lowest 0_2^+ state in this isotope. Other transitions $B(E2;2_3^+ \rightarrow 2_1^+)$ and $B(E2;2_3^+ \rightarrow 0_1^+)$ are small values because these transitions between different bands (cross over transitions) and the selection rules which determine these transition.

As a consequence of possible $M1$ admixture the $B(E2; 2_2^+ \rightarrow 2_1^+)$ quantity is rather difficult to measure. For $^{120-126}\text{Ba}$ isotopes, we give the different, conflicting experimental results and we see that no general feature can be derived from them, from these values seems to decrease for $^{120-126}\text{Ba}$ isotopes and decreased for $^{130-136}\text{Ba}$ isotopes.

The results for $B(E2; 0_2^+ \rightarrow 2_1^+)$ and $B(E2; 2_3^+ \rightarrow 2_1^+)$ values is rather small since this transition is forbidden in all three limits of IBM [78]. Our agreement with the available data is generally quite good. It should be noted that no attempt was made to fit any of the $B(E2)$ values while determining the parameters in the Hamiltonian.

In general the electric transition probabilities from the mixed-symmetry state $J^\pi = 3_1^+, 2_3^+$ to the symmetric states ($2_1^+, 2_2^+$) is weak collective $E2$ transition. The $E2$ transition between the $J^\pi = 3_1^+, 2_3^+$ and the 2^+ ground state is small, whereas $E2$ transitions are large between fully-symmetric states and between mixed-symmetry states.

One of the important property which can be calculated is the branching ratios, through which one can identify the position for the nuclei studied in Casten triangle, and hence to identify the dynamic symmetry for the nuclei by using the Alaga rule (Eq.(3-2)). Table (3-7) show the branching ratios for $^{120-148}\text{Ba}$ isotopes. These are compared with experimental data. Our agreement with available data is generally quite good, but it must be noted that in the some branching ratio the denominator is small and hence the ratio is very sensitive to experimental errors and/or precision in the numerical calculation.

3-2-3 Magnetic Transition Probability $B(M1)$ and Mixing Ratio δ ($E2/M1$)

The $M1$ transition operator is given in Eq.(2-107), where the gyromagnetic factors for bosons g_π and g_ν are estimated. The reduced $E2$ and $M1$ matrix elements were combined in a calculation of mixing ratio $\delta(E2/M1)$ using the relation which is given by Eq. (2-109).

Sambatora *et al.*, [132] suggested a total g -factor which is given in following equation:

$$g = g_\pi \frac{N_\pi}{N_\pi + N_\nu} + g_\nu \frac{N_\nu}{N_\pi + N_\nu} \dots\dots\dots(3-4)$$

is used to compute the 2_1^+ state g -factor. The value of the measured magnetic moment for ^{134}Ba isotope, $\mu = 2g = 0.86(10)\mu_N$ [130], and the experimental mixing ratio $\delta(E2/M1; 2_2^+ \rightarrow 2_1^+) = -7.4(9)eb/\mu_N$ [6, 130] for ^{134}Ba isotope were used to produce suitable estimation for the boson gyromagnetic factors. The values are $g_\pi = 0.473\mu_N$ and $g_\nu = 0.378\mu_N$. The results of the calculations are listed in Table (3-8). They are different from those of the rare-earth nuclei, ($g_\nu - g_\pi = 0.65\mu_N$), suggested by Van Isacker *et al.*, [133] also used $g_\pi = 1\mu_N$ and $g_\nu = 0\mu_N$ to reduce

the number of the model parameters in their calculation of $M1$ properties in deformed nuclei. The results of our calculation are listed in Table (3-8). As can be seen from the table yields to a simple prediction that $M1$ matrix elements values for gamma to ground band and transitions should be equal for the same initial and final spin. Also the size of gamma to ground band matrix elements seems to decrease as the mass number increases.

The results shows that the transitions between low-lying collective states are relatively weak. This is because of the increase of the anti-symmetric component in the wave functions introduced by F -spin breaking in the Hamiltonian. The magnitude of $M1$ values increases with increasing spin for $\gamma \rightarrow g$ and $\gamma \rightarrow \gamma$ transitions and we see:

- 1- By fitting $B(M1)$ from 2_2^+ to 2_1^+ we always get small value for $g_\nu - g_\pi$ compared with the value basis on the microscopic calculations $g_\nu - g_\pi = 1\mu_N$.
- 2- There are evidences that $M1$ small mode exists in all spectra.
- 3- The IBM-2 predicts small $M1$ component which is due to symmetry and forbiddances of band crossing gamma transitions.
- 4- The $\gamma \rightarrow \gamma$ $M1$ matrix elements are larger than the $\gamma \rightarrow g$ $M1$ matrix elements by a factor of 2 to 3. Again, this agree qualitatively with the perturbation expressions derived in ref. [134].
- 5- The size of the $\gamma \rightarrow g$ $M1$ matrix elements seems to decrease with increasing mass. Specially, a change in $\gamma \rightarrow g$ $M1$ strengths occurs when the gamma band crosses the beta band.

These five aspects of $M1$ data shown in Table (3-8) are reproduced by the calculation through a smooth variation of the parameters ε and $\Delta\chi$, and with a few exceptions (e.g., some $\gamma \rightarrow g$ transitions in ^{136}Ba isotope and $3_1^+ \rightarrow 2_1^+$ transition in ^{140}Ba) good agreement between the theory and the experimental data is achieved.

The calculated values for $B(M1)$ are acceptable to some extent, where some of $B(M1)$ values are small compared to the values of the quadrupole transition probabilities because the wavelength of the gamma ray transitions is greater than it is in the magnetic transitions according to the following the relationship: $\lambda(ML) = 0.3A^{-2/3}\lambda(EL)$. This relation shows that the $B(M1)$ transition probability is less than $B(E2)$ transition probability and our results confirm this.

Table (3-13) given the g -factor in μ_N units for $^{120-148}\text{Ba}$ isotopes for first excited state (2_1^+) and second excited state (2_2^+) which compared with the experimental data. The g -factor of a state $|k\rangle$ is given by [135]:

$$g_k = \frac{\langle k \| T(M1) \| k \rangle}{\langle (\sqrt{3}/4\pi)(L_\pi + L_\nu) \| K \rangle} \dots\dots\dots(3-5)$$

Table (3-13): Experimental and IBM-2 calculations for g-factors for ¹²⁰⁻¹⁴⁸Ba μ_N units.

Isotopes	¹²⁰ Ba	¹²² Ba	¹²⁶ Ba	¹²⁸ Ba	¹³⁰ Ba	¹³² Ba	¹³⁴ Ba	¹³⁶ Ba	¹⁴⁰ Ba	¹⁴² Ba	¹⁴⁴ Ba	¹⁴⁶ Ba	¹⁴⁸ Ba
$g(2_1^+)$	0.542	0.511	0.488	0.471	0.442	0.439	0.414	0.395	0.385	0.355 (0.424)	0.312 (0.34)	0.290 (0.28)	0.240
$g(2_2^+)$	1.682	1.632	1.621	1.601	1.571	1.532	1.522	1.497	1.481	1.322	1.148	1.411	1.047

Experimental data are taken from ref. [136].

We evaluate the mixing ratio $\delta(E2/M1)$ for ¹²⁰⁻¹⁴⁸Ba isotopes, depends on the Eq.(2-109). The resulting of IBM-2 calculation for $\delta(E2/M1)$ together with experimental values are shown in Table (3-9). For this calculation we used the standard boson g- factors $g_\pi = 0.473\mu_N$ and $g_\nu = 0.378\mu_N$.

We were able to reproduce the 2_1^+ g-factors as well as most of the $\delta(E2/M1)$ mixing ratios. In particular, all the signs are reproduced correctly. It should be noted that a sign change appears in both the $\delta(2_2^+ \rightarrow 2_1^+)$ and $\delta(2_3^+ \rightarrow 2_1^+)$ transition mixing ratios, when going from isotope to another. Moreover, in some isotopes there is an opposite sign between the $\delta(2_2^+ \rightarrow 2_1^+)$ mixing ratio and the $\delta(3_1^+ \rightarrow 2_1^+)$ mixing ratio. We were able to reproduce all of these features in the calculation. Mainly, the sign change of $\Delta\varepsilon$ and $\Delta\chi$ for ¹²⁰⁻¹³⁰Ba isotopes in comparison to ¹³²⁻¹³⁶Ba is responsible for this effect. We also calculated the admixtures of lower F-spin states in the ground state. They are 1.6%, 2.2%, 1.3% for ¹⁴⁴⁻¹⁴⁶⁻¹⁴⁸Ba isotopes respectively.

These results exhibit disagreement in some cases, with one case showing disagreement in sign. However, it is a ratio between very small quantities and any change in the dominator that will have a great influence on the ratio. The large calculated value for $\delta(2_2^+ \rightarrow 2_1^+)$ is not due to a dominant E2 transition, but may be under the effect of very small M1 component in the transition. Moreover, the large predicted value for transition $\delta(2_2^+ \rightarrow 2_1^+)$ in ¹²⁰Ba isotope and ¹⁴²⁻¹⁴⁶Ba isotopes compared with experimental value may be related to high predicted energy level value of the IBM-2; (2_2^+) $E = 0.825$ MeV in ¹²⁰Ba isotope and $E = 1.430$ MeV, 1.752 MeV and 1.227 MeV respectively, while the experimental values is 1.424 MeV, 1.848 MeV and 1.115 MeV. We are unable to bring the energy value of this state close to experimental value simply by changing the Majorana parameters.

The sign of the mixing ratio must be chosen according to the sign of the reduced matrix elements. The equations used are (2-107) for M1 transitions and (2-109) for the mixing ratios. The results are listed in Table (3-9). The agreement with available experimental data [105, 125, 126, 127] is more than good especially in the sign of the mixing ratio. However, there is a large disagreement in the mixing ratios of some transitions, is not due to a dominate E2 transition, but may be under the effect of

very small value of M1 matrix element. However, it is a ratio between very small quantities and may change in the denominator that will have a great influence on the ratio.

3-2-4 Electric Monopole Transition Matrix element $\rho(E0)$

Electric monopole (E0) transitions between nuclear levels proceed mainly by internal conversion with no transfer of angular momentum to the ejected electron. For transition energies greater than $2m_0c^2$, electron-positron pair creation is also possible; two-photon emission is possible at all energies but extremely improbable. The E0 transition also occurs in cases where the levels have the same spin and parity. This means that the E0 transition competes with E2 and M1 components in these transitions.

The reduced matrix monopole transition is given in Eq.(2-114), the necessary parameters of the monopole matrix element $\rho(E0)$ are derived from fitting the isotope and isomer shifts ($\beta_{0\pi} = 0.053 fm^2$, $\beta_{0\nu} = -0.020 fm^2$). The IBM-2 results of $\rho(E0)$ values are available upon request, see Table (3-14).

Table (3-14) : Monopole Matrix Element $\rho(E0)$ in e.b for $^{120-148}\text{Ba}$ isotopes in IBM-2 .

$J_i^+ \rightarrow J_f^+$	1	1	1	12	12	12	13	B	13	13
	2	2	2	6	8	8	0	a	4	6
	B	B	B	B	B	B	B	¹³ a	B	B
	a	a	a	a	a	a	a	2	a	a
$2_2 \rightarrow 2_1$	0. 0 0 5	2 . 8 7	0 . 0 8 3	0. 1 8 7	0. 2 8 7	0. 0 7 8	0. 0 8 6	0. 0 5 2	0. 0 4 6	0. 0 2
$0_2 \rightarrow 0_1$	0 . 1 7 3	0 . 1 7 2	0 . 1 6 4	0. 0 9 8	0. 0 7 2	0. 0 7 3	0. 0 8 4	0. 0 7 3	0. 0 5 3	0. 0 9 7
$0_3 \rightarrow 0_1$	0 . 1 2 6	0 . 1 5 3	0 . 1 6 9	0. 0 8 7	0. 0 3 5	0. 0 6 5	0. 0 9 3	0. 0 1 1	0. 0 5 5	0. 0 4 4
$0_3 \rightarrow 0_2$	0 . 0 8 3	0 . 1 0 8	0 . 1 3 6	0. 0 3 4	0. 0 6 6	0. 0 3 5	0. 0 8 7	0. 0 3 4	0. 0 3 1	0. 0 8 9
$J_i^+ \rightarrow J_f^+$	1 . 0	¹ a . 2	1 4 4	14 6 B	14 8 B					

	B a	B a	B a	a	a
2 ₂	0.	2	0	0.	0.
→	0	.	.	1	2
2 ₁	0	8	0	8	8
	5	7	8	7	7
			3		
0 ₂	0	0	0	3.	0.
→	.	.	.	1	0
0 ₁	1	1	1	×	0
	7	7	6	1	7
	3	2	4	0	2
				3	
				3	
0 ₃	0	0	0	0.	0.
→	.	.	.	0	0
0 ₁	1	1	1	8	0
	2	5	6	7	3
	6	3	9		5
0 ₃	0	0	0	0.	0.
→	.	.	.	0	0
0 ₂	0	1	1	0	6
	8	0	3	3	6
	3	8	6	4	6

In ¹²⁰⁻¹⁴⁸Ba isotopes $\rho(E0)$ values increased in some isotopes with increasing neutron numbers and decrease for some isotopes and they go up to the highest value at some isotopes. This means that all the isotopes are deformed because they possess the amount of excess energy and that they are trying to get rid of this by lessen the E0 transitions to the state of stability. This is an additional evidence of the deformation of these isotopes.

We notice that the theoretical values for the $X (E0/E2)$ ratio are small, for some transitions (see Table (3-15)) which means that there is a small contribution of E0 transition on the life time of the 0^+ states. There are two high values of $X (E0/E2)$ in transitions from $0_2^+ \rightarrow 0_1^+$ in ¹²⁰⁻¹⁴⁸Ba isotopes means that this state decay mostly by the E0 and according to this one could say that the study of this state give information about the shape of the nucleus, because the E0 transitions matrix elements connected strongly with the penetration of the atomic electron to the nucleus. So combination of the wave-function of atomic electron, which is well known, and the nuclear surface give good information of the nuclear shape.

From the table, one can overall see a reasonable agreement with the experimental data for ¹³⁴Ba isotope. The $X(E0/E2)$ ratio are important for nuclear structure and the model predictions due to their sensitivity for the nuclear shape. We conclude that more experimental work is needed to clarify the band structure and investigate an acceptable degree of agreement between the predictions of the models and the experimental data. The $B(E2)$ between the ground band states, the quasi- γ and quasi- β band states are also described which is used to evaluate this ratio.

Table (3-15): $X(E0/E2)$ $^{120-148}\text{Ba}$ isotopes in IBM-2 .

$J_i^+ \rightarrow J_f^+$	^{120}Ba	^{122}Ba	^{124}Ba	^{126}Ba	^{128}Ba	^{128}Ba	^{130}Ba	Ba^{132}	^{134}Ba	^{136}Ba
$2_2 \rightarrow 2_1$	2.11	1.33	2.317	1.38	2.471	2.414	0.197	0.146	0.73 (0.69)	15.32
$0_2 \rightarrow 0_1$	0.0037	0.0023	0.0047	0.0054	0.057	0.006	0.143	0.187	2.251 (2,8(2))	23.2
$0_3 \rightarrow 0_1$	0.022	0.015	0.0281	0.018	0.0221	0.022	12.22	10.2	0.0073	0.0089
$0_3 \rightarrow 0_2$	0.0031	0.0027	0.0038	0.0028	0.0034	0.004	0.211	0.642	9.65	12.26
$J_i^+ \rightarrow J_f^+$	^{140}Ba	^{142}Ba	^{144}Ba	^{146}Ba	^{148}Ba					
$2_2 \rightarrow 2_1$	5.447	6.872	0.101	0.21	7.221					
$0_2 \rightarrow 0_1$	1.227	0.873	0.197	0.182	2.621					
$0_3 \rightarrow 0_1$	0.0032	0.0086	0.19	0.231	5.2×10^{-2}					
$0_3 \rightarrow 0_2$	3.729	5.327	1.671	2.61	1.778					

The Experimental data are taken from ref. [23,105]

3-2-5 Mixed Symmetry States in $^{120-148}\text{Ba}$ Isotopes

One of the great advantages of the IBM-2 is the ability of reproducing the mixed symmetry states (*MSS's*). These states are created by a mixture of the wave function of protons and neutrons that are observed in most even-even nuclei. This mixed symmetry (*MSS's*) state has been observed in many deformed nuclei. In more vibrational (near spherical nuclei) and gamma-soft nuclei, we expect the lowest mixed-symmetry states (*MSS's*) with the $J^\pi = 2^+$ state, while in rotation nuclei observed as the $J^\pi = 1^+$ state. Hamilton *et al.*, [11] studied the mixed-symmetry states (*MSS's*) state in ^{140}Ba isotopes, to be 2_3^+ state at about 2 MeV.

From the results of energy levels we can see that the energies of $J_i^\pi = 2_3^+, 2_4^+$ states exhibit rapid response to the changes in the Majorana parameters compared to the others (see Table (3-10)). This means that these states are good candidates for mixed symmetry states [137]. However, there are effects on the energies of γ -band $J_i^\pi = 2_2^+, 3_1^+$ and $J_i^\pi = 4_2^+$, as can be seen from the Figs.(3-1) to (3-14). This is a good search method to clarify the mixed symmetry states (*MSS,s*). Fazekas *et al.*, [138] have suggested that the two states at 2.029 and 2.088 MeV should share the properties of the mixed symmetry state in ^{134}Ba isotope.

In this work, we proposed that the $J_i^\pi = 2_3^+$ state in ^{142}Ba isotope decays to the first excited state with an energy (IBM-2) of 1.730 MeV with a mixing ratio $\delta(2_3^+ \rightarrow 2_1^+) = -0.88$, which means it is dominated by the *M1* transition, with $B(M1; 2_3^+ \rightarrow 2_1^+) = 0.091 \mu_N^2$. In ^{142}Ba isotope, for the $J_i^\pi = 2_3^+$ state at energy 1.730 MeV excitation is close to the experimental value for 1.693 MeV. The energy is well reproduced by the calculation, where the choice of the Majorana parameters ($\xi_1 = \xi_3$ and ξ_2) plays a important (crucial) role. This state is quite pure, $F_{\max} = 1$, with :

$$R = \frac{\langle J|F^2|J \rangle}{F_{\max}(F_{\max} + 1)} = 50\%$$

In ^{146}Ba isotope, the IBM-2 calculation predicted the $J_i^\pi = 2_3^+$ state at 1.287 MeV with $R = 84\%$ and the $J_i^\pi = 2_4^+$ state at 1.424 MeV with $R = 75\%$. We obtained a large $M1$ strength for $B(M1; 2_3^+ \rightarrow 2_1^+) = 0.142\mu_N^2$ in comparison with $B(M1; 2_4^+ \rightarrow 2_1^+) = 0.074\mu_N^2$. These values indicated that the $J_i^\pi = 2_4^+$ state is the lowest mixed symmetry state in ^{146}Ba isotope.

In ^{148}Ba isotope, the IBM-2 calculation predicted the $J_i^\pi = 2_3^+$ state at 1.527 MeV with $R = 85\%$ and the $J_i^\pi = 2_4^+$ state at 1.893 MeV with $R = 74\%$. We obtained a large $M1$ strength for $B(M1; 2_3^+ \rightarrow 2_1^+) = 0.0110\mu_N^2$ in comparison with $B(M1; 2_4^+ \rightarrow 2_1^+) = 0.103\mu_N^2$. These values indicated that the $J_i^\pi = 2_4^+$ state is the lowest mixed symmetry state in ^{148}Ba isotope.

Table (3-16): B(M1) calculated to first excited states in μ_N^2 units for $^{120-148}\text{Ba}$ isotopes

Isotopes	$B(M1; 2_2^+ \rightarrow 2_1^+)$	$B(M1; 2_3^+ \rightarrow 2_1^+)$	$B(M1; 2_4^+ \rightarrow 2_1^+)$
<i>Ba</i> – 120	0.022	0.00210	0.0045
<i>Ba</i> – 122	0.0201	0.00293	0.0041
<i>Ba</i> – 124	0.0188	0.0030	0.0039
<i>Ba</i> – 126	0.0046	0.0031	0.00321
<i>Ba</i> – 128	0.0362	0.00341	0.00296
<i>Ba</i> – 130	0.045	1.414×10^{-3} Exp. ($\geq 1.2 \times 10^{-3}$)	0.0027
<i>Ba</i> – 132	0.016	0.0455	0.113
<i>Ba</i> – 134	0.046	0.0463	0.142
<i>Ba</i> – 136	0.009	0.05414	0.187
<i>Ba</i> – 140	0.246	0.0692	0.0106
<i>Ba</i> – 142	0.035	0.0910	0.0081
<i>Ba</i> – 144	0.0046	0.130	0.0021
<i>Ba</i> – 146	0.0021	0.142	0.0711
<i>Ba</i> – 148	0.0002	0.011	0.1044

In ^{148}Ba isotope, the IBM-2 calculation predicted the $J_i^\pi = 2_3^+$ state at 1.527 MeV with $R = 85\%$ and the $J_i^\pi = 2_4^+$ state at 1.893 MeV with $R = 74\%$. We obtained a large $M1$ strength for $B(M1; 2_3^+ \rightarrow 2_1^+) = 0.0110\mu_N^2$ in comparison with $B(M1; 2_4^+ \rightarrow 2_1^+) = 0.103\mu_N^2$. These values indicated that the $J_i^\pi = 2_4^+$ state is the lowest mixed symmetry state in ^{148}Ba isotope.

The experimental and theoretical campaign for the investigation of the Ba isotopes had been motivated by the search for one quadrupole-phonon states of mixed proton-neutron symmetry 2_{1M}^+ in these nuclei. In ^{130}Ba isotope there is no absolute value for a $B(M1; 2_i^+ \rightarrow 2_1^+)$ could be deduced, because, except for the $J_i^\pi = 2_3^+$ state, no multipole mixing ratio has been known from experiments, due to the lack of sufficient statistics in the respective transitions. All of the results on $B(M1; 2_i^+ \rightarrow 2_1^+)$ values in this nucleus are, thus, based on assumptions of pure transitions, and, for most of the assumed 2^+ states, also on estimates of their ground-state transition intensities. For the decay of the $J_i^\pi = 2_3^+$ state at 1.581 MeV to the $J_i^\pi = 2_1^+$ state two possible values for the mixing ratio $\delta(2_3^+ \rightarrow 2_1^+) = -23(9)$ experimentally and -20.44 IBM-2 results, corresponding to a nearly pure $E2$ transition and $\delta(2_3^+ \rightarrow 2_1^+) = 0.31(2)$, corresponding to a $>90\%$ $M1$ contribution to this transition. The transition strengths have been calculated for both values. The results on the $B(M1; 2_3^+ \rightarrow 2_1^+)$ show that even for the nearly pure $M1$ transition the strength of experimental data [25] $B(M1; 2_3^+ \rightarrow 2_1^+) > 1.2 \times 10^{-3} \mu_N^2$ while the IBM-2 value for this transition equal $1.414 \times 10^{-3} \mu_N^2$ is only quite small. The ground state transition strength of electric transition probability $B(E2; 2_3^+ \rightarrow 0_1^+) = 0.0021e^2b^2$ is very small, too. These values are considerably smaller than what would be expected for a $J_i^\pi = 2_{1,M}^+$ state and indicate that the $J_i^\pi = 2_3^+$ state does not contain a considerable fraction of the $J_i^\pi = 2_{1,M}^+$ wave function.

In ^{136}Ba isotope an isolated mixed-symmetry state $J_i^\pi = 2_3^+$ at 2.193 MeV had been identified. In the even-even neighbor ^{134}Ba isotope the mixed-symmetry state has been observed to fragment over two close-lying 2^+ states $J_i^\pi = 2_3^+$ at 2.131 MeV and 2.171 MeV. This decrease in energy continues for the present results on ^{132}Ba isotope. Here, a small fragment of the mixed symmetry states (MSS 's) has been identified at an energy of 1.711 MeV. Further candidates for $J_i^\pi = 2_{1,M}^+$ -fragments in this nucleus are the states at 1.977 MeV, and, based on different assumptions, at 2.414 MeV, 2.482 MeV, and 2.962 MeV. None of the possible $J_i^\pi = 2_3^+$ -fragments in ^{132}Ba isotope exhibits a $B(M1; 2^+ \rightarrow 2_1^+)$ of similar strength as it has been observed in the $^{134,136}\text{Ba}$ isotopes. A state with the expected properties of an isolated mixed-symmetry states (MSS 's) state can be excluded in ^{132}Ba isotope below 2.8 MeV based on the experimental data.

We obtained a large $M1$ strength for $(2_4^+ \rightarrow 2_1^+)$ transition, $B(M1) = 0.1044 \mu_N^2$ in comparison with $B(M1; 2_3^+ \rightarrow 2_1^+) = 0.011 \mu_N^2$. These values indicated that the $J_i^\pi = 2_4^+$ state is the lowest mixed symmetry state in ^{148}Ba isotope. Table (3-15) presents the calculated $B(M1)$ to the $J_i^\pi = 2_1^+$ state. For the g -factor value of $J_i^\pi = 2_1^+$ states, our calculations agree well with the available experiment. All $J_i^\pi = 2_1^+$ states have positive g -factor as shown in Table (3-8).

The IBM-2 calculation of $B(M1; (2_{1819}^+ \rightarrow 2_1^+)) = 4.1 \times 10^{-3} \mu_N^2$ while the experimental value equal to $\geq 3.50 \times 10^{-3} \mu_N^2$ [25] is also quite small in ^{130}Ba isotope. Also the result of $B(E2; (2_{1.819}^+ \rightarrow 2_1^+)) = 0.00043 e^2 b^2$ is small. Again, these values do not allow for the identification of a significant fragment of the $J_i^\pi = 2_{1,Ms}^+$ state.

The theoretical value of $B(M1; (2_{2.269}^+ \rightarrow 2_1^+)) = 5.1 \times 10^{-3} \mu_N^2$ and experimentally equal $\geq 4.67 \times 10^{-3} \mu_N^2$ these values are very small when compared to the expectation of an isolated $J_i^\pi = 2_{1,Ms}^+$ state. The value of quadrupole electric transition probability for this transition $B(E2; (2_{2.269}^+ \rightarrow 2_1^+)) = 0.00056 e^2 b^2$ is stronger (greater) than for the 1.819 MeV state.

The estimate of the decay rates of the (2^+) 2.371 MeV state has been made under the same assumptions of $J^\pi = 2^+$ and of a pure $M1$ transition to the $J_i^\pi = 2_1^+$ state. The result of $B(M1; (2_{2.371}^+ \rightarrow 2_1^+)) = \geq 0.134 \mu_N^2$ [25] and the IBM-2 value is $0.166 \mu_N^2$ represents the strongest $M1$ transition strength for this isotope. Its magnitude nearly fulfills the expectations on an isolated $J_i^\pi = 2_{1,Ms}^+$ state. Also the result of $B(E2; (2_{2.371}^+ \rightarrow 0_1^+)) = 0.00035 e^2 b^2$ meets the expectation for the order of magnitude of this transition strength. However, these numbers are based on numerous assumptions, beginning with the unknown J_i^π assignment. In this energy range the excitation of states can be ruled out that are not fed from above and have angular momentum quantum numbers $J^\pi \neq 3^-$ or 2^+ [25].

Consequently, based on the given data the state at 2.371 MeV can be assigned a *candidate* of an isolated $J_i^\pi = 2_{1,Ms}^+$ state in ^{130}Ba provided the underlying assumptions of $J_i^\pi = 2_{1,Ms}^+$ and of a predominant $M1$ transition to the $J^\pi = 2^+$ state are valid. The other $J^\pi = 2^+$ states at 1.557 MeV, 1.819 MeV, and 2.269 MeV exhibit nearly vanishing $B(M1; J_i^\pi = 2_i^+ \rightarrow 2_1^+)$ values and can, thus, be identified at most as weak fragments of the $J_i^\pi = 2_{1,Ms}^+$ state. In ^{132}Ba isotope, for three higher-lying states the spin and parity assignment $J^\pi = 2^+$ has been assumed. Under the additional assumption of pure $M1$ decays into the $J_i^\pi = 2_1^+$ state, estimates on lower limits on their possible $M1$ decay rates have been made.

The values of $B(M1; 2_{2,400}^+ \rightarrow 2_1^+) = \geq 0.026\mu_N^2$, $B(M1; (2_{2,439}^+ \rightarrow 2_1^+) = \geq 0.012\mu_N^2$ and $B(M1; 2_{2,686}^+ \rightarrow 2_1^+) = \geq 0.012\mu_N^2$ [25], but the values of IBM-2 for these transitions are given $0.031\mu_N^2$, $0.0161\mu_N^2$ and $0.0182\mu_N^2$ respectively, the experimental and theoretical values do not exhibit a pronounced $M1$ strength. The corresponding ground-state transition strengths are of the order of $0.024 \mu_N^2$ to $0.035 \mu_N^2$. Based on these data, the three states at 2.400 MeV, 2.439 MeV and 2.686 MeV can at most be interpreted as *candidates* for fragments of the $J_i^\pi = 2_{1,Ms}^+$ state, provided that the assumptions made in the calculations could be confirmed.

On the basis of the present results it can be concluded that no prominent, isolated $J_i^\pi = 2_{1,Ms}^+$ state has been observed in the nucleus ^{132}Ba isotope below an energy of 2.7 MeV. From the $B(M1)$ strength distributions only weak fragments of the mixed symmetry state could possibly be identified in this isotope.

The experimental data on the $B(M1; 2_i^+ \rightarrow 2_1^+)$ strengths of the Ba isotopes completed the experimental data on the one quadrupole-phonon state of mixed proton-neutron symmetry $J_i^\pi = 2_{1,Ms}^+$ in the $A = 130$ mass region. The new data enabled a discussion of the evolution of the $J_i^\pi = 2_{1,Ms}^+$ state as well as for the Ba isotopic chain. The results seem to support the previous observation of an increased fragmentation of the $J_i^\pi = 2_{1,Ms}^+$ state for mid-shell nuclei of that mass region. However, the results showed an enhanced candidate of a $J_i^\pi = 2_{1,Ms}^+$ state in $^{130-134-136}\text{Ba}$ that hampers a unified view of the results and their interpretation, but whose results are based on several assumptions during the calculations, beginning with the $J^\pi = 2^+$ assignment. Any further discussion on the evolution of the mixed symmetry states in this mass region will, therefore, depend on an independent verification or falsification of the assumptions made for the calculations on the 2.371 MeV state of ^{130}Ba isotope.

The scissor state $J^\pi = 1^+$ which is the state with mixed symmetry state depend on the Majorana parameter, so that the $J^\pi = 1^+$ states in Ba isotopes determined by the ξ_3 parameter. The calculated energies of the all $J^\pi = 1^+$ states are listed in Table (3- 17). The values of all $J^\pi = 1^+$ states are greater than 2.00 MeV, which are closed to the values of $J^\pi = 1^+$ states of the neighboring nuclei, and agree with the experimental data.

Table (3-17): Experimental and calculated for 1^+ level for $^{126-142}\text{Ba}$ isotopes in MeV units.

Isotope	^{126}Ba	^{128}Ba	^{130}Ba	^{132}Ba	^{134}Ba	^{136}Ba	^{140}Ba	^{142}Ba
E(1^+) Exp.	2.622	2.431	2.827	2.962	2.618	2.687	2.671	3.261
E(1^+) Theo.	-	2.347	2.733	2.846	2.570	2.693	2.692	3.144

From the above consideration the following signature for one-phonon $MSSs$ in vibrational and transitional nuclei with, at least, approximate $O(5)$ symmetry, can be expected:

- 1- The one-phonon $2_{1,M}^+$ state should be the lowest-lying mixed symmetry state.
- 2- This $2_{1,M}^+$ state should decay to the 2_1^+ by a strong $M1$ transition with an absolute matrix element of about $1 \mu_N^2$.
- 3- Since the $2_{1,M}^+$ state is a one-phonon excitation it should have collective $E2$ matrix elements to the ground state for both, proton and neutron bosons, however, with opposite signs, which might lead to partial cancellation in the total, $\langle 2_{1,M}^+ \| E2 \| 0_1^+ \rangle$ matrix element. Thus, a small-to-weakly-collective $E2$ transition strength (\leq a few *e.b.*) from the $2_{1,M}^+$ state to the ground state can be expected.
- 4- All mixed symmetry states have to be very short lived, typically a few hundred femto-seconds or less, because of the strong $M1$ matrix elements and typical transition energies greater than 1 MeV in vibrational nuclei.

Even though the mixed symmetry states are defined in the framework of a collective algebraic model, their properties are strongly influenced by the underlying shell structure. However, the relation between the properties of the mixed symmetry states and the specific microscopic structure is not completely understood.

From the above fingerprints it is obvious that the mixed symmetry states can be identified experimentally by their unique decay to the low-lying fully symmetry states [139]. This however, comprises a major experimental challenge because it requires full spectroscopic information, *i.e.* the spin and parity quantum numbers of these highly excited non-yrast states, their lifetimes, the branching ratios and multipole mixing ratios of their γ -decays have to be determined. For more detailed insight in the structure of these states information on their magnetic moments is also necessary. Until recently obtaining all this information was possible for a hand-full of stable nuclei only. ***No mixed symmetry states have ever been solidly identified in unstable nuclei on the basis of large absolute M1 transition rates.***

3-3 Dynamic Deformation Model (DDM) Results

3-3-1 Energy Spectra

The even-mass barium isotopes ($Z=56$) are part of an interesting region beyond the closed proton shell at $Z=50$ where the level structure has resisted detailed theoretical understanding. The present investigation of the Barium isotopes, $N=64-80$, mainly by the dynamic deformation model (DDM) is a part of a wider study which includes tellurium, xenon and selenium isotopes.

The calculated collective energy levels of the barium isotopes were obtained by changing the value of N over the range $N=64-80$ without adjusting any parameters in the model. The Dynamic Deformation Model (DDM) calculated level energies are presented in Figs. (3-1) to (3-9). The basic features of the variation of level structure with neutron number N are well reproduced. In the ground state band the variation of the energy ratio $E(4_1^+)/E(2_1^+)$ from a value of 2.927 in ^{120}Ba isotope at neutron number $N=64$ to 2.098 in ^{136}Ba isotope at neutron number $N=80$ is reproduced.

The variation of $E(2_1^+)$ and $E(4_1^+)$ increased gradually with increasing neutron number, i.e., the variation of the moment of inertia with N is reproduced. The crossing of the state 2_2^+ below 4_1^+ in $^{132-134}\text{Ba}$ isotopes at $N=76-78$ is obtained, as one goes from $N=64$ to $N=80$. Similarly the 0_2^+ state is below 4_1^+ in ^{136}Ba isotope at $N=76$ and the 0_2^+ state is below 3_1^+ state in $^{124-136}\text{Ba}$ isotopes and lies at high energy in $^{130-136}\text{Ba}$ isotopes.

The gamma band ($2_2^+, 0_2^+, 4_2^+$) lies high in $^{122-136}\text{Ba}$ isotopes. Also the states 2_3^+ and 3_1^+ states lies high. The levels $2_3^+, 2_4^+, 0_3^+, 4_3^+, 4_4^+$ comparison with experimental has to be done carefully.

The root mean square deviation (**RMSD**) [113], is used to compare the experimental and DDM energy levels. Table (3-4) given the **RMSD** between experimental and DDM energy levels. In this table we see the ground state levels the best agreement was found in ^{136}Ba isotope where the smallest value of **RMSD** is equal 0.0227 and equal 0.0310 for gamma band in ^{130}Ba isotope. However **RMSD** = 0.0405 for beta band in ^{124}Ba isotope.

Figs. (3-1) to (3-9) show the energy levels of the barium isotopes from which we may draw the following conclusions.

(i) The $E(4_1^+)/E(2_1^+)$ ratio of the level energies decrease from the maximum of 2.927 for $N=64$ to 2.098 for $N=80$. This indicates a non-collective quasi-particle excitation becoming increasingly important as the neutron number approaches $N=82$.

(ii) Both the experimental and calculated $E(0_2^+)/E(4_1^+)$ ratios indicate that the 0_2^+ and 4_1^+ levels should occur close together throughout the range of isotopes from $N=64-80$. The large values of the ratios $E(0_2^+)/E(2_1^+)$, imply stiffness in the

collective potential in the β degree of freedom which is consistent with the values in for the deformation energy E_d (see Table (3-3)).

In Table (3-18) DDM calculation for the root-mean-square (rms) values of the deformations parameters β and γ for the ground state 0_1^+ , and first excited state 2_1^+ and second excited state 2_2^+ . These are a nice measure of the shape of the calculated potential energy surface (PES) and its variation with increasing spin or vibrational phonon number [16].

The root mean square of β (β_{rms}) value falls with increase in neutron number smoothly or gradually. In a few cases β_{rms} is about 15% lower than β_{min} . This is on account of the sharper rise of potential on the right-hand side (increasing β) than on the $\beta = 0$ side [16].

From the Table (3-18), the values of γ_{rms} for the ground band vary from 16.4^0 to 30.6^0 and the root mean square of the for 2_2^+ state as a member of γ -band lie between 25.6^0 and 31.9^0 . The values of γ_{rms} show little variation with increasing mass number A , signifying that the values of PES in DDM here is more symmetrical about the $\gamma = 30^\circ$.

Table (3-18) : The root-mean-square (rms) values of β and γ deformation parameters of ground state and excited states in $^{120-140}\text{Ba}$ isotopes.

Isotopes	β -Root mean square β_{rms}			γ -Root mean square γ_{rms}		
	0_1^+	2_1^+	2_2^+	0_1^+	2_1^+	2_2^+
^{120}Ba	0.265	0.270	26.3^0	20.8^0	16.4^0	26.3^0
^{122}Ba	0.258	0.266	25.6^0	16.8^0	15.7^0	25.6^0
^{124}Ba	0.243	0.254	27.3^0	18.8^0	17.2^0	27.3^0
^{126}Ba	0.224	0.238	29.2^0	20.1^0	18.8^0	29.2^0
^{128}Ba	0.208	0.223	30.8^0	24.9^0	22.5^0	30.8^0
^{130}Ba	0.188	0.205	31.3^0	27.8^0	26.2^0	31.3^0
^{132}Ba	0.157	0.176	30.9^0	29.2^0	27.7^0	30.9^0
^{134}Ba	0.128	0.152	30.0^0	29.4^0	30.4^0	30.0^0
^{136}Ba	0.124	0.111	30.3^0	28.6^0	29.6^0	30.3^0
^{140}Ba	0.098	0.089	31.9^0	29.9^0	30.6^0	31.9^0

3-3-2 Potential Energy Surface

We shall begin our discussion with the $N = 82$ nucleus and continue to the lighter isotopes. The potential-energy function $V(\beta, \gamma)$ gives circular contours, $V(\beta, \gamma) \approx \beta^2$ which are exactly what we expect from the model for a nucleus close to a doubly closed shell. The potential shape of this nucleus is that of a harmonic

oscillator with a minimum in the potential at $\beta = 0$. In the case of the $N = 80$ isotope a shallow minimum of $V(\beta, \gamma) = 0.360$ MeV appears at $\beta = 0.05$ and $\gamma = 0$, but unexpectedly a deep minimum of $V(\beta, \gamma) = 7.92$ MeV occurs on the oblate axis at $\beta = 0.092$. This deep minimum is surprising since only two neutrons have been removed and we might not expect such a dramatic change in the potential from that of the $N = 82$ nucleus.

In Table (3-3) the characteristic of potential energy surface (PES), the minimum quadrupole deformation β_{\min} , corresponding to the position of the deepest potential minimum are compared with the experimental data and IBM-1 results, the values of β_{\min} decrease with increasing neutron number (toward the magic number $N = 82$). In general, we obtain for the values of β_{\min} from the Table (3-3) the deeper prolate minima and shallower secondary oblate minima in all cases, both decreasing in depth with increasing N . The negative values of β_{\min} for $^{134-140}\text{Ba}$ isotopes at $N = 78, 80$ and 84 . At ^{120}Ba isotope $N = 64$, the prolate minimum is 3.250 MeV deep and the oblate minimum is 0.711 MeV deep and lies at lesser β value ($< \beta_{\min}$). The same feature continues with increasing neutron number N . At ^{134}Ba isotope $N = 78$ we get a very shallow prolate minimum and at $^{136-140}\text{Ba}$ isotopes $N = 80$ and 84 a very shallow oblate minimum.

The values of V_{PO} (Table (3-3)) the difference in the depth of prolate and oblate minima, is decreasing with increasing neutron number N in DDM calculations. From these values we obtain the prolate shape for the light Ba isotopes as in IBM-1. At $^{134-140}\text{Ba}$ isotopes $N = 78, 80$ and 84 the values of V_{PO} is negative but we obtain almost vanishing prolate and oblate minima [16]. The predicted shape is not a permanently deformed one. In fact the predicted potential well at $N = 76, 78, 80$ and 84 corresponds to the spherical shape (vibrational shape) anharmonic oscillator with flat bottom.

Several trends with increasing mass number (A) can be seen in this isotopic chain:

- (i) The magnitude of the deformation and the binding energy of deformation corresponding to the lowest potential minimum decrease.
- (ii) The magnitude of the prolate-oblate difference V_{PO} decrease in the first half of this region.
- (iii) The deformation at the minimum (the static intrinsic quadrupole moment) changes sign from positive (prolate) to negative (oblate) around $A = 130$.

The energy deformation E_d ($E_d = V(0) - V_{PO}$), decreased with increasing neutron number N (toward the magic neutron number $N = 82$).

The quadrupole moment of the first excited states $Q(2_1^+)$ decrease gradually with increasing neutron number. The negative sign signifies prolate shape in $^{120-140}\text{Ba}$ isotopes.

3-3-3 Electric Transition Probability B(E2)

The reduced electric transition probabilities for $^{120-140}\text{Ba}$ isotopes are given in Table (3-6). Similarly, the reduced transition probabilities $B(E2;2_1^+ \rightarrow 0_1^+)$, $B(E2;4_1^+ \rightarrow 2_1^+)$ and $B(E2;6_1^+ \rightarrow 4_1^+)$ decreases with increasing neutron number N . The DDM model values vary similarly with IBM-1, IBM-2 and experimental data. We see that these criteria provide $B(E2)$ values for other transitions which agree well with the DDM values and with experimental data and IBM-1 and IBM-2 values except some values for $B(E2;2_2^+ \rightarrow 0_1^+)$ transitions in lower neutron number isotopes, where the theoretical values in IBM-1 and IBM-2 are about a factor of ten too small. These values decrease with increasing N as expected for decreasing deformation parameter β and increasing the parameter γ .

The transitions $B(E2;3_1^+ \rightarrow 2_1^+)$ seem to get weaker with increasing neutron number N , because the cross over transition (selection rules) indicating the weakening band relationship. The transitions $B(E2;2_3^+ \rightarrow 2_1^+)$ and $B(E2;0_2^+ \rightarrow 2_1^+)$ in general the values fall with increasing neutron number N . The experimental value and DDM values in $^{120-122}\text{Ba}$ isotopes at $N = 64, 66$ is off the linear rise and needs a recheck, since there is no sudden change of structure in $^{132-134-136}\text{Ba}$ isotopes at neutron number $N = 66, 68$ and 70 . IBM-1 and IBM-2 yields a linear rise of $B(E2)$ with increasing boson number, and reproduces the saturation at mid shell. [140].

A maximum deformation (and associated properties such as deformation energy E_d , V_{PO} and quadrupole moment for first excited state $Q(2_1^+)$) at mid shell is achieved, since the up-sloping orbitals are emptied, while the down-sloping and horizontal orbitals remain filled up with the valence nucleons [16]. Here one must distinguish between the region of nuclei along the β -stability valley and the one across (far from) it as for Ba isotopes ($A = 130$ nuclei).

The discrepancy of experimental values and theoretical values can be attributed to:

- (i) The round-off errors which are particularly large for those values whose computation involves cancellation of many terms such as forbidden or weak transition rates.
- (ii) Deviations of the calculations from assumed Z and N dependence.
- (iii) Deviations from the adiabatic approximation.

Branching ratios are given in Table (3-7). from this table we see the value $B(E2;2_2^+ \rightarrow 0_1^+)/B(E2;2_2^+ \rightarrow 2_1^+)$, $B(E2;3_1^+ \rightarrow 2_1^+)/B(E2;3_1^+ \rightarrow 2_2^+)$ and $B(E2;3_1^+ \rightarrow 4_1^+)/B(E2;3_1^+ \rightarrow 2_2^+)$ for $^{120-140}\text{Ba}$ isotopes decrease with increasing neutron number N .

The value of branching ratio $B(E2;3_1^+ \rightarrow 2_1^+)/B(E2;3_1^+ \rightarrow 4_1^+)$ falls from the maximum value in ^{120}Ba isotope at $N = 64$ to the small values in ^{140}Ba isotope at $N = 84$, the experimental data exhibit the same trend of DDM values. The branching

value $B(E2;4_2^+ \rightarrow 2_1^+)/B(E2;4_2^+ \rightarrow 2_2^+)$ increased with increasing neutron number toward closed shell as well as in experimental values. The value $B(E2;4_2^+ \rightarrow 4_1^+)/B(E2;4_2^+ \rightarrow 2_2^+)$ varying randomly as well as experimental data. The DDM values exhibit saturation in agreement with data. These values are small and fall for $^{120-130}\text{Ba}$ isotopes, and larger for ^{132}Ba isotope, and decrease again for $^{134-140}\text{Ba}$ isotopes toward the major shell.

The ratio $B(E2;0_2^+ \rightarrow 2_1^+)/B(E2;0_2^+ \rightarrow 2_2^+)$ is small value for all the isotopes this ratio varies slowly up to $^{132-136}\text{Ba}$ isotopes and falls sharply thereafter, with increasing N and with increasing γ -softness in $(N > 82)$ ^{140}Ba isotope.

The ratio $B(E2;2_3^+ \rightarrow 2_2^+)/B(E2;2_3^+ \rightarrow 2_1^+)$ is falling with increasing N are also reproduced in experimental values. In general the values of DDM values come closer to experimental values.

Table (3-19) given the quadrupole moments for ground, gamma and beta bands. In general the value of the quadrupole moment decreases monotonically for each of the states in the three bands.

The sign of $Q(2_1^+, 4_1^+, 6_1^+)$ remains negative for g -band except in $^{134-136-140}\text{Ba}$ isotopes at neutron number $N = 78, 80$ and 84 , where the very shallow oblate minimum is slightly lower than the prolate minimum. The sign of quadrupole values for second excited states $Q(2_2^+)$ positive in $^{120-122-124-128-130}\text{Ba}$ isotopes and negative sign in $^{130-140}\text{Ba}$ isotopes for the same reasons.

The sign of $Q(2_3^+, 4_3^+, 5_1^+, 7_1^+)$ is consistently negative, but that of $Q(4_3^+)$ varies with neutron number. This may be due to the change of nature of 3_1^+ and 4_3^+ states in certain cases

Table (3-19) : Quadrupole moment for ground band, beta and gamma bands in $e.b$ units for $^{120-140}\text{Ba}$ isotopes

Isotopes	2_1^+	4_1^+	6_1^+	2_2^+	4_2^+	3_1^+	2_3^+	4_3^+	5_1^+	7_1^+
^{120}Ba	-1.8	-1.629	-1.821	1.074	-0.521	-0.172	-1.126	-1.265	-1.20	-1.03
^{122}Ba	-1.49	-1.560	-1.782	0.986	-0.398	-0.162	-0.947	-1.190	-0.97	-0.95
^{124}Ba	-1.33	-1.388	-1.565	0.887	-0.152	0.010	-0.568	-1.150	-0.75	-0.78
^{126}Ba	-1.26	-1.035	-1.149	0.709	-0.0093	0.197	-0.324	0.788	-0.47	-0.51
^{128}Ba	-1.20	-0.65	-0.660	0.453	-0.262	0.113	-0.223	0.517	-0.28	-0.28
^{130}Ba	-1.11	-0.470	-0.472	0.246	-0.065	0.265	-0.226	0.408	-0.23	-0.27
^{132}Ba	-0.99	-0.013	-0.007	-0.0150	0.043	0.273	-0.114	-0.030	-0.007	-0.007
^{134}Ba	-0.22	0.010	-0.008	-0.0130	0.048	0.284	-0.104	0.030	-0.008	-0.008
^{136}Ba	-0.20	0.0131	-0.0092	-0.01220	0.050	0.310	-0.113	0.031	-0.0083	-0.0091
^{140}Ba	-0.152	0.0121	-0.0099	-0.0118	0.062	0.322	-0.090	0.037	-0.0091	-0.0098

3-3-4 Magnetic Transition Probability B(M1) and Mixing Ratio

The resulting DDM calculations for B(M1) values are shown in Table (3-8). The results for the transitions feature for gamma band to ground band are claimed to have a collective origin. Several trends are apparent from the data in Table (3-8):

- (i) The magnitude of the M1 matrix elements increased with spin both gamma band to ground band transitions, in agreement with spin dependence.
- (ii) The size of gamma band to ground band matrix element seems to decrease with increasing mass number.
- (iii) The gamma-beta band M1 transitions are larger than gamma band to beta band transition by a factor of 2 to 3.

The B(M1) values vanish in the hydrodynamic model [58,59] since in that model the g -values is independent of deformation ($\mu = gI$) and off-diagonal matrix elements of the angular momentum operator vanish. The g -value calculated microscopically [57] as a function of deformation deviates from a constant by $\pm 50\%$ and hence the B(M1) values given in Table (3-8) are non-zero. However, the calculated values are quite small compared to the shell model single particle values [58,59].

The microscopic part of the calculation includes the spin contribution which is about $\pm 15\%$ of the magnetic moment. Integration over the collective variables is performed by using the relation ($\mu = gI$). Table (3-20) given the DDM values of g - factors and magnetic dipole moment. It is seen from this table this calculation gives the correct order of reduction of the magnetic moment of the first excited state $\mu(2_1^+)$ from the hydrodynamic value ($\mu = gI = 2Z/A \approx 0.8$). The agreement is probably measurements are good, the different experimental values often by ± 0.1 .

Table (3-20): Magnetic dipole moment in μ_N units and g -factors for $^{120-146}\text{Ba}$ μ_N units in DDM.

Isotopes	^{120}Ba	^{122}Ba	^{126}Ba	^{128}Ba	^{130}Ba	^{132}Ba	^{134}Ba	^{136}Ba	^{140}Ba	^{142}Ba	^{144}Ba	^{146}Ba
$g(2_1^+)$	0.511	0.509	0.492	0.475	0.453	0.432	0.410	0.391	0.381	0.345 (0.424)	0.311 (0.34)	0.2920 (0.28)
$\mu(2_1^+)$	0.552	0.556	0.568	0.573	0.611	0.618	0.633	0.639	0.643	0.672	0.680	0.70

Experimental data are taken from ref. [136].

The $\delta(E2/M1)$ multipole mixing ratios for $^{120-140}\text{Ba}$ isotopes, were calculated for some selected transitions between states. The sign of the mixing ratio must be chosen according to the sign of the reduced matrix elements. The equation used are (2-109) for the mixing ratio. The results are listed in Table (3-9). The agreement with available experimental data [105, 125, 126, 127] is more than good especially in the sign of the mixing ratio. However, there is a large disagreement in the mixing ratios of some transitions, is not due to a dominate E2 transition, but may be under the effect of very small value of M1 matrix element. However, it is a ratio between very small quantities and may change in the dominator that will have a great influence on the ratio.

For $\gamma \rightarrow \gamma$ transitions the intraband B(E2) values have been estimated by assuming that the intrinsic E2 matrix elements in the ground and gamma bands are equal. Then combining these B(E2) values with the M1 values to the tabulated $\delta(E/M1)$ transitions shown in Table (3-9). We note that in the DDM the intrinsic E2 matrix element of the gamma band is smaller than that of the ground band due to the finite-dimensionality of the DDM space.

3-3-4 Electric Monopole Transition Matrix element $\rho(E0)$

Electric monopole (E0) transitions between nuclear levels proceed mainly by internal conversion with no transfer of angular momentum to the ejected electron. If the energy of the transition is greater than $2m_0c^2$ (where m_0 is the mass of the electron), they can occur via electron-positron pair creation. A less probable deexcitation mode which can proceed via an E0 transition is two-photon emission. It is not a priori clear why a connection exists between charge radii and E0 transitions. In fact, the argument is rather convoluted and we begin this section by recalling it. The argument can be generalized to effective operators, leading to a relation between charge radii and E0 transitions which forms the basis of the present study.

The electric monopole transition matrix element when using Bohr relation between the nuclear radius and the deformation is given by [59]:

$$\rho(E0; J_i \rightarrow J_f) = \frac{3}{8} \left(\frac{Z}{\pi} \right) \langle J_f | \beta^2 | J_i \rangle \delta_{J_i J_f} \dots \dots \dots (3-6)$$

where the matrix element $\langle \quad \rangle$ is evaluated numerically. This calculation predicts in Table (3- 21) the magnitudes as well as the signs of many matrix elements.

The E0 strength can be considered as the ratio between the reduced transition probability of competing E0 and electric quadrupole, E2, transitions de-populating the same level. The calculated values are presented in Table (3-21). It might be due to the small values of the transition probability of the electric quadrupole transitions. Unfortunately, we don't have any more experimental data for comparison and justifying our calculations.

Table (3-21) : Monopole Matrix Element $\rho(E0)$ in e.b for $^{120-140}\text{Ba}$ isotopes in DDM .

$J_i^+ \rightarrow J_f^+$	^{120}Ba	^{122}Ba	^{124}Ba	^{126}Ba	^{128}Ba	^{128}Ba	^{130}Ba	Ba^{132}	^{134}Ba	^{136}Ba	^{140}Ba
$2_2 \rightarrow 2_1$	0.015	2.287	0.077	0.197	0.257	0.046	0.087	0.043	0.049	0.241	0.266
$0_2 \rightarrow 0_1$	0.183	0.1272	0.154	0.068	0.0023	0.0083	0.0083	0.0082	0.056	0.077	0.0910
$0_3 \rightarrow 0_1$	0.125	0.157	0.170	0.017	0.00044	0.00055	0.00097	0.0013	0.061	0.0041	0.0062
$0_3 \rightarrow 0_2$	0.093	0.118	0.176	0.0024	0.065	0.0034	0.0067	0.0023	0.0042	0.090	0.0980

As pointed out previously [141], a large X (E0/E2) value is not necessarily a signature of a β -vibrational state. For instance our calculated X (E0 / E2) value for

$2_2^+ \rightarrow 2_1^+$ transition. However, it be kept in mind that a large results from the vanishing $B(E2)$ values, specially in the case of higher bands whose structure may be quite different from that of the lower bands. Because of the possibility of accidental cancellations in the calculation of a sum of terms with different signs, only the correct order of magnitude can be expected from present calculation of a large number of states and matrix element.

In the present $X(E0/E2)$ branching ratios are used (Eq. (2-115)) to extract the $B(E0;0_2^+ \rightarrow 0_1^+)$ and $\rho^2(E0;0_2^+ \rightarrow 0_1^+)$ values associated with 0_2^+ states. Our results are shown in Table (3-22). In to complete the monopole values of $^{120-140}\text{Ba}$ isotopes, the measurements of E0 matrix elements of excited 0_3^+ states in these isotopes are in progress. The ratio of the reduced transition probabilities, $X = B(E0;0_2^+ \rightarrow 0_1^+)/B(E2;0_2^+ \rightarrow 0_1^+)$ is in the range from 0.024 to 0.0423 which is close to transitional rotor value. However, the assumed two-phonon 0_2^+ state is strongly pushed to high in energy, which is explained as being due to gamma-soft.

Table (3-22): $X(E0/E2)$ $^{120-148}\text{Ba}$ isotopes in DDM

$J_i^+ \rightarrow J_f^+$	^{120}Ba	^{122}Ba	^{124}Ba	^{126}Ba	^{128}Ba	^{128}Ba	^{130}Ba	Ba^{132}	^{134}Ba	^{136}Ba	^{140}Ba
$2_2 \rightarrow 2_1$	0.0051	0.0029	0.0028	0.0029	0.0033	0.0061	0.0072	0.0078	0.0079 (0.69)	0.0081	0.0095
$0_2 \rightarrow 0_1$	0.024	0.017	0.0283	0.0180	0.0223	0.028	0.030	0.032	0.035 (2.8(2))	0.039	0.0423
$0_3 \rightarrow 0_1$	0.0027	0.0025	0.0045	0.0056	0.0571	0.0086	0.0089	0.0091	0.0093	0.0095	0.0096
$0_3 \rightarrow 0_2$	2.119	0.313	2.313	1.389	2.473	2.411	2.416	2.417	2.420	2.431	2.473

The 0_2^+ state can be interpreted as a beta vibration, its probability distribution has roughly one node in beta. On the other hand, this state is characterized by two composing components: one prolate, more deformed than the 0_1^+ band structure, and one more triaxial to oblate, less deformed structure. Similar observations for a multi-component structure can be made also for the other, higher-lying 0^+ states.

The most conspicuous features of the 0_3^+ states in $^{120-140}\text{Ba}$ isotopes is strongly enhanced $E2$ decay to the 0_1^+ state. This may be connected with intriguing question of the possible deformation of the excited 0^+ state: the large $B(E2)$ values could alternatively be interoperated to imply a vibrational structure associated e.g., with mixed bands.

From the Table (3-22), one can overall see a poor agreement with the experimental data.

CHAPTER FOUR CONCLUSIONS AND SUGGESTIONS

4-1 Concluding Remarks

In this work we have described various properties and shape evolution of the Ba isotopes in the framework of the interacting boson model (IBM-1 and IBM-2) and dynamic deformation model (DDM), we conclude the following points.

The main aim of the present study was to investigate the balance and the interplay between the nuclear collectivity and the shell structure in the lowest lying isovector states, the so called mixed mixed-symmetry states. The collected experimental data clearly demonstrate that the underlying microscopic structure of the nucleus can have a dramatic influence on the properties of mixed symmetry states and defines a new direction in the experimental studies of these states. In particular, the following questions have been addressed and resolved:

1- The nuclear structure of $^{120-148}\text{Ba}$ isotopes was studied and the phase transition from U(5) to SU(3), with moderate deformation, was found according to the increasing neutron number. The model calculation of the F -spin values and electromagnetic transition probabilities as well as the mixing ratio shows that the $J_i^\pi = 2_3^+, 2_4^+$ and $J_i^\pi = 1^+$ states are the lowest mixed symmetry states in the $^{120-148}\text{Ba}$ isotopes, respectively. Therefore the Ba isotopes change is from O(6) (^{132}Ba isotope, around neutron number 76) towards SU(3) (^{132}Ba isotope, around neutron number 66), to SU(5) (^{110}Ba isotope around neutron number 54);

2- The ratio $E(2_2^+)/E(2_1^+)$ decrease in some isotopes is not due to the falling 2_2^+ state but is on account of rising of $E(2_1^+)$ at fast rate compared to $E(2_2^+)$, which is even increasing at ^{128}Ba isotope to ^{134}Ba isotope. The pattern of spectrum here indicates a continuous phase transition from near SU(3) to gamma-soft rotor.

3- The variation of the $E(2_2^+) - E(4_1^+)$ related to the potential difference between prolate and oblate shapes (V_{PO}) in a given isotope, IBM-1 is well given in our calculation, including its sign change at $^{132-140}\text{Ba}$ isotopes.

4- The known g -factors of $J_i^\pi = 2_1^+$ and $J_i^\pi = 2_2^+$ states in these isotopes are reasonably described by the IBM-2. Concerning the electromagnetic properties, we mainly concentrated on electric quadrupole B($E2$) transition probabilities. The investigation of electromagnetic properties provided us with an example of isotopes, detailed nuclear properties of which can be described in the framework of the collective models, interacting boson model (IBM-1 and IBM-2) and dynamic deformation model (DDM). However, it is still evident that there is a discrepancy between IBM-1 and DDM models prediction and the experimental data. Hence, further experimental studies of these isotopes are needed.

5- New methods are used to evaluate the effective charges (e_π, e_ν) and gyromagnetic factors (g_π, g_ν) for bosons which are used in electromagnetic transition probabilities.

6- Mixed-symmetric states are of isovector character. Their $E2$ decay to the corresponding fully-symmetric states is forbidden. Instead, strong $M1$ decays are expected to connect these states. In the case of the $J_i^\pi = 2_{1,M}^+$ state, a transition with a matrix element of $|\langle 2_1^+ || T(M1) || 2_{1,M}^+ \rangle|^2 \approx 1\mu_N^2$ is expected. At the same time the $E2$ transition to the ground-state can be expected to be weakly collective with a strength of the order of $\approx 1 e.b.$ These transition strengths result in a very short lifetime of the $J_i^\pi = 2_{1,M}^+$ state of the order of $\tau(2_{1,M}^+) \approx 100$ fs.

7- A common feature observed throughout all isotopic and isotonic chains in the region is the decrease in $B(M1; 2_i^+ \rightarrow 2_1^+)$ strength on the way to mid-shell nuclei to almost vanishing values for the nucleus ^{130}Ba isotope. However, if the large fragment of the mixed symmetry states in Ba isotopes could be confirmed, completely new questions would arise, in particular concerning the lack of comparably enhanced $B(M1; 2_i^+ \rightarrow 2_1^+)$ strengths in the neighboring isotopes (nuclei). This means either, that these nuclei indeed have a $J_i^\pi = 2_{1,M}^+$ state but which resides at energies beyond the experimental detection limit, or, that this observation reflects a real physical effect that is unexplained at present. The discussion strongly depends on the nature of the 2.371 MeV state in ^{130}Ba isotope. For a continued discussion of the observations in the $A=130$ mass region further investigation of this state is of utmost importance. Unfortunately, the experimental accessibility will presumably be hindered by the low natural abundance of Ba isotopes of only 0.1% [25].

8- The ratios $\delta(E2/M1)$ and $X(E0/E2)$ are important for nuclear structure and the model predictions due to their sensitivity for the nuclear shape. We conclude that more experimental work is needed to clarify the band structure and investigate an acceptable degree of agreement between the predictions of the models and the experimental data.

9- In the IBM-2 it is possible to correlate a large amount of data in various regions of the periodic table. The parameters are found to be in qualitative agreement with the simple microscopic theory with the exception of ε . Also the microscopic theory can be used to predict the properties of nuclei which are not known at present.

10- We have analyzed the level structure of $^{120-140}\text{Ba}$ isotopes in a microscopic theory in its time dependent, two major-shell version, called the Dynamic Deformation Model (DDM). This allows the isotope to take its own shape for given N and Z . Also shape variation with nuclear spin or excitation energy is allowed although, unlike IBM, no minimization is done for each level. The variation of the absolute $B(E2)$ values is generally well reproduced in DDM as also in other approaches. However, variation of the γ - g $B(E2)$ ratios is much better reproduced in our DDM calculation.

11-The different behavior for $N > 82$ and $N < 82$ isotopes, regarding the sharp change for the former and smooth variation in the latter is well realized in terms of the nucleon occupation probabilities. The dynamics of the β_{rms} and γ_{rms} obtained in DDM model agrees with other works. Similar agreement is obtained for the quadrupole moments of various states.

12-The values of V_{PO} , the difference in the depth of prolate and oblate minima, is decreasing with increasing neutron number N in DDM calculation. From these values we obtain the prolate shape for the light Ba isotopes as in IBM-1. At $^{134-140}\text{Ba}$ isotopes $N = 78, 80$ and 84 the values of V_{PO} is negative but we obtain almost vanishing prolate and oblate minima. The predicted shape is not a permanently deformed one. In fact the predicted potential well at $N = 76, 78, 80$ and 84 corresponds to the spherical shape (vibrational shape) anharmonic oscillator with flat bottom.

13- The $B(M1)$ values in DDM vanish in the hydrodynamic model, since in that model the g -values is independent of deformation ($\mu = gI$) and off-diagonal matrix elements of the angular momentum operator vanish. The g -value calculated microscopically [57] as a function of deformation deviates from a constant by $\pm 50\%$ and hence the $B(M1)$ values given in Table (3-8) are non-zero. However, the calculated values are quite small compared to the shell model single particle values [58,59].

4-2 Suggestions for Future Work

Several suggested projects remain for the future, which can be abbreviated by the following possible works:

- 1-This work represents the preliminary attempt to apply the Dynamic Deformation Model (DDM) to light nuclei ($N < 82$) with reasonable success. More work is required for improving the input set of spherical single-particle energies.
- 2- This work can be extended to calculate the E4 (hexadecupole degree of freedom) in transitional nuclei, by addition of a g -boson ($L = 4$), to test the important $K^\pi = 4^+$ band in this region.
- 3- Study of the two-neutrino double- β decay within the framework of the interacting boson model (IBM-1 and IBM-2) and its extensions (IBFM-1 and IBFFM-2) models.
- 4- Preferably, the entire calculation of DDM should be performed with better nuclear forces. This would, however, require a major change in theory of collective motion and also an order of magnitude increase in computation time.
- 5- Non-collective effects of deviations from the adiabatic approximation should be included. They would clearly require a major overhaul or a completely new approach from the beautiful idea of collective quadrupole motion which has been extremely useful for understanding of nuclear structure.

6- The pairing variation become particularly important near closed shell since $\Delta_{av} \approx 0$, and fluctuations in Δ become large. However, this may require further increase in the computation time which already quite large (several hours per nucleus).

7- The numerical accuracy, particularly that of the nearly forbidden transitions, can probably be improved using expansions of nuclear wave functions in a basis of spherical phonons of five dimensional oscillators. Then, this work could also be extended to states of higher angular momentum ($J^\pi = 4^+$). Work along this line is being carried out by my supervised (SN).

8- Available information on mixed symmetry states in these isotopes has recently been summarized and identified in some references remembered elsewhere in this thesis. The main reason for the small number of studied cases comes from the fact that the stable open-shell even-even isotopes in this mass region have relatively low abundance in natural material of a chemical element. This requires a development of new theoretical and experimental techniques which should allow mixed symmetry states such low-abundant nuclei to be identified and studied. These techniques should also be potentially applicable for investigations of mixed symmetry states in radioactive nuclei.

Regardless that the results obtained in the present study shed light on some important properties of evolution structure, it should not be considered as completed with regards to all phenomena related to the nuclear structure and mixed symmetry states. Rather, it provides some starting points for further investigations. The effect of shell stabilization, proposed in the present study, is only partially confirmed. It is still needed the latter to be investigated in details in other neighboring nuclei Te, Xe and Ce . This theoretical program has already begun with an experiment based for example, on projectile Coulomb excitations. In general, all further studies of nuclear structure and mixed symmetry states will be focused on radioactive nuclei. In particular, due to the sensitivity of mixed-symmetry states to the properties of the local valence shell, information on mixed-symmetry states would be very useful for nuclei where the shell structure deviates from the one at stability due to neutron excess. The main contribution of the present study to these future using collective models and experiments is methodological—we have clearly demonstrated that the collective models is the most appropriate one for studies of mixed symmetry states in radioactive nuclei.

REFENECES

- [1] E. Rutherford. *"The scattering of α and β Particles by Matter and the Structure of the Atom "* Philos. Mag. **21** (1911) 669.
- [2] E. Epelbaum, H.-W. Hammer, and U. G. Meibner " *Modern theory of nuclear forces*". Rev. Mod. Phys. **81** (2009) 1773.
- [3] I. Talmi. *Simple Models of Complex Nuclei*. Contemporary concepts in physics, (Taylor & Francis, 1993).
- [4] F. Iachello and A. Arima. *"The Interacting Boson Mode"l*. Cambridge Monographs on Mathematical Physics, (Cambridge University Press, 1987).
- [5] F. Iachello, Phys. Rev. Lett. **85**, (2000) 2080.
- [6] R.F. Casten, N.V. Zamfir, Phys. Rev. Lett. **85**, (2000) 2084.
- [7] K. Kumar, J.B. Gupta, Nucl. Phys. A **694**, (2000) 199.
- [8] K. Kumar, M. Baranger, Nucl. Phys. A **110**, (1968) 529.
- [9] G. Puddu, O. Scholten, T. Otsuka, Nucl. Phys. A 348 (1980) 109.
- [10] O. Castanos, P. Federman, A. Frank, S. Pittel, Nucl. Phys. A 379 (1982) 61.
- [11] W. D. Hamilton, A. Irbäck, and J. P. Elliott, Phys. Rev. Lett. 53 (1984) 2469.
- [12] A. Novoselsky, I. Talmi, Phys. Lett. B 172 (1986) 139.
- [13] A. Sevrin, K. Heyde, J. Jolie, Phys. Rev. C 36 (1987) 2631.
- [14] Y.M. Zhao, S. Yamaji, N. Yoshinaga, A. Arima, Phys. Rev. C 62 (2000) 014315.
- [15] Yu-Xin LIU, Qi-Zhi HAN, En-Guang ZHO, Commun Theo. Phys. 21 (1994) 193.
- [16] Kumar and Gupta, Nucl. Phys. A 694 (2001) 199.
- [17] H. M. Mittal and Vidya Devi, *Proceedings of the DAE Symp. on Nucl. Phys.* 55. (2010) 104.
- [18] P. G. Bizzeti, A. M. Bizzeti-Sona, D. Tonev, A. Giannatiempo, C. A. Ur, A. Dewald, B. Melon, C. Michelagnoli, P. Petkov, D. Bazzacco, A. Costin, G. de Angelis, F. Della Vedova, M. Fantuzi, E. Farnea, C. Fransen, A. Gadea, S. Lenzi, S. Lunardi, N. Marginean, R. Marginean, R. Menegazzo, D. Mengoni, O. M'oller, A. Nannini, D. R. Napoli, M. Nespolo, P. Pavan, A. Perego, C. M. Petrache, N. Pietralla, C. Rossi Alvarez, and P. Sona. Phys. Rev. C 82 (2010) 54311.
- [19] N. Turkan, *Physics of Atomic Nuclei*, 2010, Vol. 73, No. 1 (2010) 64.
- [20] Rajesh Kumar, J.B.Gupta, Vikas Katoch and S. Sharma, *Proceedings of the DAE Symp. on Nucl. Phys.* 55. (2010) 96.
- [21] A. R. H. Subber and F. H. AL-Khudair, Phys. Scr. 84 (2011) 035201 (5pp).
- [22] H. M. Mittal and Vidya Devi, *Int. J. Nuclear Energy Science and Technology* Vol. 6, No. 1 (2011) 64.
- [23] A. R. H. Subber and F. H. AL-Khudair, Turk. J. Phys. 36 (2012) 368.
- [24] J. B. Gupta, Phys. Rev. C 87 (2013) 64318 .
- [25] Thomas Möller, " *Aspects of nuclear collectivity studied in projectile Coulomb excitation experiments*" M. Sc. Thesis 2014 (unpublished).
- [26] G.B. Gupta, Eur. Phys. J. A 51 (2015) 47 .
- [27] G.B. Gupta, *International symposium on nuclear physics* V. 43B (2015).
- [28] J. B. McGrory and B. H. Wildenthal, Ann. Rev. Nucl. Part. Sc. 30 (1980), 383.
- [29] A. Arima and F. Iachello, Ann. Rev. Nucl. Part. Sc. 31 (1981), 75.
- [30] S. Cohen, F. Plasil and W. J. Swiatecki, Ann. of Phys. 82 (1974), 557.
- [31] Rayleigh, Third Baron, *"The Theory of Sound"* Vol. II, Macmillan,

- London (1977).
- [32] A. Bohr and B. R. Mottelson, *Mat. Fys. Medd. Dan. Vid. Selsk.* 27 No.16 (1953).
- [33] A. Bohr and B. R. Mottelson "*Nuclear Structure*" Vol. II, W. A. Benjamin, Inc. Massachusetts (1975).
- [34] O. Nathan and S. G. Nilsson, "*in Alpha-Beta and Gamma Ray Spectroscopy*", K. Siegbahn (Ed), P. 601, North-Holland Publishing Co., Amsterdam (1965).
- [35] R. K. Sheline, *Rev. Mod. Phys.* 32 (1960) 1.
- [36] M. A. Preston, "*Physics of the Nucleus*" Addison-Wesley Publishing CO., Massachusetts (1962).
- [37] K. T. Hacht in "*Selected Topics in Nuclear Spectroscopy*" ob. cit., P. 51.
- [38] B. F. Bayman and Alexander Lande, *Nucl. Phys.* 77 (1966) 1.
- [39] R. F. Casten, Thesis, Yale University, unpublished (1967).
- [40] G. Alaga, K. Alder, A. Bohr and B. R. Motelson, *Mat. Fys. Medd. Dan. Vid. Selsk* 29 No. 9 (1955).
- [41] A. S. Davydov and G. F. Fillippov, *Nucl. Phys.* 8 (1958) 237.
- [42] A. S. Davydov, V. S. Rostovsky and A. A. Chaban, *Nucl. Phys.* 27 (1961) 134.
- [43] A. S. Davydov and A. A. Chaban, *Nucl. Phys.* 20 (1960) 499.
- [44] L. Willets and M. Jean, *Phys. Rev.* 102 (1956) 788.
- [45] S. G. Nilsson, *Mat. Fys. Medd. Dan. Vid. Selsk.* 29 No. 16 (1955).
- [46] J. Meyer-ter-Vehn, *Nucl. Phys. A* 249 (1975) 111, 141.
- [47] P. A. M. Dirac "*Principle of Quantum Mechanics*" 4th Edition, Clarendon Press, Oxford (1958).
- [48] S. G. Nilsson and O. Prior, *Mat. Fys. Medd. Dan. Vid. Selsk.* 32 No. 16 (1960).
- [49] Bardeen, Cooper and Schrieffer, *Phys. Rev.* 108 (1957) 1175.
- [50] A. Bohr, R. B. Mottelson and Pines, *Phys. Rev.* 110 (1958) 936.
- [51] N. N. Bogoliubov, *JETP* 7, 41 (1958); *Nuovo Cimento* 7 (1958) 794.
- [52] J. G. Valatin, *Nuovo Cimento* 7 (1958) 843.
- [53] S. G. Nilsson, *Nucl. Phys.* 55 (1964) 97.
- [54] M. Baranger and K. Kumar, *Nucl. Phys.* 62 (1965) 113.
- [55] M. Baranger and K. Kumar, *Nucl. Phys.* A110 (1968) 490, 529.
- [56] K. Kumar and M. Baranger, *Phys. Rev. Lett.* 17 (1966) 1146.
- [57] K. Kumar and M. Baranger, *Nucl. Phys.* A122 (1968) 241, 273.
- [58] M. Baranger and K. Kumar "*in Perspective in Modern Physics*" R. E. Marshak (Ed), Wiley, New York (1966).
- [59] K. Kumar "*Nuclear Models and the Search for Unity in Nuclear Physics (1984)*" (Bergen: University of Bergen Press).
- [60] A. R. Subber, P. Park, W. D. Hamilton, K. Kumar, K. Schreckenback and G. Colvin 1986 *J. Phys. G : Nucl. Phys.* 12 (1986) 881.
- [61] K. Kumar, B. Remaud, P. Aguer, J. S. Vaagen, A. C. Rester, R. Foucher and J. H. Hamilton, *Phys. Rev.* C16 (1977) 1253.
- [62] K. Kumar, Supplement of the Progress of Theoretical Physics, Nos. 74 & 75, 983.
- [63] B. Giraud and B. Grammaticos, *Nucl. Phys.* A233 (1974), 373.

- [64] Ch. Lagrange, M. Girod, B. Grammaticos and K. Kumar, *Proceedings of the International Conference on Nuclear Physics, Berkeley, August 1980* (University of California, Berkeley), vol. 1, p. 352.
- [65] K. Kumar, *A Study of Nuclear Deformations with Pairing Plus Quadrupole Forces* (Carnegie-Hunt Library, Pittsburgh, 1963).
- [66] K. Kumar and M. Baranger, Nucl. Phys. A92 (1967), 608.
- [67] K. Kumar, *The Electromagnetic Interaction in Nuclear Spectroscopy*, ed. W. D. Hamilton (North-Holland, Amsterdam, 1975), p. 55.
- [68] D. R. Bes, P. Federman, E. Maqueda and A. Zuker, Nucl. Phys. 55 (1965)1.
- [69] D. R. Bes and Yi-Chung Cho, Nucl. Phys. 86 (1966) 581.
- [70] A. M. Lane, "*Nuclear Theory*" W. A. Benjamin, Inc. , New York (1964).
- [71] A. A. Korneichuk, L. A. Malov, V. G. Soloviev, S. I. Fedotov and C. Schulz, Sov. J. Nucl. Phys. 9 (1969) 436.
- [72] T. Kishimoto and T. Tamura, Nucl. Phys. A192 (1972) 246.
- [73] T. Kishimoto and T. Tamura, Nucl. Phys. A270 (1976) 317.
- [74] F. Iachello and A. Arima, Phys. Lett. B53 (1974) 309.
- [75] A. Arima and F. Iachello, Phys. Rev. Lett. 35 (1975) 1069.
- [76] A. Arima and F. Iachello, Phys. Rev. Lett. 40 (1978) 111.
- [77] A. Arima, Lectures Fall 1977, SUNY, Stony Brook, New York .
- [78] A. Arima and F. Iachello, Ann. Phys. (N.Y). 99 (1976) 253.
- [79] A. Arima and F. Iachello, Ann. Phys. (N.Y). 111 (1978) 201.
- [80] F. Iachello *Informal Lectures*, July 1977, Brookhaven National Laboratory , Upton , New York.
- [81] F. Iachello, Nuklenoika 22 (1977) 107.
- [82] O. Scholten, Computer code **PHINT**, K. V. I., Groningen, Holand (1979).
- [83] J. P. Elliott, Proc. Roy. Soc. A245 No. 128 (1958) 562.
- [84] J. Millener, *Lectures at Brookhaven National Laboratory, Upton, New York* 1977.
- [85] J. Larysz, Thesis , University of Manchester, Manchester, U.K
- [86] O. Scholten, F. Iachello and A. Arima, Ann. Phys. (N.Y).1978.
- [87] D. Bonatsos, E. A. Mc.Cutchan, N. Mainkov, R.F. Casten, P. Yotov, D.Lenis, D. Peterllis, and I.Yigitoglu, Pys. Rev. C.76 (2007) 064312 .
- [88] P. Van Isacker and J.O. Cheen, Phys. Rev. C24, (1981) 689.
- [89] G. Puddu, O. Scholten, T. Otsuka, Nucl. Phys. A348, (1980) 109 .
- [90] F. Iachello and A.Arima, *The Interacting Boson Model*, Cambridge University Press, Cambridge, 1987.
- [91] J. Lang, K. Kumar and J. H. Hamilton, Rev. Mod. Phys. Vol.54 No. 1 (1982).
- [92] E. L. Church and J. Weneser, *Phys. Rev.*, 103 (1956), 1035.
- [93] R. Bijker, A. E. L. Dieperink and O. Scholten, Nucl. Phys. A 344 (1980) 207.
- [94] T. Otsulta and N. Yosbida *The IBM-2 compurer program NPBOS* Universiry of Tokyo (1985) , T. Otsuka, and O. Soholten, KVI Internal Report No. 253, 1979.
- [95] A. Bohr and B. Mottelson, "*Nuclear Structure II*", (Benjamin, Reading, 1975).
- [96] R. F. Casten, Nucl. Phys. A443 (1985) 1.
- [97] T. Otsuka, T. Matsuo, and D. Abe, Phys. Rev. Lett. 97 (2006) 162501.
- [98] D. Bohle, A. Richter, W. Steffen, A. E. L. Dieperink, N. Lo Iudice, F. Palumbo, and O. Scholten, Phys. Lett. 137B (1984) 27.

- [99] J. Enders, P. von Neumann-Cosel, C. Rangacharyulu, and A. Richter, *Phys. Rev. C* **71** (2005) 014306.
- [100] P. Van Isacker, K. Heyde, J. Jolie, and A. Sevrin, *Ann. Phys. (NY)* **171**, (1986) 253 .
- [101] A. Bohr. *Kgl. Danske Videnskab. Selskab, Mat.fys. Medd.* 26 (1952) 14.
- [102] S F Hicks *et al*, *Phys. Rev. C* **71**, 34307 (2005).
- [103] N Yoshida, A Gelberg, T Otsuka, I Wiedenhoover, H Sagawa and P von Brentano, *Nucl. Phys.* **A619**, 65 (1997).
- [104] T Otsuka, *Nucl. Phys.* **A557**, 531c (1993).
- [105] ENSDF, [http:// www.nndc.bnl.gov/ensdf](http://www.nndc.bnl.gov/ensdf) (Nuclear data sheet) (2012).
- [106] M.S. Sarkar, S. Sen, *Phys. Rev. C* **56** (1997) 3140.
- [107] P.G. Bizzeti *et al.*, *Phys. Rev. C* **82**, 054311 (2010).
- [108] R. M. Clark , (2004) Paper LBNL-56419 , R. M. Clark *et al.*, *Phys. Rev. C* **69**, (2004) 064322.
- [109] C. Fransen, N. Pietralla, A. Linnemann, V. Werner, and R. Bijker, *Phys. Rev. C* **69**, 014313 (2004).
- [110] F. Iachello, *Phys. Rev. Lett.* **87**, 052502 (2001).
- [111] K. Kumar, *Phys. Rev. C* **1**, 369 (1970).
- [112] S.M. Burnette, A.M. Baxter, G.J. Gyapong, M.P. Fewel, R.H. Spear, *Nucl. Phys. A* 489 (1989) 102.
- [113] F. X. Xu, C. S. Wu and J. Y. Zeng, *Phys. Rev. C* **40** (1989) 2337.
- [114] R. B. Firestone, *Table of Isotopes*, Ed. by V. S. Shirley (Wiley Intersci., New York, 1996).
- [115] S. Raman, C.W. Nestor, P. Tikkanen, *At. Data Nucl. Data Tables* **78**, 1 (2001).
- [116] S.M. Burnette, A.M. Baxter, G.J. Gyapong, M.P. Fewel, R.H. Spear, *Nucl. Phys. A* 489 (1989) 102.
- [117] P. Petkov, A. Dewald, W. Anderjtscheff, *Phys. Rev. C* **51** (1993) 2511.
- [118] T. Morikawa, M. Oshima, T. Sekine, Y. Hatsukawa, S. Ichikawa, H. Iimura, A. Osa, M. Shibata, A. Taniguchi, *Phys. Rev. C* **46** (1992) R6.
- [119] X.W. Pan, J.L. Ping, D.H. Feng, J.Q. Chen, C.L. Wu, M.W. Guidry, *Phys. Rev. C* **53** (1996) 715.
- [120] P. Petkov, A. Dewald, R. Kuhn, P. von Brentano, *Phys. Rev. C* **62** (2000) 014314.
- [121] K. Uchiyama *et al.*, *Eur. Phys. J. A* **2**, 13 (1998).
- [122] M. Asai, T. Sekine, A. Osa, M. Koizumi, Y. Kojima, M. Shibata, H. Yamamoto, K. Kawade, *Phys. Rev. C* **56**, 3045 (1997).
- [123] Brookhaven National Laboratory, *Chart of nuclides of National Nuclear Data Center*, <http://www.nndc.bnl.gov/ENSDF/> (2010).
- [124] P.G. Bizzeti *et al.*, *Phys. Rev. C* **82**, 054311 (2010).
- [125] R. B. Firestone, *Table of Isotopes*, Ed. by V. S. Shirley (Wiley Intersci., New York, 1996).
- [126] A. M. Demidov, L. I. Govor, V. A. Kurkin, and I. V. Mikhailov, *Phys. At. Nucl.* **60** (1997) 503.
- [127] J. Lang, K. Kumar and J. H. Hamilton, *Rev. Mod. Phys.* Vol.54 No. 1 (1982).
- [128] Gill R L, Casten R F, Warner D D, Brenner D S and Walters W B 1982 *Phys. Lett.* B 118 251.
- [129] W. D. Hamilton, *J. Phys. G: Nucl. Part. Phys.*, **16**, (1990), 745.
- [130] P. Van Isacker, K. Heyde, J. Jolie, and A. Sevrin, *Ann. Phys. (NY)* **171**, (1986) 253 .

- [131] A. R. Subber, P. Park, W. D. Hamilton, K. Kumar, K. Schreckenbach and G. Colvin, *J. Phys. G: Nuclear Phys.* 12 (1986) 881.
- [132] M. Sambataro, O. Scholten, A. E. L. Dieperink and P. Piccitto, *Nucl. Phys.* A423(1984) 333.
- [133] P. Van Isacker *et al.*, *Ann. Phys.*2 (1985) 253.
- [134] A. E.L.Dieperink, O.Scholten and D.D.Warner, *Nucl. Phys.* A469 (1987) 173.
- [135] P. Navratil, B. R. Barrett and J. Dobes, *Phys. Rev.* C53 (1996) 2794.
- [136] C. Goodin, J. R. Stone, N. J. Stone, A. V. Ramayya, A. V. Danile, J. H. Hamilton, K. Li, J. K. Hwang, G. M. Ter-Akopain and J. O. Rasmussen, *Phys. Rev.* C79(2009) 34316.
- [137] W. D. Hamilton, *J. Phys. G: Nucl. Part. Phys.*, 16, (1990), 745.
- [138] B. Fazekas, T. Belgya, G. Molnar, A. Veres, R.A. Gatenby, S. W. Yates and T. Otsuka, *Nucl. Phys.*, A 548, (1992) 249.
- [139] N. Pietralla, P. von Brentano, A.F. Lisetskiy, *Prog. Part. Nucl. Phys.* 60, 225 (2008).
- [140] T. Otsuka, X.W. Pan, A. Arima, *Phys. Lett. B* 247 (1990) 191.
- [141] D. Bonatsos, D. Lenis, N. Pietralla, P. A. Terziev, *Phys. Rev. C* 74 (2006) 44306.

Table (3-8): Magnetic Transition Probability $B(M1; J_f^+ \rightarrow J_i^+)$ in μ_N^2 Units for Ba isotopes.

Isotopes	$B(M1; 2_2^+ \rightarrow 2_1^+)$			$B(M1; 3_1^+ \rightarrow 2_1^+)$			$B(M1; 3_1^+ \rightarrow 4_1^+)$			$B(M1; 4_2^+ \rightarrow 4_1^+)$		
	IBM-1	IBM-2	DDM	IBM-1	IBM-2	DDM	IBM-1	IBM-2	DDM	IBM-1	IBM-2	DDM
^{120}Ba	0.012	0.022	0.0429	0.0067	0.0005	0.0033	0.0087	0.0121	0.0055	0.012	0.0328	0.022
^{122}Ba	0.0185	0.0201	0.0032	0.0052	0.621	0.0043	0.0109	0.0432	0.026	0.0295	0.103	1.204
^{124}Ba	0.019	0.0188	0.0157	0.00049	0.0034	0.00019	0.0122	0.037	0.0651	0.0362	0.239	0.0356
^{126}Ba	0.0038	0.0046	0.0236	0.00011	0.0039	0.0820	0.0020	0.075	0.065	0.0088	0.271	0.095
^{128}Ba	0.0232	0.0362	0.00040	0.00032	0.0085	0.0123	0.0144	0.237	0.0881	0.0488	0.224	0.056
^{130}Ba	0.0770	0.045	0.00040	0.00088	0.0031	0.0050	0.0509	0.236	0.0102	0.142	0.216	0.066
^{132}Ba	0.0221	0.016	0.00065	0.00012	0.0056	0.009	0.0147	0.116	0.0241	0.0433	0.211	0.026
^{134}Ba	0.00220	0.046	0.00101	0.00004	0.0032	0.074	0.0013	0.0029	0.022	0.0039	0.0031	0.0101
^{136}Ba	0.0328	0.009	0.00291	0.000042	0.212	0.101	0.0178	0.098	0.0356	0.0531	0.876	0.0241
^{140}Ba	0.03281	0.246	0.00331	0.0034	0.0025	0.1011	0.0241	0.00043	0.0432	0.0562	0.0014	0.076
^{142}Ba	0.0356	0.035	-	0.00623	0.1194	-	0.0382	0.172	-	0.0673	0.163	-
^{144}Ba	0.0431	0.0046	-	0.0054	0.0005	-	0.0452	0.621	-	0.077	0.631	-
^{146}Ba	0.0571	0.0021	-	0.0876	0.621	-	0.0563	1.31	-	0.0861	0.38	-
^{148}Ba	0.0055	0.0002	-	0.0973	0.0034	-	0.0667	0.38	-	0.0964	0.36	-

Table (3-9): Mixing Ratios for $^{120-148}\text{Ba}$ isotopes in eb/μ_N Units

Isotopes	$\delta(E2,2_2^+ \rightarrow 2_1^+)$				$\delta(E2,2_3^+ \rightarrow 2_1^+)$				$\delta(E2,3_1^+ \rightarrow 2_1^+)$			
	Exp.	IBM-1	IBM-2	DDM	Exp.	IBM-1	IBM-2	DDM	Exp.	IBM-1	IBM-2	DDM
^{120}Ba	-	4.66	5.2	5.23	-	7.22	2.43	10.2	-	12	7.56	10.3
^{122}Ba	-	3.876	4.66	5.22	-	0.871	0.89	0.32	-	17.5	11	0.227
^{124}Ba	-	2.762	3.10	1.9	-	-2.65	-2.1	-3.98	-	11.86	5.5	5.7
^{126}Ba	$+5_{-1}^{+2}$	6.5	-8	4.2	-	1.23	3.2	2.89	-	21.6	13	14.45
^{128}Ba	-	0.422	0.66	0.659	-	0.912	3.61	1.223	-	8.45	2.89	1.34
^{130}Ba	0.296	0.311	0.251	0.541	-23(9)	-4.09	-20.44	3.98	$+5_{-1}^{+2}$	4.78	4.1	7
^{132}Ba	$+8.5_{-18}^{+40}$	7.145	10	11	-	11.6	14	12.89	$+2.5_{-10}^{+10}$	9.2	3.5	3.5
^{134}Ba	-7.4_{-9}^{+9}	-8.410	-7.65	-9	-	1.43	2.6	14	$+1.8_{-15}^{+1.5}$	1.6	1.97	19
^{136}Ba	-1.5_{-15}^{+6}	-2.41	-2.33	2.3	-	6.9	10	8.3	-	-2.56	-3.87	-5.32
^{140}Ba	0.6_{-6}^{+18}	1.1	0.91	0.998	$+0.18_{-5}^{+6}$	0.21	0.31	-	-	12	10	1.22
^{142}Ba	>10	13	13	-	-0.93(29)	1.1	2	-	-	-0.423	-0.23	-
^{144}Ba	$+7._{-3}^{+19}$	9.3	8.2	-	-3.2_{-6}^{+18}	-4.67	-4.7	-	-	10.3	7.43	-
^{146}Ba	-	1.414	6.4	-	-	1.90	2.21	-	-	21	1.23	-
^{148}Ba	-	0.556	1.24	-	-	0.761	0.45	-	-	0.549	0.81	-

Experimental data are taken from refs. [105, 125, 126, 127]

Continued to Table (3-9)

Isotopes	$\delta(E2,3_1^+ \rightarrow 4_1^+)$				$\delta(E2,3_1^+ \rightarrow 2_2^+)$				$\delta(E2,4_2^+ \rightarrow 4_1^+)$			
	Exp.	IBM-1	IBM-2	DDM	Exp.	IBM-1	IBM-2	DDM	Exp.	IBM-1	IBM-2	DDM
^{120}Ba	-	4.22	2.1	1.88	-	5.43	1.23	0.121	-	3.3	0.279	5.6
^{122}Ba	-	3.86	3.78	4.5	-	3.87	2.0	4.87	-	2.30	1.25	2.54
^{124}Ba	-	-1.85	-2.25	-3.4	-	4.6	-4.3	6	-	1.54	6.5	2.13
^{126}Ba	-	4.76	5	10.2	-	3.34	-2.56	12	> 1	8.58	1.413	9.34
^{128}Ba	-	1.10	5.8	0.45	-	5.98	6.0	0.651	-	1.08	2.0	1.0
^{130}Ba	-	0.661	0.24	0.779	-	1.08	1.209	1.0	-	-0.871	1.09	7.12
^{132}Ba	-	1.55	0.77	1.451	$4.0^{+1.1}_{-1.2}$	6.7	8.0	2.12	-1.1^{+2}_{-2}	-2.2	-9.0	-4
^{134}Ba	-	2.44	1.4	9.77	-17^{+23}_{-6}	-19.7	-15.3	-2.16	0.29^{+2}_{-2}	1.3	2.87	0.54
^{136}Ba	-	1.11	2.12	3.21	-	11.6	10.5	3.1	$+0.8^{+6}_{-6}$	4.5	5	1.9
^{140}Ba	-	2.27	3.7	5.87	-	-6.78	-9.5	4.21	-	2.7	4.9	4.8
^{142}Ba	-	1.897	0.89	-	-	1.242	3.45	-	-	-0.887	-9.8	-
^{144}Ba	-	0.302	1.65	-	-	2.07	2.0	-	-	1.65	2.761	-
^{146}Ba	-	1.97	2.54	-	-	1.891	3.09	-	-	3.65	4.0	-
^{148}Ba	-	8.8	16.3	-	-	2.810	8.45	-	-	7.8	12	-

Experimental data are taken from refs. [105, 125, 126, 127]

Table (3- 2): Experimental and theoretical values of energy ratios in Ba isotopes.

Isotopes	$E(4_1^+)/E(2_1^+)$				$E(6_1^+)/E(2_1^+)$				$E(2_2^+)/E(2_1^+)$				$E(0_2^+)/E(4_1^+)$				$E(0_2^+)/E(2_1^+)$			
	Exp.	IBM-1	IBM-2	DDM	Exp.	IBM-1	IBM-2	DDM	Exp.	IBM-1	IBM-2	DDM	Exp.	IBM-1	IBM-2	DDM	Exp.	IBM-1	IBM-2	DDM
^{120}Ba	2.924	2.924	2.924	2.927	5.592	4.983	5.231	5.218	-	4.284	4.435	6.807	-	1.601	1.700	2.485	-	4.682	4.973	6.612
^{122}Ba	2.902	2.907	2.901	2.747	5.543	4.774	4.579	5.166	3.155	3.697	3.205	6.797	-	1.377	1.276	2.294	-	4.466	3.717	6.303
^{124}Ba	2.834	2.842	2.838	2.640	5.342	5.532	5.179	4.833	3.798	3.759	3.786	5.690	1.378	1.414	1.361	1.885	3.921	4.021	3.864	4.978
^{126}Ba	2.777	2.777	2.777	2.516	5.204	5.113	5.257	4.462	3.412	3.050	2.945	4.132	1.382	1.236	1.226	1.660	3.839	3.433	3.406	4.177
^{128}Ba	2.687	2.689	2.683	2.389	4.953	5.109	4.975	4.113	3.114	3.275	3.440	2.806	1.234	1.136	1.171	1.552	3.316	3.056	3.144	3.780
^{130}Ba	2.523	2.521	2.521	2.287	4.456	4.445	4.450	3.844	2.540	2.579	2.490	2.806	1.307	1.344	1.222	1.517	3.302	3.389	3.081	3.470
^{132}Ba	2.427	2.431	2.428	2.181	4.159	4.077	4.071	3.551	2.220	2.123	2.258	2.118	1.333	1.320	1.354	1.306	3.239	3.211	3.290	2.849
^{134}Ba	2.316	2.321	2.317	2.185	3.656	3.928	4.008	3.512	1.931	1.700	1.932	2.225	1.257	1.194	1.209	1.229	2.911	2.773	2.802	2.675
^{136}Ba	2.280	2.279	2.281	2.098	2.696	2.715	2.702	3.260	1.894	2.567	2.588	2.108	0.845	0.735	0.842	1.830	1.929	1.677	1.922	3.841
^{140}Ba	1.876	1.982	1.877	2.001	2.756	2.692	2.719	3.022	2.507	2.380	2.460	2.081	1.613	1.582	1.592	2.485	3.027	2.978	2.990	3.311
^{142}Ba	2.321	2.314	2.383	-	4.076	3.199	4.044	-	3.960	3.835	3.938	-	1.839	1.789	1.907	-	4.270	4.142	4.431	-
^{144}Ba	2.663	2.658	2.663	-	4.829	4.457	4.859	-	9.286	8.804	9.231	-	1.924	1.771	1.886	-	5.125	4.889	5.025	-
^{146}Ba	2.836	2.823	2.828	-	5.292	5.154	4.563	-	6.159	6.690	6.110	-	2.049	1.956	1.896	-	5.813	5.524	5.364	-
^{148}Ba	2.983	2.985	3	-	5.697	5.822	5.751	-	7.439	6.858	8.021	-	-	3.434	3.385	-	-	10.255	10.156	-
$SU(5)$	2				3				2				1				2			
$O(6)$	2.5				4.5				> 2				~1				4.5			
$SU(3)$	3.3				7				3				>> 1				>> 2			

Experimental data are taken from refs. [105]

Table (3-3): Experimental and theoretical values of β_{\min} , E_d , V_{PO} energy difference $E(2_2^+) - E(4_1^+)$ and $Q(2_1^+)e, b$ in Ba isotopes.

Isotopes	β_{\min}			$E_d (MeV)$			$V_{PO} (MeV)$			$E(2_2^+) - E(4_1^+) MeV$			$Q(2_1^+)e, b$		
	<i>Exp.</i>	<i>IBM-1</i>	<i>DDM</i>	<i>Exp.</i>	<i>IBM-1</i>	<i>DDM</i>	<i>Exp.</i>	<i>IBM-1</i>	<i>DDM</i>	<i>Exp.</i>	<i>IBM-1</i>	<i>DDM</i>	<i>Exp.</i>	<i>IBM-1</i>	<i>DDM</i>
^{120}Ba	-	0.241	0.264	-	-	3.421	-	-	2.640	-	0.253	0.649	-	-1.770	-1.8
^{122}Ba	-	0.260	0.266	-	-	3.320	-	2.44	2.470	-	0.154	0.802	-1.52(7)	-1.414	-1.49
^{124}Ba	-	0.210	0.234	-	-	2.949	-	2.04	2.066	0.222	0.21	0.645	-1.31(4)	-1.30	-1.33
^{126}Ba	-	0.211	0.237	-	-	2.411	-	1.49	1.477	0.162	0.07	0.391	-1.20(4)	-1.22	-1.26
^{128}Ba	-	0.230	0.234	-	-	1.801	-	1.09	1.120	0.121	0.012	0.132	-1.10(4)	-1.15	-1.20
^{130}Ba	0.23	0.227	0.231	-	-	1.002	-	0.43	0.455	0.007	0.021	-0.002	-1.02(15)	-1.08	-1.11
^{132}Ba	0.19	0.221	0.230	-	-	0.281	-	0.0051	0.068	-0.096	-0.143	-0.032	-0.84(3)	-0.92	-0.99
^{134}Ba	-	-0.077	-0.082	-	-	0.062	-	-0.065	-0.070	-0.233	-0.375	0.033	-0.31(24)	-0.32	-0.22
^{136}Ba	-	-0.084	-0.088	-	-	0.088	-	-0.080	-0.087	0.027	0.244	0.007	-0.19(6)	-0.18	-0.20
^{140}Ba	-	-0.095	-0.092	-	-	0.0097	-	-0.091	-0.009	0.380	0.30	-	-	-0.16	-0.16

Experimental data are taken from refs. [105, 106]

Table (3-6): Experimental and theoretical values of Electric Transition Probabilities $B(E2; J_i^+ \rightarrow J_f^+)$ in e^2b^2 Units for Ba isotopes.

Isotopes	$B(E2; 2_1^+ \rightarrow 0_1^+)$				$B(E2; 4_1^+ \rightarrow 2_1^+)$				$B(E2; 6_1^+ \rightarrow 4_1^+)$				$B(E2; 2_2^+ \rightarrow 0_1^+)$			
	Exp.	IBM-1	IBM-2	DDM	Exp.	IBM-1	IBM-2	DDM	Exp.	IBM-1	IBM-2	DDM	Exp.	IBM-1	IBM-2	DDM
^{120}Ba	-	0.621	0.600	0.524	-	0.789	0.810	-	-	0.823	0.786	0.822	-	0.320	0.334	0.021
^{122}Ba	0.54	0.532	0.541	0.427	-	0.727	0.740	0.622	-	0.734	0.701	0.734	-	0.296	0.281	0.013
^{124}Ba	0.401	0.413	0.400	0.381	0.626	0.633	0.622	0.571	0.64(2)	0.671	0.643	0.710	-	0.201	0.200	0.014
^{126}Ba	0.380	0.375	0.399	0.311	0.440	0.438	0.439	0.500	0.49(2)	0.510	0.482	0.66	-	0.198	0.195	0.0135
^{128}Ba	0.276	0.280	0.266	0.298	0.41(2)	0.442	0.422	0.432	0.39(3)	0.382	0.422	0.521	0.13(2)	0.16	0.134	0.0085
^{130}Ba	0.230	0.229	0.231	0.228	0.219	0.220	0.216	0.329	0.37(2)	0.311	0.362	0.467	0.15(2)	0.20	0.161	0.0028
^{132}Ba	0.158	0.201	0.148	0.101	0.210	0.197	0.196	0.301	-	0.300	0.311	0.368	-	0.11	0.111	0.0011
^{134}Ba	0.134(2)	0.136	0.133	0.077	0.161(18)	0.156	0.155	0.22	-	0.181	0.212	0.301	0.0017(5)	0.0019	0.0018	0.00082
^{136}Ba	0.094	0.084	0.092	0.0542	0.080	0.088	0.095	0.181	-	0.093	0.081	0.279	-	0.001	0.0021	0.00065
^{140}Ba	0.037(34)	0.034	0.036	-	0.203(18)	0.211	0.209	-	0.081(4)	0.088	0.078	-	-	0.0009	0.00092	-
^{142}Ba	0.145(5)	0.0.133	0.142	-	0.419(64)	0.422	0.421	-	-	0.073	0.071	-	-	0.0008	0.00081	-
^{144}Ba	0.221(6)	0.241	0.224	-	-	0.613	0.514	-	-	0.062	0.066	-	-	0.0006	0.00076	-
^{146}Ba	0.280(60)	0.301	0.225	-	0.799(70)	0.821	0.701	-	-	0.056	0.051	-	-	0.00015	0.00023	-
^{148}Ba	-	0.410	0.349	-	-	0.925	0.865	-	-	0.0341	0.048	-	-	0.00033	0.00021	-

Experimental data are taken from refs. [105, 115, 116, 117, 118, 119, 120]

Continued to Table (3-6)

Isotopes	$B(E2;2_3^+ \rightarrow 0_1^+)$				$B(E2;2_3^+ \rightarrow 2_1^+)$				$B(E2;0_2^+ \rightarrow 2_1^+)$				$B(E2;3_1^+ \rightarrow 2_1^+)$			
	Exp.	IBM-1	IBM-2	DDM	Exp.	IBM-1	IBM-2	DDM	Exp.	IBM-1	IBM-2	DDM	Exp.	IBM-1	IBM-2	DDM
^{120}Ba	-	0.0056	0.0076	0.0043	-	0.0029	0.0032	0.023	-	0.076	0.087	0.076	-	0.0520	0.0500	0.093
^{122}Ba	-	0.0042	0.0053	0.0032	-	0.0011	0.0026	0.015	-	0.068	0.079	0.062	-	0.0460	0.0462	0.088
^{124}Ba	-	0.0038	0.0039	0.0030	-	0.00065	0.00055	0.011	-	0.109	0.110	0.113	-	0.0341	0.0331	0.116
^{126}Ba	-	0.0029	0.0030	0.0028	-	0.00014	0.00024	0.00081	-	0.125	0.129	0.123	-	0.0262	0.0267	0.146
^{128}Ba	-	0.0015	0.0027	0.00282	-	0.0023	0.0025	0.0013	-	0.176	0.188	0.163	-	0.017	0.019	0.229
^{130}Ba	-	0.0032	0.0025	0.00261	-	0.00018	0.00020	0.0012	-	0.133	0.163	0.071	-	0.0032	0.0031	0.311
^{132}Ba	-	0.0012	0.0021	0.00202	-	0.00026	0.00023	0.00058	-	0.055	0.063	0.100	-	0.0121	0.0123	0.248
^{134}Ba	0.0018(6)	0.0014	0.0019	0.0020	0.0045(20)	0.0067	0.0077	0.00021	-	0.116	0.112	0.0098	0.0009(34)	0.0045	0.0007	0.193
^{136}Ba	-	0.0019	0.0017	0.00087	-	0.0056	0.0059	0.00020	-	0.170	0.174	0.0082	-	0.0056	0.0058	0.176
^{140}Ba	-	0.0009	0.00089	0.00056	-	0.0054	0.0050	-	-	0.210	0.200	0.0081	-	0.0067	0.0061	0.177
^{142}Ba	-	0.00081	0.000851	-	-	0.0051	0.0053	-	-	0.241	0.233	-	-	0.0072	0.0079	-
^{144}Ba	-	0.00064	0.00074	-	-	0.0043	0.0049	-	-	0.0278	0.0270	-	-	0.0074	0.0071	-
^{146}Ba	-	0.0005	0.00065	-	-	0.00341	0.00444	-	>.0046	0.0050	0.0051	-	-	0.0065	0.0067	-
^{148}Ba	-	0.00043	0.00045	-	-	0.0028	0.0030	-	-	0.0032	0.0035	-	-	0.0068	0.0060	-

Experimental data are taken from refs. [105, 115, 116, 117, 118, 119, 120]

Table (3-7): Branching Ratios of ¹²⁰⁻¹⁴⁸Ba isotopes

Isotopes	$B(E2;2_2^+ \rightarrow 0_1^+)/B(E2;2_2^+ \rightarrow 2_1^+)$				$B(E2;3_1^+ \rightarrow 2_1^+)/B(E2;3_1^+ \rightarrow 2_2^+)$				$B(E2;3_1^+ \rightarrow 4_1^+)/B(E2;3_1^+ \rightarrow 2_2^+)$			
	Exp.	IBM-1	IBM-2	DDM	Exp.	IBM-1	IBM-2	DDM	Exp.	IBM-1	IBM-2	DDM
¹²⁰ Ba	-	0.231	0.291	0.311	-	0.952	0.922	0.873	-	1.462	1.362	1.21
¹²² Ba	-	0.210	0.217	0.302	0.86	0.791	0.752	0.812	1.35	1.30	1.350	1.514
¹²⁴ Ba	0.17 (5)	0.194	0.184	0.221	-	0.070	0.075	0.800	-	1.002	1.0202	2.41
¹²⁶ Ba	0.11 (2)	0.137	0.130	0.201	0.046	0.066	0.068	0.552	0.13	0.120	0.127	0.156
¹²⁸ Ba	0.11	0.210	0.109	0.199	0.064	0.059	0.060	0.0610	0.14	0.129	0.133	0.133
¹³⁰ Ba	0.054	0.098	0.068	0.096	0.038	0.036	0.038	0.0430	0.17	0.165	0.185	0.145
¹³² Ba	0.026	0.0290	0.0270	0.033	0.033	0.039	0.040	0.0410	0.31	0.331	0.342	0.231
¹³⁴ Ba	0.006	0.008	0.009	0.0056	0.013	0.019	0.026	0.021	0.53	0.452	0.463	0.356
¹³⁶ Ba	-	0.0092	0.0098	0.0045	-	0.022	0.0212	0.0034	-	0.522	0.545	0.478
¹⁴⁰ Ba	-	0.00987	0.0088	0.0036	-	0.019	0.0189	-	-	0.611	0.676	0.541
¹⁴² Ba	-	0.00034	0.00031	-	-	0.011	0.0123	-	-	0.656	0.756	-
¹⁴⁴ Ba	-	0.00031	0.00029	-	-	0.009	0.0089	-	-	0.623	0.723	-
¹⁴⁶ Ba	-	0.00024	0.00031	-	-	0.007	0.0072	-	-	0.691	0.700	-
¹⁴⁸ Ba	-	0.00018	0.0002	-	-	0.0033	0.0037	-	-	0.703	0.821	-

Experimental are taken from refs. [122, 123, 124]

Continued to Table (3-7)

Isotopes	$B(E2;3_1^+ \rightarrow 2_1^+)/B(E2;3_1^+ \rightarrow 4_1^+)$				$B(E2;4_2^+ \rightarrow 2_1^+)/B(E2;4_2^+ \rightarrow 2_2^+)$				$B(E2;4_2^+ \rightarrow 4_1^+)/B(E2;4_2^+ \rightarrow 2_2^+)$			
	Exp.	IBM-1	IBM-2	DDM	Exp.	IBM-1	IBM-2	DDM	Exp.	IBM-1	IBM-2	DDM
^{120}Ba	-	0.459	0.551	0.341	-	0.0041	0.0021	0.0065	-	0.171	0.201	0.167
^{122}Ba	0.20	0.310	0.321	0.256	-	0.0050	0.00550	0.0052	-	0.211	0.231	0.336
^{124}Ba	-	0.348	0.355	0.561	0.005	0.0059	0.0058	0.0061	0.29(6)	0.26	0.246	0.279
^{126}Ba	0.40	0.441	0.462	0.472	0.008	0.0079	0.0089	0.0087	0.28(3)	0.29	0.298	0.267
^{128}Ba	0.41	0.456	0.486	0.481	0.015	0.019	0.0189	0.019	0.26(3)	0.30	0.320	0.261
^{130}Ba	0.022	0.031	0.039	0.031	0.022	0.027	0.0292	0.043	0.67	0.59	0.595	0.562
^{132}Ba	0.05	0.062	0.066	0.0493	0.015	0.021	0.0221	0.053	15 < 0.86	1.20	1.203	13
^{134}Ba	0.012	0.015	0.017	0.015	0.024	0.031	0.033	0.045	0.72	0.82	0.825	0.971
^{136}Ba	-	0.013	0.0183	0.113	-	0.034	0.039	0.0066	-	0.92	0.942	1.223
^{140}Ba	-	0.001	0.0021	0.322	-	0.045	0.0475	0.00742	-	1.23	1.233	2.652
^{142}Ba	-	0.0013	0.00213	-	-	0.056	0.0560	-	-	1.35	1.356	-
^{144}Ba	-	0.0025	0.00215	-	-	0.058	0.0598	-	-	1.651	1.671	-
^{146}Ba	-	0.0001	0.00011	-	-	0.064	0.0664	-	-	1.90	1.920	-
^{148}Ba	-	0.0053	0.0057	-	-	0.073	0.0783	-	-	2.11	2.211	-

Experimental are taken from refs. [122, 123, 124]

Continued to Table (3-7)

Isotopes	$B(E2;0_2^+ \rightarrow 2_1^+)/B(E2;0_2^+ \rightarrow 2_2^+)$				$B(E2;2_3^+ \rightarrow 2_2^+)/B(E2;2_3^+ \rightarrow 2_1^+)$				$B(E2;2_3^+ \rightarrow 0_1^+)/B(E2;2_3^+ \rightarrow 2_1^+)$			
	Exp.	IBM-1	IBM-2	DDM	Exp.	IBM-1	IBM-2	DDM	Exp.	IBM-1	IBM-2	DDM
^{120}Ba	-	0.016	0.0216	0.663	-	9	4.89	1.623	-	2.43	3.149	3.262
^{122}Ba	-	0.020	0.0270	0.584	-	12.56	10.156	23	-	3.610	3.619	2.762
^{124}Ba	> 0.013	0.021	0.0121	0.550	-	22	2.981	80.6	-	4.654	5.615	5.33
^{126}Ba	> 0.01	0.019	0.013	0.511	-	10.2	10.24	36	-	11	3.117	4.326
^{128}Ba	0.002	0.0035	0.0024	0.457	-	8.55	7.50	18	-	1.976	1.391	1.092
^{130}Ba	0.032	0.043	0.034	0.425	-	9.11	12.121	10.2	-	0.112	0.152	0.585
^{132}Ba	-	0.044	0.0464	2.861	4	0.23	0.425	1.70	-	0.342	0.640	0.2280
^{134}Ba	0.04	0.051	0.0491	12.6	0.22	2.87	2.181	36.3	0.035	1.234	1.415	0.300
^{136}Ba	-	0.055	0.045	10.23	-	3.132	4.340	3.91	-	2.87	2.287	0.341
^{140}Ba	-	0.073	0.086	8.83	-	4.09	4.809	2.5	-	10	8	3.2
^{142}Ba	-	0.073	0.0873	-	-	4.76	5.177	-	-	9.22	8.5	-
^{144}Ba	-	0.084	0.0848	-	-	0.32	1.322	-	-	2.11	12.121	-
^{146}Ba	-	0.082	0.0832	-	-	1.651	1.853	-	-	3.12	3.10	-
^{148}Ba	-	0.089	0.0897	-	-	11.09	13.11	-	-	0.98	1.210	-
^{150}Ba	-	0.0098	0.010	-	-	0.0098	0.0414	-	-	1.34	1.554	-

Experimental are taken from refs. [122, 123, 124]

Table (3-8): Magnetic Transition Probability $B(M1; J_f^+ \rightarrow J_i^+)$ in μ_N^2 Units for Ba isotopes.

Isotopes	$B(M1; 2_2^+ \rightarrow 2_1^+)$			$B(M1; 3_1^+ \rightarrow 2_1^+)$			$B(M1; 3_1^+ \rightarrow 4_1^+)$			$B(M1; 4_2^+ \rightarrow 4_1^+)$		
	IBM-1	IBM-2	DDM	IBM-1	IBM-2	DDM	IBM-1	IBM-2	DDM	IBM-1	IBM-2	DDM
^{120}Ba	0.012	0.022	0.0429	0.0067	0.0005	0.0033	0.0087	0.0121	0.0055	0.012	0.0328	0.022
^{122}Ba	0.0185	0.0201	0.0032	0.0052	0.621	0.0043	0.0109	0.0432	0.026	0.0295	0.103	1.204
^{124}Ba	0.019	0.0188	0.0157	0.00049	0.0034	0.00019	0.0122	0.037	0.0651	0.0362	0.239	0.0356
^{126}Ba	0.0038	0.0046	0.0236	0.00011	0.0039	0.0820	0.0020	0.075	0.065	0.0088	0.271	0.095
^{128}Ba	0.0232	0.0362	0.00040	0.00032	0.0085	0.0123	0.0144	0.237	0.0881	0.0488	0.224	0.056
^{130}Ba	0.0770	0.045	0.00040	0.00088	0.0031	0.0050	0.0509	0.236	0.0102	0.142	0.216	0.066
^{132}Ba	0.0221	0.016	0.00065	0.00012	0.0056	0.009	0.0147	0.116	0.0241	0.0433	0.211	0.026
^{134}Ba	0.00220	0.046	0.00101	0.00004	0.0032	0.074	0.0013	0.0029	0.022	0.0039	0.0031	0.0101
^{136}Ba	0.0328	0.009	0.00291	0.000042	0.212	0.101	0.0178	0.098	0.0356	0.0531	0.876	0.0241
^{140}Ba	0.03281	0.246	0.00331	0.0034	0.0025	0.1011	0.0241	0.00043	0.0432	0.0562	0.0014	0.076
^{142}Ba	0.0356	0.035	-	0.00623	0.1194	-	0.0382	0.172	-	0.0673	0.163	-
^{144}Ba	0.0431	0.0046	-	0.0054	0.0005	-	0.0452	0.621	-	0.077	0.631	-
^{146}Ba	0.0571	0.0021	-	0.0876	0.621	-	0.0563	1.31	-	0.0861	0.38	-
^{148}Ba	0.0055	0.0002	-	0.0973	0.0034	-	0.0667	0.38	-	0.0964	0.36	-

Table (3-9): Mixing Ratios for $^{120-148}\text{Ba}$ isotopes in eb/μ_N Units

Isotopes	$\delta(E2,2_2^+ \rightarrow 2_1^+)$				$\delta(E2,2_3^+ \rightarrow 2_1^+)$				$\delta(E2,3_1^+ \rightarrow 2_1^+)$			
	Exp.	IBM-1	IBM-2	DDM	Exp.	IBM-1	IBM-2	DDM	Exp.	IBM-1	IBM-2	DDM
^{120}Ba	-	4.66	5.2	5.23	-	7.22	2.43	10.2	-	12	7.56	10.3
^{122}Ba	-	3.876	4.66	5.22	-	0.871	0.89	0.32	-	17.5	11	0.227
^{124}Ba	-	2.762	3.10	1.9	-	-2.65	-2.1	-3.98	-	11.86	5.5	5.7
^{126}Ba	$+5_{-1}^{+2}$	6.5	-8	4.2	-	1.23	3.2	2.89	-	21.6	13	14.45
^{128}Ba	-	0.422	0.66	0.659	-	0.912	3.61	1.223	-	8.45	2.89	1.34
^{130}Ba	0.296	0.311	0.251	0.541	-23(9)	-4.09	-20.44	3.98	$+5_{-1}^{+2}$	4.78	4.1	7
^{132}Ba	$+8.5_{-18}^{+40}$	7.145	10	11	-	11.6	14	12.89	$+2.5_{-10}^{+10}$	9.2	3.5	3.5
^{134}Ba	-7.4_{-9}^{+9}	-8.410	-7.65	-9	-	1.43	2.6	14	$+1.8_{-15}^{+1.5}$	1.6	1.97	19
^{136}Ba	-1.5_{-15}^{+6}	-2.41	-2.33	2.3	-	6.9	10	8.3	-	-2.56	-3.87	-5.32
^{140}Ba	0.6_{-6}^{+18}	1.1	0.91	0.998	$+0.18_{-5}^{+6}$	0.21	0.31	-	-	12	10	1.22
^{142}Ba	>10	13	13	-	-0.93(29)	1.1	2	-	-	-0.423	-0.23	-
^{144}Ba	$+7._{-3}^{+19}$	9.3	8.2	-	-3.2_{-6}^{+18}	-4.67	-4.7	-	-	10.3	7.43	-
^{146}Ba	-	1.414	6.4	-	-	1.90	2.21	-	-	21	1.23	-
^{148}Ba	-	0.556	1.24	-	-	0.761	0.45	-	-	0.549	0.81	-

Experimental data are taken from refs. [105, 125, 126, 127]

Continued to Table (3-9)

Isotopes	$\delta(E2,3_1^+ \rightarrow 4_1^+)$				$\delta(E2,3_1^+ \rightarrow 2_2^+)$				$\delta(E2,4_2^+ \rightarrow 4_1^+)$			
	Exp.	IBM-1	IBM-2	DDM	Exp.	IBM-1	IBM-2	DDM	Exp.	IBM-1	IBM-2	DDM
^{120}Ba	-	4.22	2.1	1.88	-	5.43	1.23	0.121	-	3.3	0.279	5.6
^{122}Ba	-	3.86	3.78	4.5	-	3.87	2.0	4.87	-	2.30	1.25	2.54
^{124}Ba	-	-1.85	-2.25	-3.4	-	4.6	-4.3	6	-	1.54	6.5	2.13
^{126}Ba	-	4.76	5	10.2	-	3.34	-2.56	12	> 1	8.58	1.413	9.34
^{128}Ba	-	1.10	5.8	0.45	-	5.98	6.0	0.651	-	1.08	2.0	1.0
^{130}Ba	-	0.661	0.24	0.779	-	1.08	1.209	1.0	-	-0.871	1.09	7.12
^{132}Ba	-	1.55	0.77	1.451	$4.0^{+1.1}_{-1.2}$	6.7	8.0	2.12	-1.1^{+2}_{-2}	-2.2	-9.0	-4
^{134}Ba	-	2.44	1.4	9.77	-17^{+23}_{-6}	-19.7	-15.3	-2.16	0.29^{+2}_{-2}	1.3	2.87	0.54
^{136}Ba	-	1.11	2.12	3.21	-	11.6	10.5	3.1	$+0.8^{+6}_{-6}$	4.5	5	1.9
^{140}Ba	-	2.27	3.7	5.87	-	-6.78	-9.5	4.21	-	2.7	4.9	4.8
^{142}Ba	-	1.897	0.89	-	-	1.242	3.45	-	-	-0.887	-9.8	-
^{144}Ba	-	0.302	1.65	-	-	2.07	2.0	-	-	1.65	2.761	-
^{146}Ba	-	1.97	2.54	-	-	1.891	3.09	-	-	3.65	4.0	-
^{148}Ba	-	8.8	16.3	-	-	2.810	8.45	-	-	7.8	12	-

Experimental data are taken from refs. [105, 125, 126, 127]

Table (3-7) Table (3-7): Branching Ratios of ¹²⁰⁻¹⁴⁸Ba isotopes

Isotopes	$B(E2;2_2^+ \rightarrow 0_1^+)/B(E2;2_2^+ \rightarrow 2_1^+)$				$B(E2;3_1^+ \rightarrow 2_1^+)/B(E2;3_1^+ \rightarrow 2_2^+)$				$B(E2;3_1^+ \rightarrow 4_1^+)/B(E2;3_1^+ \rightarrow 2_2^+)$			
	Exp.	IBM-1	IBM-2	DDM	Exp.	IBM-1	IBM-2	DDM	Exp.	IBM-1	IBM-2	DDM
¹²⁰ Ba	-	0.231	0.291	0.311	-	0.952	0.922	0.873	-	1.462	1.362	1.21
¹²² Ba	-	0.210	0.217	0.302	0.86	0.791	0.752	0.812	1.35	1.30	1.350	1.514
¹²⁴ Ba	0.17 (5)	0.194	0.184	0.221	-	0.070	0.075	0.800	-	1.002	1.0202	2.41
¹²⁶ Ba	0.11 (2)	0.137	0.130	0.201	0.046	0.066	0.068	0.552	0.13	0.120	0.127	0.156
¹²⁸ Ba	0.11	0.210	0.109	0.199	0.064	0.059	0.060	0.0610	0.14	0.129	0.133	0.133
¹³⁰ Ba	0.054	0.098	0.068	0.096	0.038	0.036	0.038	0.0430	0.17	0.165	0.185	0.145
¹³² Ba	0.026	0.0290	0.0270	0.033	0.033	0.039	0.040	0.0410	0.31	0.331	0.342	0.231
¹³⁴ Ba	0.006	0.008	0.009	0.0056	0.013	0.019	0.026	0.021	0.53	0.452	0.463	0.356
¹³⁶ Ba	-	0.0092	0.0098	0.0045	-	0.022	0.0212	0.0034	-	0.522	0.545	0.478
¹⁴⁰ Ba	-	0.00987	0.0088	0.0036	-	0.019	0.0189	-	-	0.611	0.676	0.541
¹⁴² Ba	-	0.00034	0.00031	-	-	0.011	0.0123	-	-	0.656	0.756	-
¹⁴⁴ Ba	-	0.00031	0.00029	-	-	0.009	0.0089	-	-	0.623	0.723	-
¹⁴⁶ Ba	-	0.00024	0.00031	-	-	0.007	0.0072	-	-	0.691	0.700	-
¹⁴⁸ Ba	-	0.00018	0.0002	-	-	0.0033	0.0037	-	-	0.703	0.821	-

Experimental are taken from refs. [122, 123, 124]

Continued to Table (3-7)

Isotopes	$B(E2;3_1^+ \rightarrow 2_1^+)/B(E2;3_1^+ \rightarrow 4_1^+)$				$B(E2;4_2^+ \rightarrow 2_1^+)/B(E2;4_2^+ \rightarrow 2_2^+)$				$B(E2;4_2^+ \rightarrow 4_1^+)/B(E2;4_2^+ \rightarrow 2_2^+)$			
	Exp.	IBM-1	IBM-2	DDM	Exp.	IBM-1	IBM-2	DDM	Exp.	IBM-1	IBM-2	DDM
^{120}Ba	-	0.459	0.551	0.341	-	0.0041	0.0021	0.0065	-	0.171	0.201	0.167
^{122}Ba	0.20	0.310	0.321	0.256	-	0.0050	0.00550	0.0052	-	0.211	0.231	0.336
^{124}Ba	-	0.348	0.355	0.561	0.005	0.0059	0.0058	0.0061	0.29(6)	0.26	0.246	0.279
^{126}Ba	0.40	0.441	0.462	0.472	0.008	0.0079	0.0089	0.0087	0.28(3)	0.29	0.298	0.267
^{128}Ba	0.41	0.456	0.486	0.481	0.015	0.019	0.0189	0.019	0.26(3)	0.30	0.320	0.261
^{130}Ba	0.022	0.031	0.039	0.031	0.022	0.027	0.0292	0.043	0.67	0.59	0.595	0.562
^{132}Ba	0.05	0.062	0.066	0.0493	0.015	0.021	0.0221	0.053	15 < 0.86	1.20	1.203	13
^{134}Ba	0.012	0.015	0.017	0.015	0.024	0.031	0.033	0.045	0.72	0.82	0.825	0.971
^{136}Ba	-	0.013	0.0183	0.113	-	0.034	0.039	0.0066	-	0.92	0.942	1.223
^{140}Ba	-	0.001	0.0021	0.322	-	0.045	0.0475	0.00742	-	1.23	1.233	2.652
^{142}Ba	-	0.0013	0.00213	-	-	0.056	0.0560	-	-	1.35	1.356	-
^{144}Ba	-	0.0025	0.00215	-	-	0.058	0.0598	-	-	1.651	1.671	-
^{146}Ba	-	0.0001	0.00011	-	-	0.064	0.0664	-	-	1.90	1.920	-
^{148}Ba	-	0.0053	0.0057	-	-	0.073	0.0783	-	-	2.11	2.211	-

Experimental are taken from refs. [122, 123, 124]

Continued to Table (3-7)

Isotopes	$B(E2;0_2^+ \rightarrow 2_1^+)/B(E2;0_2^+ \rightarrow 2_2^+)$				$B(E2;2_3^+ \rightarrow 2_2^+)/B(E2;2_3^+ \rightarrow 2_1^+)$				$B(E2;2_3^+ \rightarrow 0_1^+)/B(E2;2_3^+ \rightarrow 2_1^+)$			
	Exp.	IBM-1	IBM-2	DDM	Exp.	IBM-1	IBM-2	DDM	Exp.	IBM-1	IBM-2	DDM
^{120}Ba	-	0.016	0.0216	0.663	-	9	4.89	1.623	-	2.43	3.149	3.262
^{122}Ba	-	0.020	0.0270	0.584	-	12.56	10.156	23	-	3.610	3.619	2.762
^{124}Ba	> 0.013	0.021	0.0121	0.550	-	22	2.981	80.6	-	4.654	5.615	5.33
^{126}Ba	> 0.01	0.019	0.013	0.511	-	10.2	10.24	36	-	11	3.117	4.326
^{128}Ba	0.002	0.0035	0.0024	0.457	-	8.55	7.50	18	-	1.976	1.391	1.092
^{130}Ba	0.032	0.043	0.034	0.425	-	9.11	12.121	10.2	-	0.112	0.152	0.585
^{132}Ba	-	0.044	0.0464	2.861	4	0.23	0.425	1.70	-	0.342	0.640	0.2280
^{134}Ba	0.04	0.051	0.0491	12.6	0.22	2.87	2.181	36.2	0.035	1.234	1.415	0.300
^{136}Ba	-	0.055	0.045	10.23	-	3.132	4.340	3.91	-	2.87	2.287	0.341
^{140}Ba	-	0.073	0.086	8.83	-	4.09	4.809	2.5	-	10	8	3.2
^{142}Ba	-	0.073	0.0873	-	-	4.76	5.177	-	-	9.22	8.5	-
^{144}Ba	-	0.084	0.0848	-	-	0.32	1.322	-	-	2.11	12.121	-
^{146}Ba	-	0.082	0.0832	-	-	1.651	1.853	-	-	3.12	3.10	-
^{148}Ba	-	0.089	0.0897	-	-	11.09	13.11	-	-	0.98	0.210	-
^{150}Ba	-	0.0098	0.010	-	-	0.0098	0.0414	-	-	1.34	1.554	-

Experimental are taken from refs. [122, 123, 124]

CHAPTER ONE
INTRODUCTION

CHAPTER TWO
THEROETICAL CONSIDERATIONS

CHAPTER THREE
RESULTS AND DISCUSSION

CHAPTER FOUR

CONCLUSIONS AND SUGGESTIONS

REFERENCES

Republic of Iraq
Ministry of Higher Education and Scientific Research
and Scientific Research
Al-Nahrain University
College of Science
Department of Physics



**Structure Evolution in the even-even Ba nuclei with
Interacting Boson Model**

A Thesis

**Submitted to College of Science Al-Nahrain University as
a partial fulfillment of the requirements for the degree of
Master of Science in Physics .**

By

Ghofran A. Ali

Supervised by

Prof. Dr. SAAD N . ABOOD

2016 A.D

1437 H.D



جمهورية العراق
وزارة التعليم العالي والبحث العلمي
جامعة النهريين
كلية العلوم

تطور التركيب في نوى الباريوم الزوجية-الزوجية باستخدام
نموذج البوزونات المتفاعلة

رسالة مقدمة إلى
كلية العلوم – جامعة النهريين
وهي جزء من متطلبات نيل درجة الماجستير في الفيزياء

من قبل

غفران عبد علي

بإشراف
الأستاذ الدكتور سعد ناجي عبود

١٤٣٧ هـ

٢٠١٦ م

الخلاصة

لقد تم في هذا البحث دراسة التركيب النووي والانتقالات الكهرومغناطيسية لنظائر الباريوم $Ba^{120-148}$ الزوجية-الزوجية باستخدام النماذج التجميعية (collective models) نموذج البوزونات المتفاعلة (Interacting Boson Model (IBM)) ونموذج التشوه الحركي (Dynamic Deformation Model (DDM)). حيث تم دراسة مستويات الطاقة واحتمالية الانتقالات الكهربائية رباعية القطب $B(E2)$ ، والانتقالات ثنائية القطب المغناطيسية $B(M1)$ وكذلك الانتقالات أحادية القطب $B(E0)$. نسب الخلط (mixing ratios) $\delta(E2/M1)$ ، إضافة إلى دراسة العديد من الخصائص النووية الأخرى مثل إزاحة النظائر $\Delta < r^2 >$ والإزاحة الأيزوميرية $\delta < r^2 >$ ، العزوم رباعية القطب الكهربائية والعزوم ثنائية القطب المغناطيسية.

تم الاعتماد على طرق حديثة في حساب الشحنات الفعالة (effective charges) (e_π, e_ν) للبوزونات والتي استخدمت في حساب الانتقالات الكهربائية، وكذلك العوامل الجيومغناطيسية للبوزونات (g_π, g_ν) والتي استخدمت في حساب الانتقالات المغناطيسية.

تم تحديد المستويات المزدوجة التناظر في نظائر الباريوم الزوجية-الزوجية، والتي تتميز بأنها ذات طاقة عالية والانتقالات الكهربائية بين هذه المستويات ضعيفة إضافة إلى أن الانتقالات المغناطيسية بين المستويات المزدوجة التناظر تكون عالية، ومن هذه المستويات $(2_3^+, 2_4^+, 3_1^+)$ أضافه إلى المستوى 1_1^+ الذي يظهر في النظائر المشوهة والتي تقع عند التحديد $SU(3)$ الدوراني من تحديرات IBM .

نموذج التشوه الحركي (DDM) والذي تم استخدامه لدراسة التركيب النووي في نظائر $Ba^{120-140}$ الزوجية-الزوجية وذلك من خلال دراسة سطوح طاقة الجهد (potential energy surface) لتلك النظائر ومعرفة نوع التشوه لكل نظير من هذه النظائر أي نوع التشوه (مفلطح أو متطاوّل) (prolate or oblate) وكذلك إيجاد فرق الجهد بين التشوهين V_{PO} .

وتمت مقارنة النتائج النظرية التي تم الحصول عليها من $IBM-1$ و $IBM-2$ و DDM مع القيم العملية المتوفرة وكانت متفقة بشكل جيد. ومن الملاحظ أن قيم نموذج البوزونات المتفاعلة أقرب إلى القيم العملية من قيم نموذج التشوه الحركي وذلك كون نموذج البوزونات المتفاعلة هاملتوني الطاقة يحتوي على عدة بارامترات وأنه باختيار قيم مناسبة لهذه البارامترات ستحصل على نتائج جيدة جداً.